



Center for Aeronautical Research

Bureau of Engineering Research
The University of Texas at Austin
Austin, Texas

CAR 90-1

**A DECENTRALIZED LINEAR QUADRATIC CONTROL DESIGN
METHOD FOR FLEXIBLE STRUCTURES**

by

JOHNSON
GRANT

Tzu-Jeng Su
Roy R. Craig, Jr.

IN-18-CR

NASA Contract No. NAG9-357
May, 1990

329382

P118

(NASA-CR-187860) A DECENTRALIZED LINEAR
QUADRATIC CONTROL DESIGN METHOD FOR FLEXIBLE
STRUCTURES Interim Report (Texas Univ.)
118 p CSCL 22B

N91-16059

Unclas
63/18 0329382

A DECENTRALIZED LINEAR QUADRATIC CONTROL DESIGN
METHOD FOR FLEXIBLE STRUCTURES

Tzu-Jeng Su*
Roy R. Craig, Jr.†

Interim Report
NASA Contract NAG9-357

Report No. CAR 90-1

Center for Aeromechanics Research
Department of Aerospace Engineering and Engineering Mechanics
Bureau of Engineering Research
College of Engineering
The University of Texas at Austin
Austin, Texas 78712

May, 1990

*Postdoctoral Fellow, Aerospace Engineering

†Professor, Department of Aerospace Engineering and Engineering Mechanics

10

11

ACKNOWLEDGEMENTS

This work was supported by NASA Contract NAG9-357 of the NASA Lyndon B. Johnson Space Center. The authors wish to thank Mr. John Sunkel for his interest in this work.



ABSTRACT

A decentralized suboptimal linear quadratic control design procedure which combines substructural synthesis, model reduction, decentralized control design, subcontroller synthesis, and controller reduction is proposed for the design of reduced-order controllers for flexible structures. The procedure starts with a definition of the continuum structure to be controlled. An evaluation model of finite dimension is obtained by the finite element method. Then, the finite element model is decomposed into several substructures by using a natural decomposition called *substructuring decomposition*. Each substructure, at this point, still has too large a dimension and must be reduced to a size that is "Riccati-solvable." Model reduction of each substructure can be performed by using any existing model reductions method, e.g., modal truncation, balanced reduction, Krylov model reduction, or mixed-mode method. Then, based on the reduced substructure model, a subcontroller is designed by an LQ optimal control method for each substructure independently. After all subcontrollers have been designed, a controller synthesis method called *Substructural Controller Synthesis* is employed to synthesize all subcontrollers into a global controller. The assembling scheme used is the same as that employed for the structure matrices. Finally, a controller reduction scheme, called the *Equivalent Impulse Response Energy Controller* (EIREC) reduction algorithm, is used to reduce the global controller to a reasonable size for implementation. The EIREC reduced controller preserves the impulse response energy of the full-order controller and has the property of matching low-frequency moments and

low-frequency power moments. An advantage of the Substructural Controller Synthesis method is that it relieves the computational burden associated with dimensionality. Besides that, the SCS design scheme is also a highly adaptable controller synthesis method for structures with varying configuration, or varying mass and stiffness properties.

TABLE OF CONTENTS

ACKNOWLEDGEMENTS	ii
ABSTRACT	iii
TABLE OF CONTENTS	v
1. INTRODUCTION	1
1.1 Substructural Controller Synthesis	7
1.2 Preview	11
2. SUBSTRUCTURING DECOMPOSITION AND CONTROLLER SYNTHESIS	13
2.1 Substructuring Decomposition	16
2.2 Substructuring Decomposition of Structural Dynamics Systems	19
2.2.1 Coupling Matrix	23
2.3 Substructural Controller Synthesis	24
2.4 Examples	34
2.4.1 Identical Substructures With Almost-Colocated Sensor And Actuator Allocations	35
2.4.2 Unsymmetric Case	39
3. MODEL REDUCTION OF FLEXIBLE STRUCTURES	48
3.1 Model Reduction	50

3.1.1	Modal Truncation	50
3.1.2	Balanced Reduction	51
3.1.3	Balanced Gains	53
3.1.4	Krylov Model Reduction	54
3.1.5	Ritz Vectors and Mixed-Mode Method	55
3.2	Plane Truss Example	56
3.2.1	Open-Loop Comparison	57
3.2.2	Control Design	59
4.	CONTROLLER REDUCTION	69
4.1	LQG Controller Reduction Problem	72
4.2	Equivalent Impulse Response Energy Controller Reduction Algorithm	74
4.3	Some Properties of the Equivalent Impulse Response Energy Controller	79
4.4	Examples	89
4.4.1	Controllers For A Four-Disk System	89
4.4.2	Controllers For A Solar Optical Telescope Spacecraft	92
5.	CONCLUSIONS	103
	BIBLIOGRAPHY	105

Chapter 1

INTRODUCTION

Largely because the highly advanced space technology has made the construction of large space structures possible in the very near future, the problem of control of flexible structures has received a great deal of attention in recent years. In fact, control of flexible structures has emerged as an interdisciplinary research topic called Control/Structure Interaction (CSI), which attracts researchers from both controls and structural dynamics areas. A number of conferences and workshops specialized on control of flexible structures have been held recently to promote technical exchange between the structural dynamics and control disciplines. Reference [31] provides a lengthy bibliography to survey the developments of particular importance to dynamic modelling and control of large space structures.

CSI problems involve combining advanced structural dynamics analysis and identification techniques with advanced control methods. A major difficulty that makes control of flexible structures different from other control problems is due to the fact that a flexible structure is a distributed system and, hence, has an infinite number of degrees of freedom. This very nature of structural systems hinders the direct application of the existing well-developed control methods. Although there is a branch of study on the control of distributed systems[1, 27], its application is limited to simple structures like beams

and plates, but it is not applicable to structures with complicated geometry. In practice, a structural system is usually modelled by the finite element method, along with modifications based upon system identification test data. For a large space structure, e.g., Fig. 1.1, such a model attains at least tens of thousands of degrees of freedom, which is a major computational task for dynamic analysis not to mention too large a scale for control design. Therefore, for the purposes of efficient computation and easy control implementation, model reduction is an inevitable procedure for dynamic analysis and control design of large structures.

There are various open-loop model reduction approaches for structural dynamics systems, such as static condensation, Guyan-Irons reduction, mode-superposition method, component mode synthesis, and the Lanczos method. The purpose of model order reduction is to construct a simplified but representative model upon which a controller design can be based.

Although there is a wealth of new and sophisticated control methods, e.g., H^∞ control theory, linear quadratic optimal control methodology (for which Ref. [21] has a fine review) still is the one that has provided the most complete multivariable design and synthesis theory yet available. For this reason, LQ control theory is the method frequently used by control engineers to design controllers for flexible structures. As mentioned before, it is not possible to design an optimal LQ controller for a large scale structural dynamics system because the size of the system exceeds the available computing capability, i.e., the system is not "Riccati-solvable." Therefore, a traditional approach to synthesize a controller for a flexible structure is to use a suboptimal LQ design strategy. A flow chart similar to the one in Ref. [2] is shown in Fig. 1.2 to

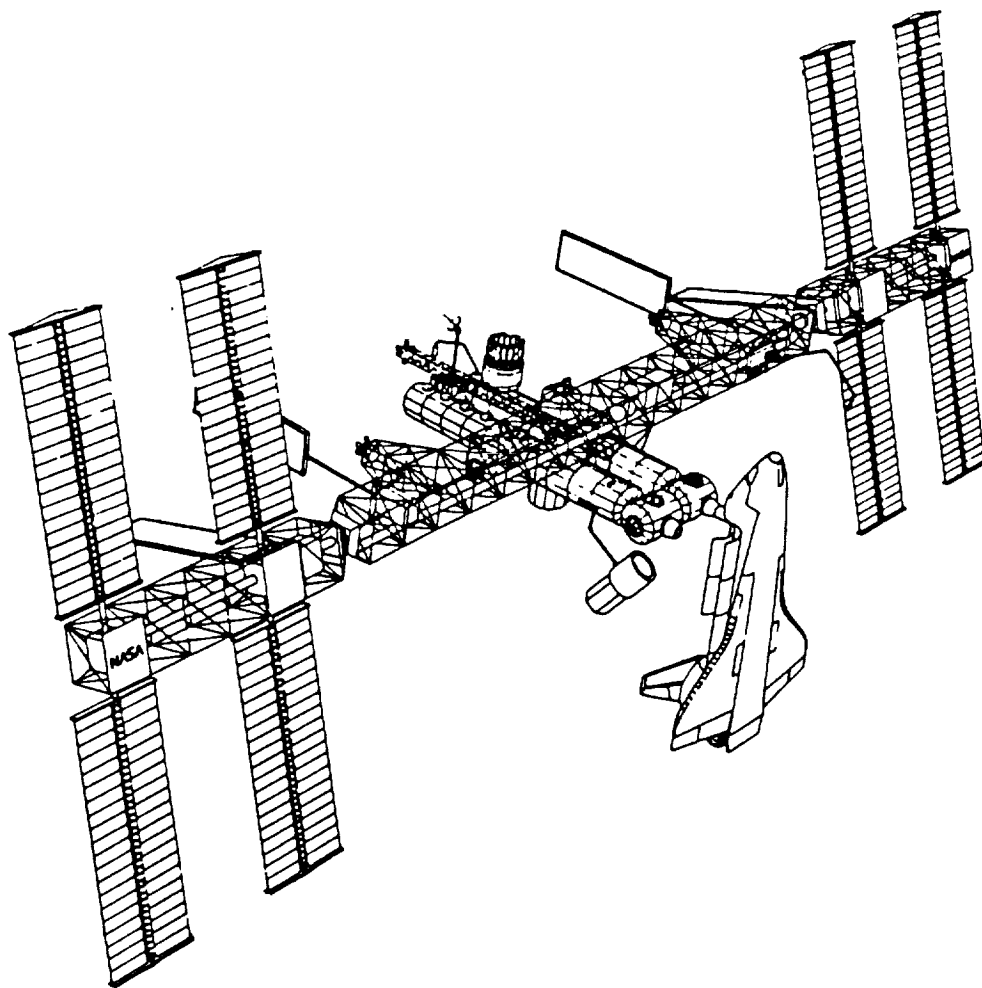


Figure 1.1: Large space structure (CETF Phase 1 Model)

summarize the suboptimal LQ design procedure. It is called a “centralized” suboptimal LQ design procedure for a reason to be clarified later.

There are three alternative centralized suboptimal LQ design approaches illustrated in Fig. 1.2. All approaches begin with the definition of a continuum structure, which theoretically has infinite dimension. An evaluation model of order N , which is too large for controller design purposes, is obtained by the finite element method. The objective of each of the three fundamental approaches is to synthesize a low order controller of dimension $r \ll N$. In the first case (path A), the structure is reduced directly to order r and then an LQ method is employed to produce a controller which is optimal for the r -th order model. In the second case (path B), the structure is first reduced to a large order n such that it is still Riccati-solvable and an LQ controller can be synthesized based upon the n -th order model. The controller obtained is then reduced to order r by employing some controller reduction method. This approach is referred as Linear-Quadratic Reduction in Ref. [13]. Controller reduction by Component Cost Analysis[45] and balanced controller reduction[9, 22, 28, 40] belong to this approach. In the third case (path C), the structure is reduced to order m ($r < m \leq n$). Then, a parameter optimization method is used to determine the controller of order r by minimizing some performance criterion. The optimal projection method of Hyland and Bernstein[17] belongs to this approach. The resulting r -th order controller is optimal for the m -order structure in that it is derived from a direct optimization of a steady-state quadratic performance index for the closed-loop equations including the controller. For all three cases, the last step is to apply the r -th order controller obtained to the evaluation model for a stability study and performance evaluation.

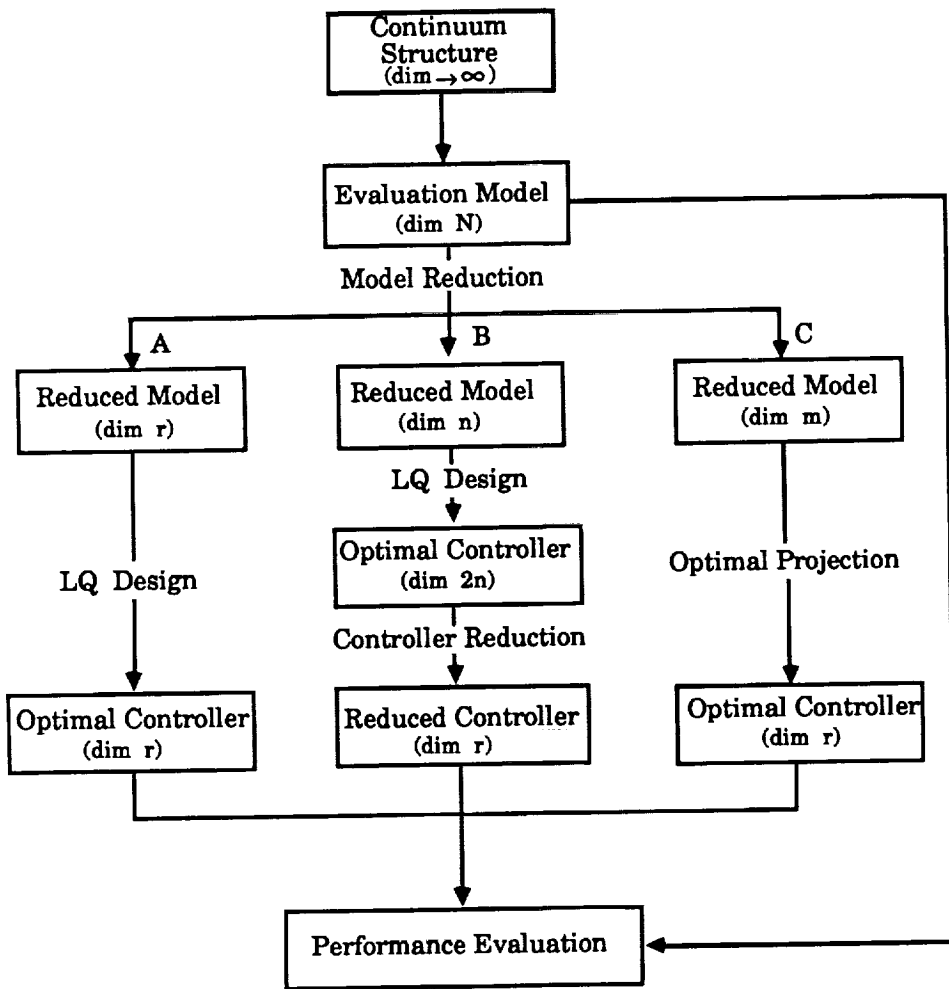


Figure 1.2: Centralized suboptimal LQ control design for flexible structures

The most costly computing part in the suboptimal LQ design is the synthesis of controller. Among the three alternatives, the computational burden of path A is the lowest because the control design is of r -th dimension. However, it requires an r -th order reduced model which can approximate the input-output characteristics of the evaluation model very well. If r is very much smaller than N , which is usually the case, the existing reliable model reduction methods may all fail to meet this requirement. Therefore, path A is not a favorable approach and is not recommended. For the optimal projection method (path C), the computational burden is very high because it requires iteration to solve a coupled set of matrix Lyapunov and Riccati equations of dimension $m + r$. These coupled Lyapunov and Riccati equations are derived from the first-order necessary conditions for optimality. In general, convergence of the iterative scheme is not assured, and the resulting solution is not guaranteed to be globally optimal, especially when m is large. Therefore, the optimal projection method is strongly restricted by the available computing capability. Path B seems to be the most reasonable approach among the three alternatives to a suboptimal LQ controller design. It combines reliable plant model reduction and controller reduction into an integrated approach for the control design of large structures, as long as dimension of the reduced-order model, n , does not exceed the computer capability for solutions of Riccati equations.

As mentioned before, the suboptimal LQ design procedure shown in Fig. 1.2 is classified as a centralized design scheme. The term "centralized" means that the controller design is based on a reduced model for the "whole" structure. In this report, a decentralized control design scheme called *Substructural Controller Synthesis* (SCS) is proposed for the controller design of flexible struc-

tures. A decentralized design scheme has advantages over a centralized design in many respects.

1.1 Substructural Controller Synthesis

First, the definition of the term *decentralized* needs to be clarified. There has been an increasing interest in decentralized control of large scale systems in very recent years (see the literature included in Refs. [49] and [50]). In these decentralized problems, the system to be controlled has several local control stations with the controller of each station being constrained to measure only local system outputs and control only local system inputs. In this sense, decentralized control means that “control implementation” is decentralized in the sense that each local controller works independently. However, the interactions among all local stations must be taken into consideration in the design of each local controller in order to coordinate the overall performance, since, in actual fact, all controllers are involved in controlling the whole system. The decentralized control design scheme proposed in this section, is, rigorously speaking, not a decentralized control, because the final controller employed to control the system is a global controller, but not a group of local controllers. Nevertheless, the control design is decentralized in that the global controller is assembled from subcontrollers which are designed solely based on local system input-output characteristics. Therefore, the Substructural Controller Synthesis method proposed here is a decentralized control *design* scheme, but not a decentralized control *implementation* scheme. This difference is pointed out here to avoid confusion with the definition used by some decentralized control researchers, although in some literature a global control implementation with

decentralized design is also called decentralized control, e.g., Ref. [20].

The procedure of Substructural Controller Synthesis is summarized by the flow chart shown in Fig. 1.3. It is a suboptimal LQ control design with controller design decentralized. The procedure starts with a definition of the continuum structure to be controlled. An evaluation model of finite dimension is obtained by the finite element method. Then, the finite element model is decomposed into several substructures by using a natural decomposition called *substructuring decomposition*. Substructuring decomposition is based on the well-known property of structural dynamics systems: the system matrices of the whole structure can be obtained by assembling the system matrices of substructures. Although structural dynamics systems are frequently described in matrix second-order form, substructuring decomposition is formulated in first-order form since the control design is based on the first-order equation form. Each substructure, at this point, still has too large a dimension and must be reduced to a size that is Riccati-solvable. Any existing reliable model reduction method can be employed to reduce the substructure, e.g., modal truncation, component mode synthesis, or Krylov model reduction. Then, based on the reduced substructure model, a *subcontroller* is designed by an LQ optimal control method independently for each substructure. The name *subcontroller* does not imply a sub-controller, which works like a low authority controller, but is used to indicate that it is a controller optimal to and designed for a substructure. After all subcontrollers have been designed, a controller synthesis method called *Substructural Controller Synthesis* (SCS) is employed to synthesize all subcontrollers into a global controller. The assembling scheme used is the same as that employed for the structure matrices. Finally, a controller reduction scheme

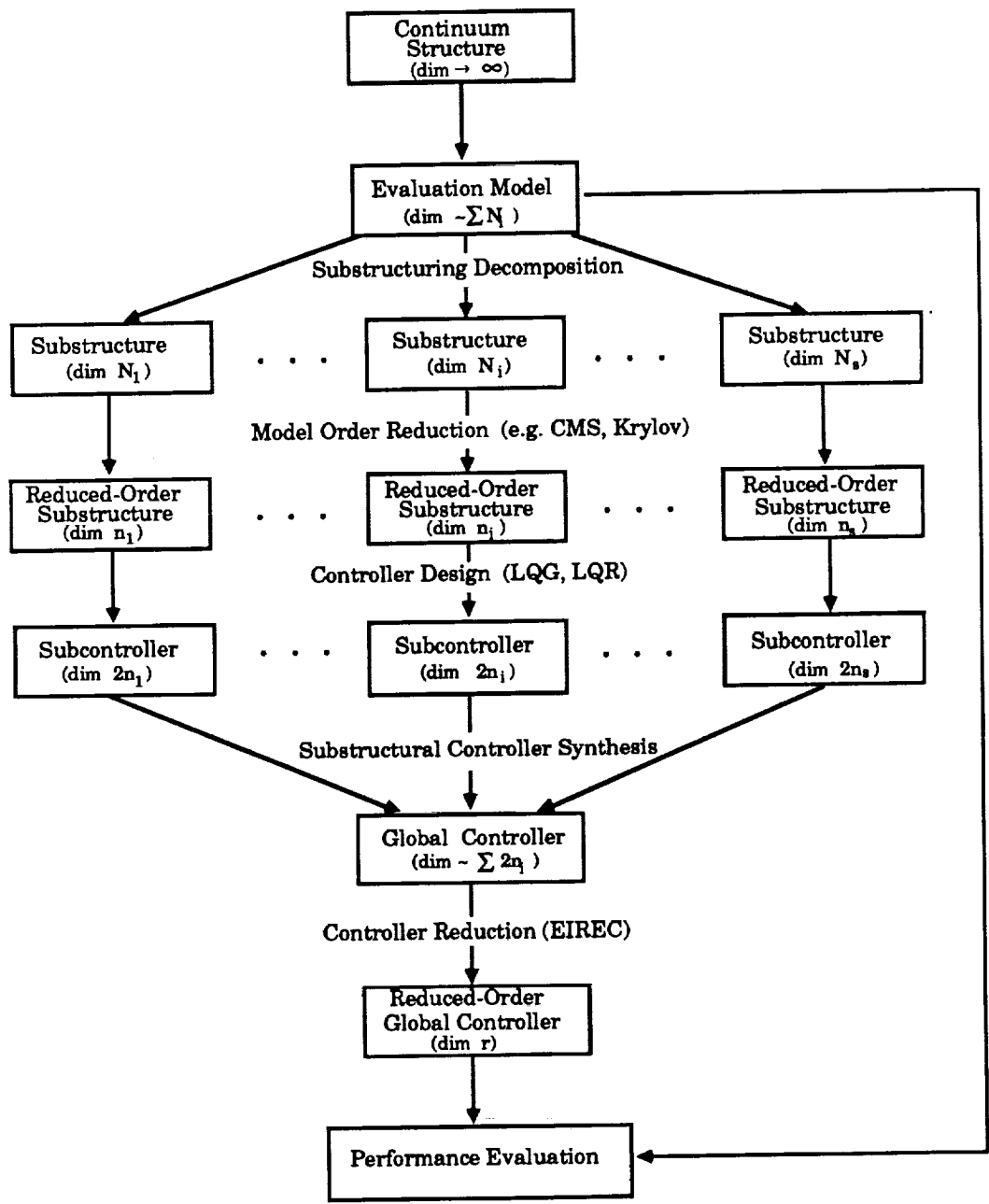


Figure 1.3: Decentralized suboptimal LQ control design for flexible structures

called *Equivalent Impulse Response Energy Controller* (EIREC) reduction algorithm is used to reduce the global controller obtained to a reasonable size for implementation.

The SCS method has many advantages over the traditional centralized suboptimal LQ design approach. First of all, the computational burden associated with dimensionality is substantially reduced because the control design is carried out at the substructure level, which is of smaller size than a structure level control design. In a centralized suboptimal LQ design, the dimension of the reduced structure model is restricted to an order for which solution of the Riccati equation is possible. For the SCS design, this restriction is imposed on substructures instead of the whole structure, which means the structure overall is approximated by a reduced model of order equal to the sum of orders of all substructures. An even bolder statement is that open-loop model reduction is not required in SCS design if the structure is decomposed into hundreds of small substructures, each of Riccati-solvable size. Secondly, the SCS controller can be updated very economically if part of the structure changes. A space structure like the one shown in Fig. 1.1 is a changing system because the space shuttle docks and leaves, the solar panels change directions, and the payload grows. For a changing structure like this, an SCS controller is highly adaptable as long as an on-line computer can keep up with the system changes. Since the SCS controller is synthesized from subcontrollers, if one substructure has a configuration or system parameter change, the only subcontroller which needs to be redesigned is the one associated with that substructure. On the other hand, for a controller based on a centralized design scheme, a slight change of the structure may require a full-scale redesign.

1.2 Preview

The organization of this report is as follows. The definitions, background, and literature related to the problem of control of flexible structures are described in Chapter 1. It also includes flow charts to describe the traditional centralized suboptimal LQ design and a novel decentralized suboptimal LQ design for the control of flexible structures.

In Chapter 2, the decentralized control design summarized in Fig. 1.3 is formulated. First, substructuring decomposition is defined for a general linear time-invariant system described in a first-order form. Then, it is shown that substructuring decomposition is a natural decomposition for structural dynamics systems. Based on the substructuring decomposition, a Substructural Controller Synthesis method is derived for the control design of flexible structures. Two plane truss examples are used to study the performance of an SCS controller.

In Chapter 3, some model reduction methods frequently used for structural dynamics systems are briefly reviewed. The methods reviewed are: modal truncation, balanced reduction, balanced gain method, Krylov model reduction, and mixed-mode method.

In Chapter 4, an efficient controller reduction algorithm is developed. The reduced-order controller is called an *Equivalent Impulse Response Energy Controller* (EIREC) because it has the same impulse response energy as the full-order controller. The proposed controller reduction method is, in fact, a model-order reduction method applied to a controller. It is shown that the EIREC controller has interesting and useful properties, such as moment-matching, min-

inality, and stability. Efficacy of the proposed controller reduction is validated by two examples. Comparison of computational effort with existing controller reduction methods is also made.

Finally, in Chapter 5, a number of conclusions are drawn. Recommendations and future research directions are also addressed.

Chapter 2

SUBSTRUCTURING DECOMPOSITION AND CONTROLLER SYNTHESIS

Although many decentralized control methods have been developed for general linear systems, the application of decentralized control to flexible structures is still in its infancy. Most of the existing decentralized control methods for flexible structures either adopt or extend the concepts and methodology developed for general linear systems. In Ref. [43], Young applies the overlapping decomposition method, which was developed by Ikeda and Šiljak for large scale systems [18], to the control design for structures. In order for the overlapping decomposition method to be applied effectively, Young developed an approximate finite element model for the structure resulting in a first-order equation with system matrices in block tri-diagonal form. Later, in Ref. [44], Young combined the well-developed Component Mode Synthesis (CMS) method, for which Ref. [7] has an extensive review, with the overlapping decomposition concept to develop a Controlled Component Synthesis (CCS) method. The finite element models for the components are produced by an approach, called Isolated Boundary Loading, which is based on the boundary stiffness and inertia loading process of Benfield and Hrudá [3]. The controller design is carried out at the component level. Then the large complex structure is synthesized from the controlled components. The idea behind the CCS approach is the same as that behind the CMS method. However, the way the structure is de-

composed is not the same. Recently, in an attempt to simplify the decentralized control design for structures, Yousuff extended the concept of inclusion principle, which was developed along with the overlapping decomposition method by Ikeda et.al.[19], to systems described in matrix second-order form [48]. The substructural model in Yousuff's work is an expanded component, i.e., the original boundary of the component is expanded into the adjacent component, which is similar to the substructure used in Young's CCS method. The expanded component is a result of overlapping decomposition.

In this chapter, a decentralized control design process called *Substructural Controller Synthesis* (SCS) is proposed. First, a natural decomposition, called substructuring decomposition, of structural dynamics systems is defined. It is well known that for dynamics equations described in matrix second-order form, the system matrices of the whole structure can be assembled from the system matrices of substructures. Since the optimal control design is based on the first-order equations, the substructuring decomposition method is formulated in first-order form. It is shown that for dynamics equations in matrix first-order form, it is still true that the system matrices of the whole structure can be assembled from the system matrices of substructures. Based on substructuring decomposition of the structure, control design can be carried out substructure by substructure. For each substructure, a subcontroller is designed by an optimal control design method. Then, the global controller, which is to be used to control the whole structure, is synthesized from the subcontrollers by using the same assembling scheme as that employed for structure matrices. The final control implementation is centralized, which means the final controller for implementation is a system controller. However, the control

design is decentralized, because each subcontroller is designed independently.

The substructure used in the Substructural Controller Synthesis method is a natural component, i.e., not an expanded component like that in Young's method. One advantage of using natural components is that SCS can be effectively incorporated with the Component Mode Synthesis method to design controllers for large scale structures. The substructures can be modelled by a CMS method and then assembled together to form an approximate model for the whole structure. The subcontrollers can be designed based on the CMS substructures and can then be assembled together to form a global controller for the whole structure. Another attractive feature of the SCS controller is that it can be updated economically if part of the structure changes. Since the global controller is synthesized from subcontrollers, if one substructure has a configuration or system parameter change, the only subcontroller which needs to be redesigned is the one associated with that substructure. Therefore, the SCS controller is, in fact, an adaptable controller for structures with varying configuration and/or with varying mass and stiffness properties.

The organization of this chapter is as follows. In Section 2.1, substructuring decomposition is defined for a general linear time-invariant system described by a first-order equation. It is shown that all linear systems have substructuring decompositions, although there might not be an appropriate physical interpretation for such decompositions. In Section 2.2, a substructuring decomposition for structural dynamics systems is developed. Then, based on the substructuring decomposition, a Substructural Controller Synthesis method is formulated in Section 2.3. An LQGSCS Algorithm for the process of Substructural Controller Synthesis based on the LQG optimal control design method is

established. Finally, in Section 2.4, a plane-truss example is used to illustrate the applicability of the proposed method. The decentralized control design approach for structural control developed in this chapter is summarized by Figure 1.3 in Chapter 1. Part of the material in this chapter is presented in Ref. [39, 38].

2.1 Substructuring Decomposition

Consider a linear time-invariant system described by

$$\begin{aligned} S\dot{z} &= Az + Bu \\ y &= Cz \end{aligned} \tag{2.1}$$

where $z \in R^n$ is the state vector, $u \in R^l$ is the input vector, and $y \in R^m$ is the output vector. S , A , B , and C are the system matrices with appropriate dimensions. The difference between the above description and the conventional state-space form of a linear system is the S matrix, which, of course, can be eliminated if the state equation is premultiplied by S^{-1} . There exist some linear systems, for instance, structural dynamics systems, which are easier to analyze if the system is described in the form of Eq. (2.1). Therefore, we consider Eq. (2.1), a more general form for the representation of linear time-invariant systems. The conventional state-space form is a special case of Eq. (2.1) with S equal to the identity matrix.

Next, consider another linear time-invariant system described by

$$\begin{aligned} \tilde{S}\dot{\tilde{z}} &= \tilde{A}\tilde{z} + \tilde{B}u \\ y &= \tilde{C}\tilde{z} \end{aligned} \tag{2.2}$$

with the system matrices in the following block diagonal form

$$\tilde{S} = \begin{bmatrix} S_1 & & & \\ & S_2 & & \\ & & \ddots & \\ & & & S_\nu \end{bmatrix} \quad \tilde{A} = \begin{bmatrix} A_1 & & & \\ & A_2 & & \\ & & \ddots & \\ & & & A_\nu \end{bmatrix}$$

$$\tilde{B} = \begin{bmatrix} B_1 & & & \\ & B_2 & & \\ & & \ddots & \\ & & & B_\nu \end{bmatrix} \quad \tilde{C} = \begin{bmatrix} C_1 & & & \\ & C_2 & & \\ & & \ddots & \\ & & & C_\nu \end{bmatrix}$$

and

$$\tilde{z} = \begin{Bmatrix} z_1 \\ z_2 \\ \vdots \\ z_\nu \end{Bmatrix} \quad u = \begin{Bmatrix} u_1 \\ u_2 \\ \vdots \\ u_\nu \end{Bmatrix} \quad y = \begin{Bmatrix} y_1 \\ y_2 \\ \vdots \\ y_\nu \end{Bmatrix}$$

The dimensions of the variables are $z_i \in R^{n_i}$, $u_i \in R^{l_i}$, and $y_i \in R^{m_i}$. It is assumed that system (2.1) and system (2.2) have the same set of inputs ($\sum_{i=1}^{\nu} l_i = l$) and the same set of outputs ($\sum_{i=1}^{\nu} m_i = m$). Therefore, it is appropriate to use u and y in Eq. (2.2) as well as in Eq. (2.1). Because of the block diagonal form of the system matrices, system (2.2) is, in fact, a collection of ν decoupled subsystems

$$\begin{aligned} S_i \dot{z}_i &= A_i z_i + B_i u_i \\ y_i &= C_i z_i \end{aligned} \quad i = 1, 2, \dots, \nu \quad (2.3)$$

Now let us define a substructuring decomposition. System (6.2) is said to be a *substructuring decomposition* of system (2.1) if there exists a *coupling matrix* \tilde{T} such that the following relationships hold

$$S = \tilde{T}^T \tilde{S} \tilde{T} \quad A = \tilde{T}^T \tilde{A} \tilde{T} \quad B = \tilde{T}^T \tilde{B} \quad C = \tilde{C} \tilde{T} \quad (2.4)$$

and if the states of the two systems can be related by

$$\tilde{z} = \tilde{T}z \quad (2.5)$$

The above relationships merely state that the system matrices of system (2.1) are assemblages of the system matrices of the subsystems in Eq. (2.3). Therefore, system (2.1) will be referred to as the *assembled system* and system (2.2) will be referred to as the *unassembled system*.

All multi-input multi-output systems are, in fact, substructurally decomposable. For instance,

$$\begin{aligned} \begin{bmatrix} \alpha S & 0 \\ 0 & \beta S \end{bmatrix} \begin{Bmatrix} \dot{z}_1 \\ \dot{z}_2 \end{Bmatrix} &= \begin{bmatrix} \alpha A & 0 \\ 0 & \beta A \end{bmatrix} \begin{Bmatrix} z_1 \\ z_2 \end{Bmatrix} + \begin{bmatrix} B_1 & 0 \\ 0 & B_2 \end{bmatrix} \begin{Bmatrix} u_1 \\ u_2 \end{Bmatrix} \\ y = \begin{Bmatrix} y_1 \\ y_2 \end{Bmatrix} &= \begin{bmatrix} C_1 & 0 \\ 0 & C_2 \end{bmatrix} \begin{Bmatrix} z_1 \\ z_2 \end{Bmatrix} \end{aligned}$$

is a substructuring decomposition of system (2.1) for all $\alpha + \beta = 1$ if $[B_1 \ B_2] = B$, $[C_1^T \ C_2^T] = C^T$. The coupling matrix is $\tilde{T} = [I_n \ I_n]^T$.

As another example, consider the system

$$\begin{aligned} \begin{bmatrix} S_{11} & S_{12} & 0 \\ S_{21} & S_{22} & S_{23} \\ 0 & S_{32} & S_{33} \end{bmatrix} \begin{Bmatrix} \dot{z}_1 \\ \dot{z}_2 \\ \dot{z}_3 \end{Bmatrix} &= \begin{bmatrix} A_{11} & A_{12} & 0 \\ A_{21} & A_{22} & A_{23} \\ 0 & A_{32} & A_{33} \end{bmatrix} \begin{Bmatrix} z_1 \\ z_2 \\ z_3 \end{Bmatrix} \\ &+ \begin{bmatrix} B_{11} & 0 \\ B_{21} & B_{22} \\ 0 & B_{32} \end{bmatrix} \begin{Bmatrix} u_1 \\ u_2 \end{Bmatrix} \quad (2.6) \\ y = \begin{Bmatrix} y_1 \\ y_2 \end{Bmatrix} &= \begin{bmatrix} C_{11} & C_{12} & 0 \\ 0 & C_{22} & C_{23} \end{bmatrix} \begin{Bmatrix} z_1 \\ z_2 \\ z_3 \end{Bmatrix} \end{aligned}$$

which has block tri-diagonal system matrices. It can be shown that the above

system is an assemblage of the following two subsystems

$$\begin{bmatrix} S_{11} & S_{12} \\ S_{21} & \alpha S_{22} \end{bmatrix} \begin{Bmatrix} \dot{z}_1 \\ \dot{z}_2 \end{Bmatrix} = \begin{bmatrix} A_{11} & A_{12} \\ A_{21} & \alpha A_{22} \end{bmatrix} \begin{Bmatrix} z_1 \\ z_2 \end{Bmatrix} + \begin{bmatrix} B_{11} \\ B_{21} \end{bmatrix} u_1 \quad (2.7)$$

$$y_1 = [C_{11} \ C_{12}] \begin{Bmatrix} z_1 \\ z_2 \end{Bmatrix}$$

$$\begin{bmatrix} \beta S_{22} & S_{23} \\ S_{32} & S_{33} \end{bmatrix} \begin{Bmatrix} \dot{z}_2 \\ \dot{z}_3 \end{Bmatrix} = \begin{bmatrix} \beta A_{22} & A_{23} \\ A_{32} & A_{33} \end{bmatrix} \begin{Bmatrix} z_2 \\ z_3 \end{Bmatrix} + \begin{bmatrix} B_{22} \\ B_{32} \end{bmatrix} u_2 \quad (2.8)$$

$$y_2 = [C_{22} \ C_{23}] \begin{Bmatrix} z_2 \\ z_3 \end{Bmatrix}$$

with the coupling matrix being

$$\tilde{T} = \begin{bmatrix} I & 0 & 0 \\ 0 & I & 0 \\ 0 & I & 0 \\ 0 & 0 & I \end{bmatrix}$$

and with the condition that $\alpha + \beta = 1$. It is seen that z_2 serves as the *interface state* between the two subsystems.

For many real-world systems, there might not be a physical interpretation for the above substructuring decomposition, although mathematically it can always be done. However, there do exist some systems which, by nature, provide a strong physical motivation for such a substructuring decomposition. Structural dynamics systems are the ones that interest us at this point.

2.2 Substructuring Decomposition of Structural Dynamics Systems

In this section, the substructuring decomposition of a structural dynamics system is formulated. Without loss of generality, we will consider a structure composed of two substructures which have a common interface, as shown in

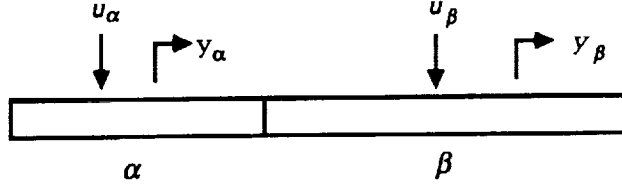


Figure 2.1: Two-component structure

Figure 2.1. It is assumed that the control inputs and the measurement outputs are localized. In the present context, “localized control inputs” means that the actuators are distributed such that u_α is applied to the α -substructure only and u_β is applied to the β -substructure only. “Localized measurements” means that y_α measures only the response of the α -substructure and y_β measures only the response of the β -substructure.

Let the equations of motion of the two substructures be represented by

$$\begin{aligned} M_i \ddot{x}_i + D_i \dot{x}_i + K_i x_i &= P_i u_i \\ y_i &= V_i x_i + W_i \dot{x}_i \end{aligned} \quad i = \alpha, \beta \quad (2.9)$$

It is noted here that the above dynamics equations for the substructures do not have to be exact (full-order) models. They can be approximate (reduced-order) models obtained by any model reduction method, say a Component Mode Synthesis method [7]. The dynamics of the the assembled structure (the structure as a whole) is described by

$$\begin{aligned} M \ddot{x} + D \dot{x} + K x &= P u \\ y &= V x + W \dot{x} \end{aligned} \quad (2.10)$$

Since the two substructures have a common interface and are parts of the assembled structure, the displacement vectors of the substructures and the

displacement vector of the assembled structure are related. There exists a coupling matrix T which relates x_α , x_β , to x as follows:

$$\begin{Bmatrix} x_\alpha \\ x_\beta \end{Bmatrix} = Tx = \begin{bmatrix} T_\alpha \\ T_\beta \end{bmatrix} x \quad (2.11)$$

Given the coupling matrix T , it can be shown that the system matrices of the assembled structure and the system matrices of the substructures satisfy the following relations:

$$\begin{aligned} M &= T^T \begin{bmatrix} M_\alpha & 0 \\ 0 & M_\beta \end{bmatrix} T, \quad D = T^T \begin{bmatrix} D_\alpha & 0 \\ 0 & D_\beta \end{bmatrix} T, \quad K = T^T \begin{bmatrix} K_\alpha & 0 \\ 0 & K_\beta \end{bmatrix} T \\ P &= T^T \begin{bmatrix} P_\alpha & 0 \\ 0 & P_\beta \end{bmatrix}, \quad V = \begin{bmatrix} V_\alpha & 0 \\ 0 & V_\beta \end{bmatrix} T, \quad W = \begin{bmatrix} W_\alpha & 0 \\ 0 & W_\beta \end{bmatrix} T \end{aligned} \quad (2.12)$$

The above relationships can be proved by using the method of Lagrange's equation of motion [6]. Therefore, it is an inherent property of structural dynamics systems that the system matrices of the assembled structure can be obtained by assembling the system matrices of the substructures. This property is, in fact, the essence of all "matrix assemblage" methods, e.g., the Finite Element Method and Component Mode Synthesis. The above formulation is based on the matrix second-order equation of motion. For control design purposes, a first-order formulation which leads to a substructuring decomposition of the structural dynamics system is required.

Let us rewrite the equation of motion (2.9) in the following first-order form

$$\begin{aligned} \begin{bmatrix} D_i & M_i \\ M_i & 0 \end{bmatrix} \begin{Bmatrix} \dot{x}_i \\ \ddot{x}_i \end{Bmatrix} &= \begin{bmatrix} -K_i & 0 \\ 0 & M_i \end{bmatrix} \begin{Bmatrix} x_i \\ \dot{x}_i \end{Bmatrix} + \begin{bmatrix} P_i \\ 0 \end{bmatrix} u_i \\ (S_i) \quad (\dot{z}_i) \quad (A_i) \quad (z_i) \quad (B_i) \quad & i = \alpha, \beta \quad (2.13) \end{aligned}$$

$$y_i = \begin{bmatrix} V_i & W_i \end{bmatrix} \begin{Bmatrix} x_i \\ \dot{x}_i \end{Bmatrix}$$

$$(C_i) \quad (z_i)$$

where the symbol under each matrix denotes that this equation corresponds to Eq. (2.3). Similarly, Eq. (2.10) can be rewritten as

$$\begin{bmatrix} D & M \\ M & 0 \end{bmatrix} \begin{Bmatrix} \dot{x} \\ \ddot{x} \end{Bmatrix} = \begin{bmatrix} -K & 0 \\ 0 & M \end{bmatrix} \begin{Bmatrix} x \\ \dot{x} \end{Bmatrix} + \begin{bmatrix} P \\ 0 \end{bmatrix} u \quad (2.14)$$

(S) (z) (A) (z) (B)

$$y = [V \ W] \begin{Bmatrix} x \\ \dot{x} \end{Bmatrix} \quad (2.14)$$

(C) (z)

where the symbol under each matrix denotes that this equation corresponds to Eq. (2.1).

Combination of the two substructure equations in Eq. (2.13) gives the first-order equation of motion of the unassembled system in the form of Eq. (2.2).

$$\begin{bmatrix} S_\alpha & 0 \\ 0 & S_\beta \end{bmatrix} \begin{Bmatrix} \dot{z}_\alpha \\ \dot{z}_\beta \end{Bmatrix} = \begin{bmatrix} A_\alpha & 0 \\ 0 & A_\beta \end{bmatrix} \begin{Bmatrix} z_\alpha \\ z_\beta \end{Bmatrix} + \begin{bmatrix} B_\alpha & 0 \\ 0 & B_\beta \end{bmatrix} \begin{Bmatrix} u_\alpha \\ u_\beta \end{Bmatrix} \quad (2.15)$$

(\tilde{S}) (\tilde{z}) (\tilde{A}) (\tilde{z}) \tilde{B}

$$y \equiv \begin{Bmatrix} y_\alpha \\ y_\beta \end{Bmatrix} = \begin{bmatrix} C_\alpha & 0 \\ 0 & C_\beta \end{bmatrix} \begin{Bmatrix} z_\alpha \\ z_\beta \end{Bmatrix} \quad (2.15)$$

(\tilde{C})

It can be shown that the unassembled system (2.15) is a substructuring decomposition of the assembled system (2.14). That is, (S, A, B, C) in Eq. (2.14) and $(\tilde{S}, \tilde{A}, \tilde{B}, \tilde{C})$ in Eq. (2.15) satisfy the relations in Eq. (2.4). The state vector of the assembled structure and the state vectors of the substructures are related by a coupling matrix \tilde{T} as

$$\begin{Bmatrix} x_\alpha \\ \dot{x}_\alpha \\ x_\beta \\ \dot{x}_\beta \end{Bmatrix} = \begin{bmatrix} T_\alpha & 0 \\ 0 & T_\alpha \\ T_\beta & 0 \\ 0 & T_\beta \end{bmatrix} \begin{Bmatrix} x \\ \dot{x} \end{Bmatrix} \quad (2.16)$$

(\tilde{z}) (\tilde{T}) (z)

2.2.1 Coupling Matrix

Physically, the coupling matrix \tilde{T} that relates the state vectors of the substructures and the state vector of the assembled structure simply describes the compatibility conditions which must be imposed on the interface degrees of freedom. Let x_i represent the physical displacement coordinates of substructures i , and let the physical coordinates of the substructures in Figure 2.1 be partitioned into two sets: Interior coordinates (I-set) and Boundary coordinates (B-set), as shown in Figure 2.2.

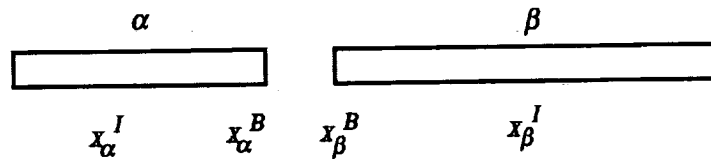


Figure 2.2: Interior Coordinates and Boundary Coordinates

The displacement compatibility condition requires that $x_\alpha^B = x_\beta^B$. If the displacement vector of the assembled structure is represented by

$$x = \begin{Bmatrix} x_\alpha^I \\ x^B \\ x_\beta^I \end{Bmatrix}$$

where x^B is the vector of interface degrees of freedom, then the three displacement vectors x_α , x_β , and x are related by

$$\begin{Bmatrix} x_\alpha \\ x_\beta \end{Bmatrix} \equiv \begin{Bmatrix} x_\alpha^I \\ x_\alpha^B \\ x_\beta^I \\ x_\beta^B \end{Bmatrix} = \begin{bmatrix} I & 0 & 0 \\ 0 & I & 0 \\ 0 & 0 & I \\ 0 & I & 0 \end{bmatrix} \begin{Bmatrix} x_\alpha^I \\ x^B \\ x_\beta^I \end{Bmatrix} \equiv \begin{bmatrix} T_\alpha \\ T_\beta \end{bmatrix} x \quad (2.17)$$

with

$$T_\alpha = \begin{bmatrix} I & 0 & 0 \\ 0 & I & 0 \end{bmatrix}, \quad T_\beta = \begin{bmatrix} 0 & 0 & I \\ 0 & I & 0 \end{bmatrix}$$

The velocity compatibility condition requires that $\dot{x}_\alpha^B = \dot{x}_\beta^B$, which leads to

$$\dot{x}_\alpha = T_\alpha \dot{x}, \quad \dot{x}_\beta = T_\beta \dot{x} \quad (2.18)$$

Combination of Eqs. (2.17) and (2.18) shows that the state vectors of the substructures and the state vector of the assembled structure are related by a coupling matrix \tilde{T} as in Eq. (2.16).

In general applications, the x_α , x_β , and x vectors do not have to be described in physical coordinates. For instance, in the application of Component Mode Synthesis (CMS) method, dynamics of the substructures are represented by a set of static modes called component modes. In this case, the column vectors in the T_α and T_β matrices would be the representation of those component modes. Even though the displacement vectors are in generalized coordinates instead of physical coordinates, the compatibility condition can still be described by Eq. (2.16).

2.3 Substructural Controller Synthesis

The derivation in this section is based on the two-component structure in Section 2.2. The system is assumed to be subject to disturbance and observation noise. Therefore, the formulation is a stochastic case. At the end of this section, a control design procedure called LQGSCS Algorithm is used to summarize the Substructural Controller Synthesis scheme. The method proposed can also be applied to a deterministic problem with only slight modification.

First, let the dynamics of the *assembled structure* (the structure as a whole) in Figure 2.1 be described by

$$\begin{aligned} S\dot{z} &= Az + Bu + N\varpi \\ y &= Cz + v \end{aligned} \quad (2.19)$$

where input disturbance ϖ and output disturbance v are assumed to be uncorrelated zero-mean white noise processes. For a linear stochastic system with incomplete measurement, optimal state feedback control design requires a state estimator called Kalman filter to reconstruct the states for feedback. The state estimator of a plant described by Eq. (2.19) has the form

$$S\dot{q} = Aq + Bu + F^o(y - Cq) \quad (2.20)$$

where F^o is determined by solving a Riccati equation. If a feedback control scheme $u = G^o q$ is incorporated with Eq. (2.20) to control the plant, the estimator becomes a controller in the form

$$\begin{aligned} S\dot{q} &= (A + BG^o - F^o C)q + F^o y \\ u &= G^o q \end{aligned} \quad (2.21)$$

where superscript o denotes optimal design. The feedback gain matrix G^o is determined by minimizing a performance index

$$J = \lim_{t \rightarrow \infty} \frac{1}{2} E[z^T Q z + u^T R u] \quad (2.22)$$

For structural control problem, the weighting matrix Q is usually chosen to be

$$Q = \begin{bmatrix} K & 0 \\ 0 & M \end{bmatrix} \quad (2.23)$$

such that the first term in the performance index represents the total energy of the structure

$$\frac{1}{2} z^T Q z = \frac{1}{2} (x^T K x + \dot{x}^T M \dot{x})$$

For a purpose to be clarified later, the control weighting matrix R is chosen to be

$$R = \begin{bmatrix} R_\alpha & 0 \\ 0 & R_\beta \end{bmatrix} \quad (2.24)$$

The above centralized design scheme for a linear optimal compensator is well known. Now, a decentralized controller synthesis method, called the *Substructural Controller Synthesis* (SCS) method, will be formulated. The development of the Substructural Controller Synthesis method is stimulated by the substructuring decomposition and the Component Mode Synthesis method. The plant to be controlled is first decomposed into several substructures by the substructuring decomposition method. Then, for each substructure a subcontroller is designed by using linear quadratic optimal control theory. The collection of all the subcontrollers is considered as the substructuring decomposition of a global controller which is to be employed to control the whole plant. Finally, a coupling scheme the same as that employed for the plant is used to synthesize the subcontrollers.

Let the dynamic equations of the two substructures in Figure 2.1 be represented by

$$\begin{aligned} S_i \dot{z}_i &= A_i z_i + B_i u_i + N_i \varpi_i \\ y_i &= C_i z_i + v_i \end{aligned} \quad i = \alpha, \beta \quad (2.25)$$

With each substructure is associated a performance index

$$J_i = \lim_{t \rightarrow \infty} \frac{1}{2} E[z_i^T Q_i z_i + u_i^T R_i u_i] \quad i = \alpha, \beta \quad (2.26)$$

with

$$Q_\alpha = \begin{bmatrix} K_\alpha & 0 \\ 0 & M_\alpha \end{bmatrix}, \quad Q_\beta = \begin{bmatrix} K_\beta & 0 \\ 0 & M_\beta \end{bmatrix} \quad (2.27)$$

All the substructures are assumed to be completely controllable and observable with the given performance weightings and the noise distribution. For each substructure, an LQG design can be carried out to obtain an optimal controller in the form

$$\begin{aligned} S_i \dot{q}_i &= (A_i + B_i G_i^o - F_i^o C_i) q_i + F_i^o y_i \\ u_i &= G_i^o q_i \end{aligned} \quad i = \alpha, \beta \quad (2.28)$$

The above optimal controllers are designed for the substructures. Therefore, they are called *subcontrollers*. Superscript o in Eq. (2.28) denotes that each subcontroller is optimal to its corresponding substructure.

In order to show more clearly how the concept of substructuring decomposition is employed to assemble the subcontrollers, the collection of the two substructures is now considered as a single system, the *unassembled system*. The dynamic equation of the unassembled system can be written in a compact form

$$\begin{aligned} \tilde{S} \dot{\tilde{z}} &= \tilde{A} \tilde{z} + \tilde{B} u + \tilde{N} \varpi \\ y &= \tilde{C} \tilde{z} + v \end{aligned} \quad (2.29)$$

with

$$\begin{aligned} \tilde{S} &= \begin{bmatrix} S_\alpha & 0 \\ 0 & S_\beta \end{bmatrix}, & \tilde{A} &= \begin{bmatrix} A_\alpha & 0 \\ 0 & A_\beta \end{bmatrix}, & \tilde{B} &= \begin{bmatrix} B_\alpha & 0 \\ 0 & B_\beta \end{bmatrix} \\ \tilde{N} &= \begin{bmatrix} N_\alpha & 0 \\ 0 & N_\beta \end{bmatrix}, & \tilde{C} &= \begin{bmatrix} C_\alpha & 0 \\ 0 & C_\beta \end{bmatrix} \end{aligned}$$

and

$$\tilde{z} = \begin{Bmatrix} z_\alpha \\ z_\beta \end{Bmatrix}, \quad u \equiv \begin{Bmatrix} u_\alpha \\ u_\beta \end{Bmatrix}, \quad y \equiv \begin{Bmatrix} y_\alpha \\ y_\beta \end{Bmatrix}, \quad \varpi \equiv \begin{Bmatrix} \varpi_\alpha \\ \varpi_\beta \end{Bmatrix}, \quad v \equiv \begin{Bmatrix} v_\alpha \\ v_\beta \end{Bmatrix}$$

The distribution of the input noise is assumed to be substructurally decomposable, i.e., $N = \tilde{T}^T \tilde{N}$, so that system (2.29) is a substructuring decomposition

of system (2.19). This assumption is not a serious restriction since, in general, distribution and intensity of the noise are uncertain quantities. Therefore, for design purpose, a reasonable assumption can be made by control engineers.

The performance index of the unassembled system is simply the summation of the performance indexes of the substructures

$$\tilde{J} = J_\alpha + J_\beta = \lim_{t \rightarrow \infty} \frac{1}{2} E[\tilde{z}^T \tilde{Q} \tilde{z} + u^T \tilde{R} u] \quad (2.30)$$

with

$$\tilde{Q} = \begin{bmatrix} Q_\alpha & 0 \\ 0 & Q_\beta \end{bmatrix}, \quad \tilde{R} = \begin{bmatrix} R_\alpha & 0 \\ 0 & R_\beta \end{bmatrix}$$

It is noted that \tilde{R} is the same as the control weighting R in the performance index of the assembled system (Eq. (2.24)). The \tilde{Q} matrix and the state weighting matrix Q in the performance index of the assembled system are related as $Q = \tilde{T}^T \tilde{Q} \tilde{T}$. This relationship can be proved by using the relations among the stiffness and mass matrices of the substructures and the stiffness and mass matrices of the assembled structure as depicted in Eq. (2.12).

$$\begin{aligned} \tilde{T}^T \tilde{Q} \tilde{T} &= \begin{bmatrix} T_\alpha^T & 0 & T_\beta^T & 0 \\ 0 & T_\alpha^T & 0 & T_\beta^T \end{bmatrix} \begin{bmatrix} K_\alpha & 0 & 0 & 0 \\ 0 & M_\alpha & 0 & 0 \\ 0 & 0 & K_\beta & 0 \\ 0 & 0 & 0 & M_\beta \end{bmatrix} \begin{bmatrix} T_\alpha & 0 \\ 0 & T_\alpha \\ T_\beta & 0 \\ 0 & T_\beta \end{bmatrix} \\ &= \begin{bmatrix} T_\alpha^T K_\alpha T_\alpha + T_\beta^T K_\beta T_\beta & 0 \\ 0 & T_\alpha^T M_\alpha T_\alpha + T_\beta^T M_\beta T_\beta \end{bmatrix} \\ &= \begin{bmatrix} K & 0 \\ 0 & M \end{bmatrix} \equiv Q \end{aligned}$$

By using the relations $\tilde{z} = \tilde{T} z$, $Q = \tilde{T}^T \tilde{Q} \tilde{T}$, and $\tilde{R} = R$, the performance index of the unassembled system can be rewritten as

$$\begin{aligned} \tilde{J} &= \lim_{t \rightarrow \infty} \frac{1}{2} E[z^T \tilde{T}^T \tilde{Q} \tilde{T} z + u^T \tilde{R} u] \\ &= \lim_{t \rightarrow \infty} \frac{1}{2} E[z^T Q z + u^T R u] \end{aligned}$$

which is equal to the performance index of the assembled system. This equivalence shows that with the weighting matrices Q and R chosen as in Eqs. (2.23) and (2.24), the performance index is substructurally decomposable. However, this is only a symbolic equivalence. Because the compatibility condition $\tilde{z} = \tilde{T}z$ is not enforced in the design of the subcontrollers, the values of \tilde{J} and J are, in general, not equal.

The controller for the unassembled system is the collection of the two subcontrollers in Eq. (2.28), which can be rewritten in a more compact form as

$$\begin{aligned}\tilde{S}\dot{\tilde{q}} &= (\tilde{A} + \tilde{B}\tilde{G}^\circ - \tilde{F}^\circ\tilde{C})\tilde{q} + \tilde{F}^\circ y \\ u &= \tilde{G}^\circ\tilde{q}\end{aligned}\quad (2.31)$$

with

$$\tilde{G}^\circ = \begin{bmatrix} G_\alpha^\circ & 0 \\ 0 & G_\beta^\circ \end{bmatrix}, \quad \tilde{F}^\circ = \begin{bmatrix} F_\alpha^\circ & 0 \\ 0 & F_\beta^\circ \end{bmatrix}\quad (2.32)$$

It needs no proof that the unassembled controller, Eq. (2.31), is optimal for the unassembled structure, Eq. (2.29), because the unassembled system matrices are decoupled and each subcontroller is optimal for its corresponding substructure. Combination of Eq. (2.29) and Eq. (2.31) gives the closed-loop equation of the unassembled system

$$\begin{bmatrix} \tilde{S} & 0 \\ 0 & \tilde{S} \end{bmatrix} \begin{Bmatrix} \dot{\tilde{z}} \\ \dot{\tilde{q}} \end{Bmatrix} = \begin{bmatrix} \tilde{A} & \tilde{B}\tilde{G}^\circ \\ \tilde{F}^\circ\tilde{C} & \tilde{A} + \tilde{B}\tilde{G}^\circ - \tilde{F}^\circ\tilde{C} \end{bmatrix} \begin{Bmatrix} \tilde{z} \\ \tilde{q} \end{Bmatrix} + \begin{bmatrix} \tilde{N} & 0 \\ 0 & \tilde{F}^\circ \end{bmatrix} \begin{Bmatrix} \varpi \\ v \end{Bmatrix}\quad (2.33)$$

The last step is to assemble the subcontrollers by using the same coupling scheme as used for assembling the substructures. The assembled controller for the assembled system is represented by

$$\begin{aligned}S\dot{q} &= (A + BG^\circ - F^\circ C)q + F^\circ y \\ u &= G^\circ q\end{aligned}\quad (2.34)$$

with

$$F^\oplus = \tilde{T}^T \tilde{F}^\circ, \quad G^\oplus = \tilde{G}^\circ \tilde{T} \quad (2.35)$$

where superscript \oplus denotes that the controller is not optimal but is considered as suboptimal. The control design matrices F^\oplus and G^\oplus for the assembled structure are obtained by assembling the optimal control design matrices F_i° and G_i° for the substructures by using the coupling matrix \tilde{T} . Under this assembling scheme, it can be shown that the unassembled controller, Eq. (2.31) is a substructuring decomposition of the assembled controller, Eq. (2.34).

If the assembled controller is employed to control the assembled structure, Eq. (2.19), the following closed-loop equation is obtained

$$\begin{bmatrix} S & 0 \\ 0 & S \end{bmatrix} \begin{Bmatrix} \dot{z} \\ \dot{q} \end{Bmatrix} = \begin{bmatrix} A & BG^\oplus \\ F^\oplus C & A + BG^\oplus - F^\oplus C \end{bmatrix} \begin{Bmatrix} z \\ q \end{Bmatrix} + \begin{bmatrix} N & 0 \\ 0 & F^\oplus \end{bmatrix} \begin{Bmatrix} \varpi \\ v \end{Bmatrix} \quad (2.36)$$

The unassembled closed-loop equation, Eq. (2.33) is a substructuring decomposition of the assembled closed-loop equation, Eq. (2.36), under the coupling matrix $\begin{bmatrix} \tilde{T} & 0 \\ 0 & \tilde{T} \end{bmatrix}$. Since the unassembled control system is an optimal design for the unassembled system, the assembled control system can be considered to be suboptimal for the assembled system if it yields a stable design. A suboptimality study similar to the one developed along with the overlapping decomposition method [20] is a future research topic.

The coupling matrix \tilde{T} plays the major role in the above formulation of the Substructural Controller Synthesis method. To have a clearer idea about how the compatibility condition $\tilde{z} = \tilde{T}z$ is involved in the SCS control design, consider the following three optimization problems:

Problem 1:

$$\begin{aligned} \text{Minimize } J &= \int_0^\infty \frac{1}{2}(z^T Q z + u^T R u) dt \\ \text{Subject to } S \dot{z} &= A z + B u \end{aligned}$$

Problem 2:

$$\begin{aligned} \text{Minimize } \tilde{J} &= \int_0^\infty \frac{1}{2}(\tilde{z}^T \tilde{Q} \tilde{z} + u^T \tilde{R} u) dt \\ \text{Subject to } \tilde{S} \dot{\tilde{z}} &= \tilde{A} \tilde{z} + \tilde{B} u \end{aligned}$$

Problem 3:

$$\begin{aligned} \text{Minimize } \tilde{J} &= \int_0^\infty \frac{1}{2}(\tilde{z}^T \tilde{Q} \tilde{z} + u^T \tilde{R} u) dt \\ \text{Subject to } \begin{cases} \tilde{S} \dot{\tilde{z}} = \tilde{A} \tilde{z} + \tilde{B} u \\ \tilde{z} = \tilde{T} z \end{cases} \end{aligned}$$

Problem 1 is the optimal state feedback control problem for the assembled system. Problem 2 is the optimal state feedback control problem for the unassembled system. The difference between Problem 3 and Problem 2 is that Problem 3 has one more constraint condition $\tilde{z} = \tilde{T}z$. Hence, Problem 3 is the optimal state feedback control problem for the unassembled system with the compatibility condition enforced on the boundary degrees of freedom, which means that Problem 3 is, in fact, exactly equivalent to Problem 1. (Also recall that, symbolically, \tilde{J} is equal to J .) In the SCS design, it is Problem 2 instead of Problem 3 that is solved to obtain the subcontrollers. Therefore, in some sense, the SCS design method can be interpreted as simplifying the assembled optimal control design problem (Problem 3) by throwing away some constraints (the compatibility condition). After the optimal control law of Problem 2, $u = \tilde{G}^o \tilde{z}$, is obtained, the compatibility condition is, then, imposed on the feedback law to obtain the global feedback gain matrix G^\oplus .

$$u = \tilde{G}^o \tilde{z} = \tilde{G}^o(\tilde{T}z) = (\tilde{G}^o \tilde{T})z = G^\oplus z$$

The above interpretation of the SCS method may give some helpful direction to the suboptimality study in the future.

Closed-loop stability of a Substructural Controller Synthesis design is, in general, not guaranteed. This is the same disadvantage that most indirect control design methods have. Indirect control design means that the controller is not designed based upon the exact full-order structure but is based on an approximate model or reduced-order model. From the form of Eq. (2.36), it is seen that the separation principle is applicable to the SCS control system. The closed-loop poles of the assembled system are the union of the regulator poles (eigenvalues of $S^{-1}(A + BG^*)$) and the observer poles (eigenvalues of $S^{-1}(A - F^*C)$). Therefore, stability of the assembled closed-loop system can be checked by examining the locations of these two sets of eigenvalues.

One advantage of using Substructural Controller Synthesis to design a controller is that an SCS controller is highly adaptable. For a structure with varying configuration or varying mass and stiffness properties, like some space structures, the Substructural Controller Synthesis method may be especially efficient. The SCS controller can be updated economically by simply carrying out redesign of subcontrollers associated with those substructures that have changed. On the other hand, for a controller based on a centralized design scheme, a slight change of the structure may require a full-scale redesign. This favorable decentralized feature of the Substructural Controller Synthesis method is similar to that of the Component Mode Synthesis method in the application to model modification. It is emphasized again that the dynamic models of the substructures do not have to be exact models. They can be approximate (reduced-order) models obtained by a Component Mode Synthesis

method or any existing model reduction method, e.g., the methods reviewed in Chapter 3. If the subcontroller is designed based on an approximate substructural model, then it is not optimal to the substructure. Nevertheless, the aforementioned decentralized feature is still true.

The following algorithm summarizes the Substructural Controller Synthesis scheme, with the LQG optimal control theory as the design basis.

Algorithm 2.1 (LQGSCS Algorithm)

- (1.) *Set up the LQG problem for the assembled structure.*

$$\begin{aligned} S\dot{z} &= Az + Bu + N\varpi \\ y &= Cz + v \\ \text{Minimize } J &= \lim_{t \rightarrow \infty} E[z^T Qz + u^T Ru] \end{aligned}$$

- (2.) *Construct a substructuring decomposition of the LQG problem in (1).*

$$\begin{aligned} \tilde{S}\dot{\tilde{z}} &= \tilde{A}\tilde{z} + \tilde{B}u + \tilde{N}\varpi \\ y &= \tilde{C}\tilde{z} + v \\ \text{Minimize } \tilde{J} &= \lim_{t \rightarrow \infty} E[\tilde{z}^T \tilde{Q}\tilde{z} + u^T Ru] \end{aligned}$$

where

$$\begin{aligned} S &= \tilde{T}^T \tilde{S} \tilde{T} & A &= \tilde{T}^T \tilde{A} \tilde{T} & B &= \tilde{T}^T \tilde{B} & C &= \tilde{C} \tilde{T} \\ N &= \tilde{T}^T \tilde{N}, & Q &= \tilde{T}^T \tilde{Q} \tilde{T} & \tilde{z} &= \tilde{T} z & \tilde{J} &= J \end{aligned}$$

Due to the decoupling of the substructuring decomposition, the unassembled LQG problem can be split into ν substructure-level LQG problems:

$$\begin{aligned} S_i \dot{z}_i &= A_i z_i + B_i u_i + N_i \varpi_i \\ y_i &= C_i z_i + v_i & i &= 1, 2, \dots, \nu \\ \text{Minimize } J_i &= \lim_{t \rightarrow \infty} E[z_i^T Q_i z_i + u_i^T R_i u_i] \end{aligned}$$

- (3.) Carry out an LQG design to obtain an optimal subcontroller for each substructure in (2).

$$\begin{aligned} S_i \dot{q}_i &= (A_i + B_i G_i^o - F_i^o C_i) q_i + F_i^o y_i \\ u_i &= G_i^o q_i \end{aligned} \quad i = 1, 2, \dots, \nu$$

where F_i^o and G_i^o are obtained by solving Riccati equations.

- (4.) By using the coupling matrix \tilde{T} , assemble all the subcontrollers to obtain a global controller.

$$\begin{aligned} S \dot{q} &= (A + B G^{\oplus} - F^{\oplus} C) q + F^{\oplus} y \\ u &= G^{\oplus} q \end{aligned}$$

where $G^{\oplus} = \tilde{G}^o \tilde{T}$, $F^{\oplus} = \tilde{T}^T \tilde{F}^o$ with $\tilde{G}^o = \text{diag}[G_i^o]$ and $\tilde{F}^o = \text{diag}[F_i^o]$.

- (5.) Calculate the eigenvalues of $S^{-1}(A + B G^{\oplus})$ and $S^{-1}(A - F^{\oplus} C)$ to check closed-loop stability.

A similar algorithm can be developed for the deterministic case. The only difference between the LQRSCS algorithm (for the deterministic case) and the LQGSCS algorithm (for the stochastic case) is that a pole assignment scheme is required to determine the F_i^o matrices in the former case.

2.4 Examples

In this section, two plane truss structure examples are used to demonstrate the applicability of the Substructural Controller Synthesis method. The first example has two identical substructures and almost-colocated sensor and actuator allocations. The second example is a more general case.

2.4.1 Identical Substructures With Almost-Colocated Sensor And Actuator Allocations

The truss structure considered is depicted in Figure 2.3, which consists of six bays and has twenty degrees-of-freedom. Two force actuators and two displacement sensors are allocated symmetrically at f and d , respectively. The actuators are contaminated by disturbances with intensity 10^{-3} . The sensors are contaminated by noises with intensity 10^{-12} . These levels of noise intensities are chosen arbitrarily just for the purpose of example study, and are not justified by the experience of any real case. (In Ref. [45], there is an example with input noise intensity 10^{-4} and output noise intensity 10^{-15} .) All disturbances are assumed to be uncorrelated zero-mean white noise processes. The mass and stiffness matrices for the structure are obtained by the finite element method. The damping matrix is chosen to be 1/1000 of the stiffness matrix. The eigenvalues of the open-loop system have damping ratios ranging from 0.05% to 1.5%. The structure is divided into two substructures as shown in Figure 2.3.

SCS control design has been carried out and compared with the full-order optimal controller for five different cases. Conditions, assumptions, formulations, and results for the five cases studied are summarized in the following.

Case 1: (Two-input and two-output)

For this case, the two substructures are identical due to symmetry. Therefore, only one substructural level control design need be carried out. The other subcontroller can be obtained by using symmetry. The results are shown in Table 2.1 and Figure 2.5, in which R is the weighting of control cost in the

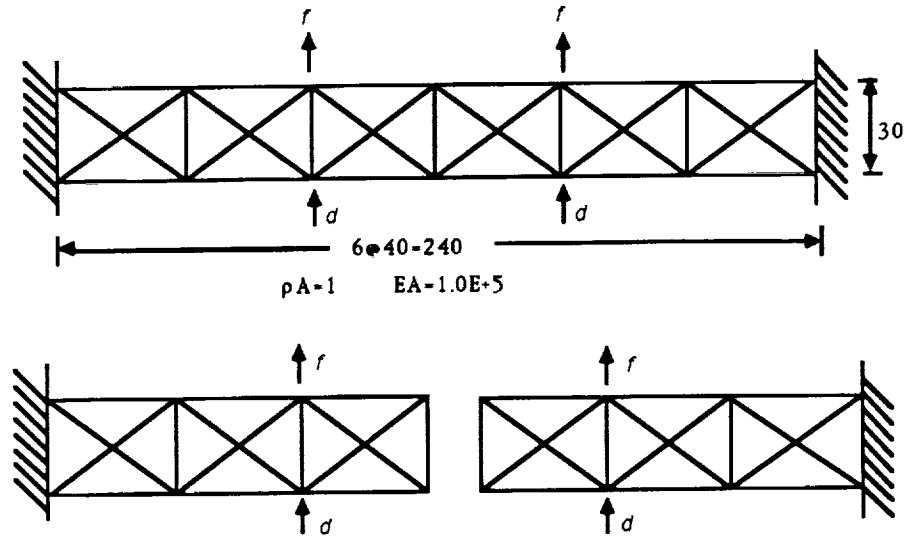


Figure 2.3: Details of the plane truss for the SCS design example (identical substructures and colocated sensor/actuator allocations)

performance index. It is seen that the SCS controller has a near-optimal performance. The performance value of the SCS controller is less than 4% higher than the performance value of the optimal controller. The substructures and subcontrollers for this case are symbolically represented by the following equations.

Left substructure

$$S_1 \dot{z}_1 = A_1 z_1 + B_1 u_1 + B_1 \varpi_1$$

$$y_1 = C_1 z_1 + v_1$$

Left subcontroller

$$S_1 \dot{q}_1 = (A_1 + B_1 G_1^o - F_1^o C_1) q_1 + F_1^o y_1$$

$$u_1 = G_1^o q_1$$

Right substructure

$$S_2 \dot{z}_2 = A_2 z_2 + B_2 u_2 + B_2 \varpi_2$$

$$y_2 = C_2 z_2 + v_2$$

Right subcontroller

$$S_2 \dot{q}_2 = (A_2 + B_2 G_2^o - F_2^o C_2) q_2 + F_2^o y_2$$

$$u_2 = G_2^o q_2$$

Case 2: (Single-input and two-output)

Assume that the actuator on the right substructure has malfunctioned.

In this case, the right substructure is, in fact, not controllable since there is no actuator on it. However, the right sensor is still functioning and can collect information about the state of the right substructure. Therefore, an observer for the right substructure is designed and is called the *generalized subcontroller* for the right substructure, although there is really no control law involved. The design of the left subcontroller is the same as that for Case 1. The global controller is obtained by assembling the right generalized subcontroller and the left subcontroller. Comparisons of the SCS controller and the full-optimal controller for this case are summarized by Table 2.2 and Figure 2.6. Again, it is seen that the SCS controller is near-optimal. The substructures and subcontrollers for this case are symbolically represented by the following equations.

Left substructure

$$S_1 \dot{z}_1 = A_1 z_1 + B_1 u_1 + B_1 \varpi_1$$

$$y_1 = C_1 z_1 + v_1$$

Left subcontroller

$$S_1 \dot{q}_1 = (A_1 + B_1 G_1^o - F_1^o C_1) q_1 + F_1^o y_1$$

$$u_1 = G_1^o q_1$$

Right substructure

$$S_2 \dot{z}_2 = A_2 z_2 + B_2 \varpi_2$$

$$y_2 = C_2 z_2 + v_2$$

Right generalized subcontroller

$$S_2 \dot{q}_2 = (A_2 - F_2^o C_2) q_2 + F_2^o y_2$$

Case 3: (Single-input and single-output)

Assume that both the actuator and sensor on the right substructure have malfunctioned. In this case, the right substructure is neither controllable nor observable. The generalized subcontroller for the right substructure is defined by the state equation that describes the right substructure itself. The results of this case are summarized by Table 2.3 and Figure 2.7, which show that the SCS controller is near-optimal. The substructures and subcontrollers for this

case are symbolically represented by the following equations.

Left substructure

$$S_1 \dot{z}_1 = A_1 z_1 + B_1 u_1 + B_1 \varpi_1$$

$$y_1 = C_1 z_1 + v_1$$

Left subcontroller

$$S_1 \dot{q}_1 = (A_1 + B_1 G_1^o - F_1^o C_1) q_1 + F_1^o y_1$$

$$u_1 = G_1^o q_1$$

Right substructure

$$S_2 \dot{z}_2 = A_2 z_2$$

Right generalized subcontroller

$$S_2 \dot{q}_2 = A_2 q_2$$

Case 4: (Two-input and single-output)

Assume that the right sensor has malfunctioned. In this case, the right substructure is not observable. The generalized subcontroller for the right substructure is defined to be a full-state feedback controller, although there is really no state estimator available. Comparisons of the SCS controller and the full-order optimal controller are summarized by Table 2.4 and Figure 2.8. It is seen that the performance of the SCS controller for this case is not so good as that for the previous three cases. The substructures and subcontrollers for this case are symbolically represented by the following equations.

Left substructure

$$S_1 \dot{z}_1 = A_1 z_1 + B_1 u_1 + B_1 \varpi_1$$

$$y_1 = C_1 z_1 + v_1$$

Left subcontroller

$$S_1 \dot{q}_1 = (A_1 + B_1 G_1^o - F_1^o C_1) q_1 + F_1^o y_1$$

$$u_1 = G_1^o q_1$$

Right substructure

$$S_2 \dot{z}_2 = A_2 z_2 + B_2 u_2 + B_2 \varpi_2$$

Right generalized subcontroller

$$S_2 \dot{q}_2 = (A_2 + B_2 G_2^o) q_2$$

$$u_2 = G_2^o q_2$$

Case 5: (Two-input and single-output, right substructure free of noise)

We suspect that the poor performance of the SCS controller in Case 4 is due to the fact that there is not an observer to filter the noise on the

right substructure. Therefore, as another case for study, we consider the same actuator/sensor configuration as that of Case 4, but assume that the right substructure is free of disturbance. The results are summarized by Table 2.5 and Figure 2.9. As we can see, the SCS controller for this case has a near-optimal performance. The substructures and subcontrollers for this case are symbolically represented by the following equation.

<p>Left substructure</p> $S_1 \dot{z}_1 = A_1 z_1 + B_1 u_1 + B_1 \varpi_1$ $y_1 = C_1 z_1 + v_1$ <p>Left subcontroller</p> $S_1 \dot{q}_1 = (A_1 + B_1 G_1^o - F_1^o C_1) q_1 + F_1^o y_1$ $u_1 = G_1^o q_1$	<p>Right substructure</p> $S_2 \dot{z}_2 = A_2 z_2 + B_2 u_2$ <p>Right generalized subcontroller</p> $S_2 \dot{q}_2 = (A_2 + B_2 G_2^o) q_2$ $u_2 = G_2^o q_2$
---	--

From the results of the above five cases, it is seen that the performance of the SCS controller is, in general, near-optimal. The only case that the SCS controller exhibited a poor performance is Case 4, in which the right substructure is subject to disturbance but has no output measurement as a feedback to filter the noise. A conclusion from the study of Case 4 and Case 5 is that an estimator is required for each substructure subject to noise disturbance in order to obtain a near-optimal SCS controller.

2.4.2 Unsymmetric Case

The second example is a more general case. The structure considered is a sixteen degree-of-freedom plane truss structure as shown in Figure 2.4. The structure is decomposed into two substructures in order to perform the SCS design. There are two sensors located on bar elements denoted by s and two

actuators located on bar elements denoted by *a*. The sensors are strain gauges that can measure the strains in the bar elements. The actuators are load cells that can control the relative displacements of the two ends of the bar elements. No attempt was made to optimize the locations of sensors and actuators. It is assumed that the actuators are contaminated by disturbances with intensity 10^{-3} and the sensors are contaminated by noises with intensity 10^{-9} . The damping matrix is equal to 1/1000 of the stiffness matrix. The corresponding system damping factors range from 0.07% to 1.0%.

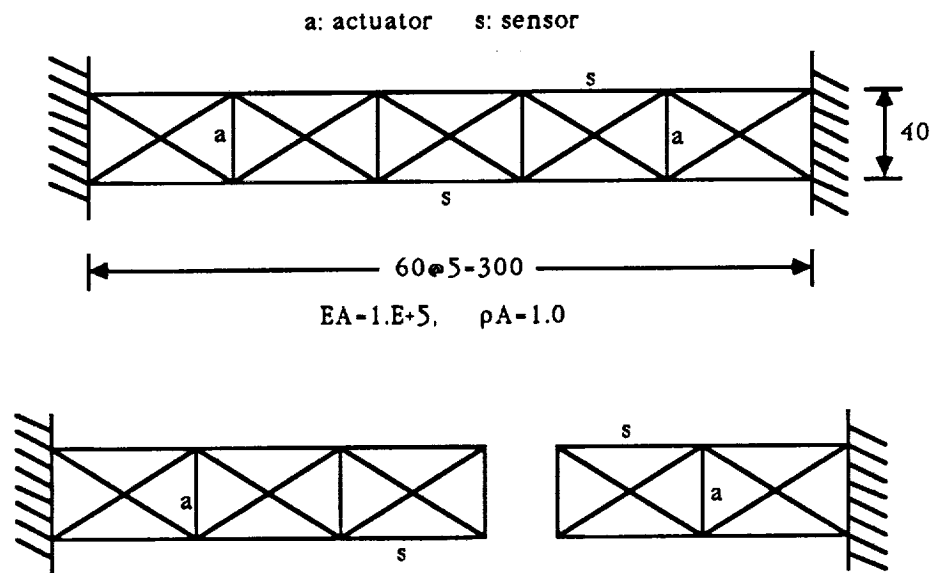


Figure 2.4: Details of the plane truss for the SCS design example (unsymmetric case)

The results are summarized in Table 2.6 and Figure 2.10. It is seen that the performance curve of the SCS controller for this example is not as close to the optimal performance curve as that for the symmetric case in the previous

subsection. However, the performance values in Table 2.6 still show that the SCS controller is near-optimal. It is also noted that for large control bandwidth (small R), the SCS controller tends to deviate further from the optimal one.

Although further examples must be examined before any general conclusions can be reached about the efficiency of the proposed SCS controller design procedure, the results of the above two examples are very encouraging. Examples which apply SCS design to reduced-order substructure models definitely must be considered.

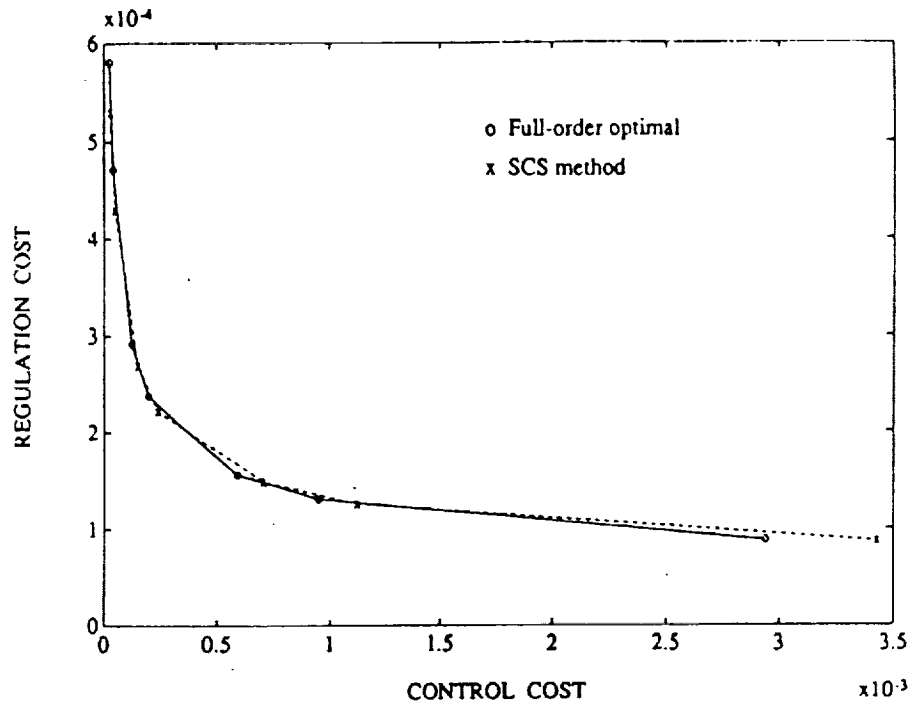


Figure 2.5: Performance plot of Case 1

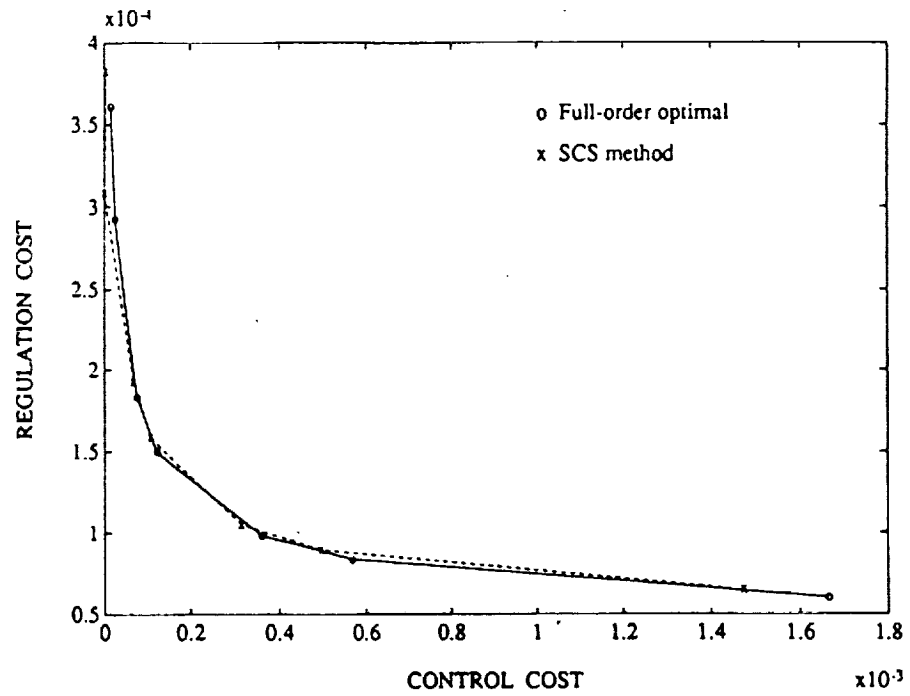


Figure 2.6: Performance plot of Case 2

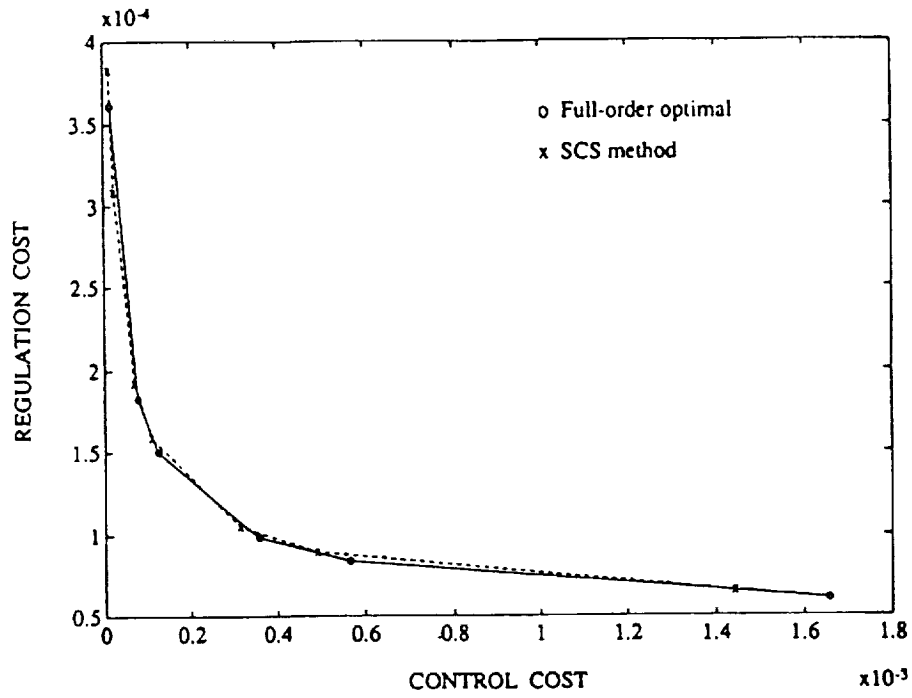


Figure 2.7: Performance plot of Case 3

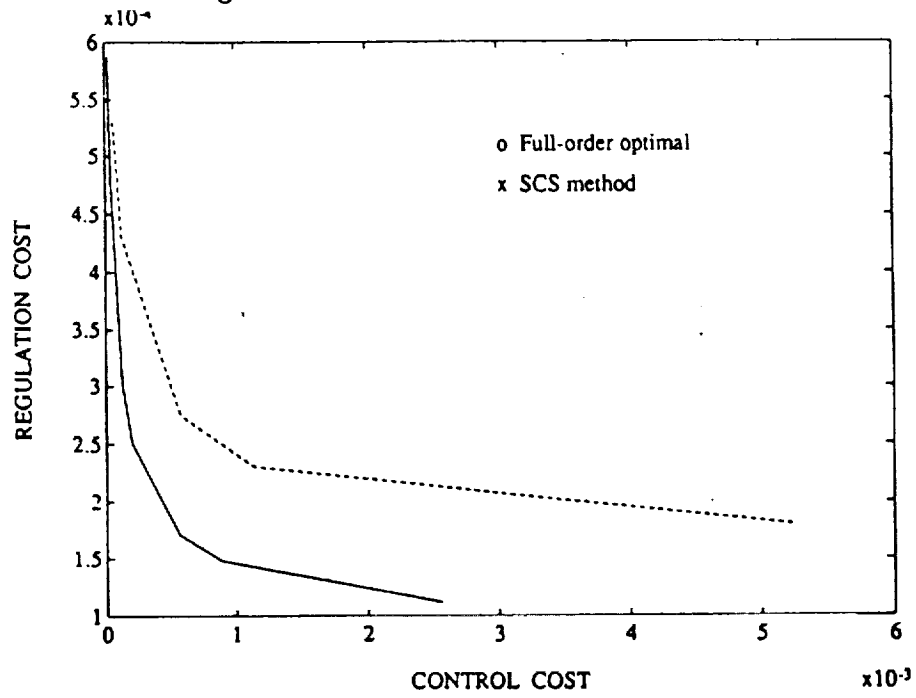


Figure 2.8: Performance plot of Case 4

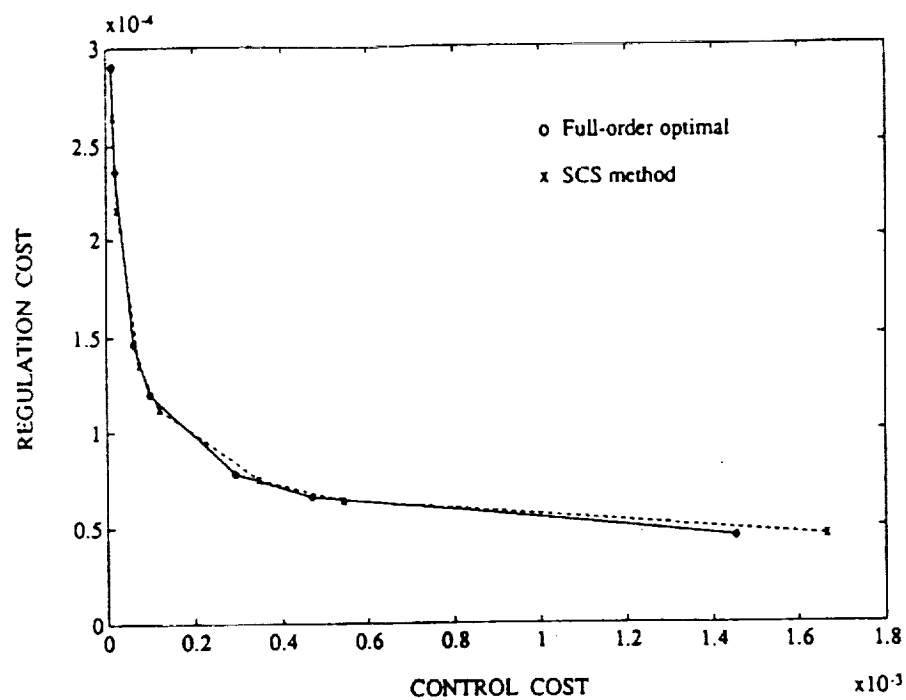


Figure 2.9: Performance plot of Case 5

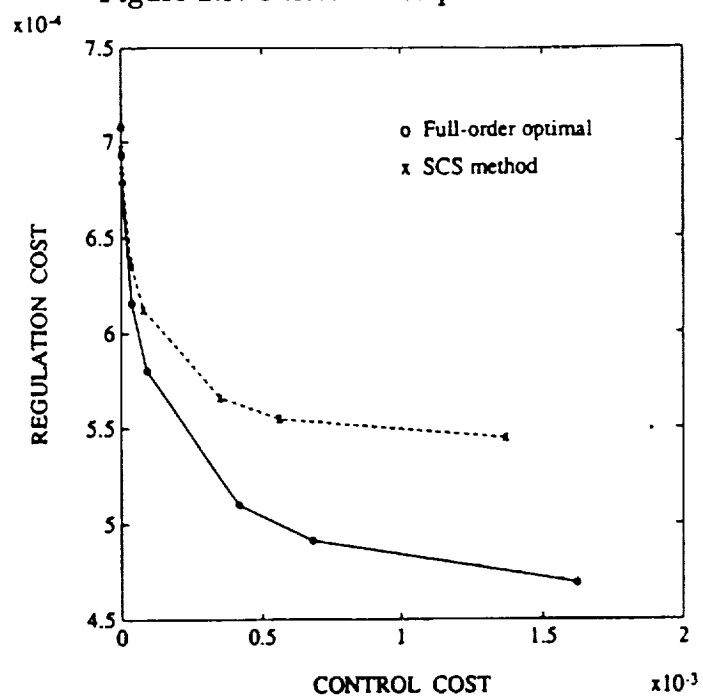


Figure 2.10: Performance plot of the unsymmetric example

Table 2.1: Performance values of Case 1

R=	0.01	0.05	0.1	0.5	1	5	10
Optimal	1.1737E-4	1.7796E-4	2.1445E-4	3.3929E-4	4.1689E-4	6.7621E-4	8.3436E-4
SCS method	1.2155E-4	1.8168E-4	2.1856E-4	3.4522E-4	4.2385E-4	6.8522E-4	8.4451E-4
Difference	3.6%	2.1%	1.9%	1.7%	1.7%	1.3%	1.2%

Table 2.2: Performance values of Case 2

R=	0.01	0.05	0.1	0.5	1	5	10
Optimal	7.6963E-5	1.1228E-4	1.3449E-4	2.1154E-4	2.5916E-4	4.1879E-4	5.1610E-4
SCS method	7.9660E-5	1.1442E-4	1.3654E-4	2.1342E-4	2.6109E-4	4.2213E-4	5.2082E-4
Difference	3.5%	1.9%	1.5%	0.89%	0.74%	0.79%	0.91%

Table 2.3: Performance values of Case 3

R=	0.01	0.05	0.1	0.5	1	5	10
Optimal	7.7358E-5	1.1255E-4	1.3472E-4	2.1168E-4	2.5927E-4	*	5.1618E-4
SCS method	7.9850E-5	1.1450E-4	1.3659E-4	2.1344E-4	2.6112E-4	4.2213E-4	5.2082E-4
Difference	3.2%	1.7%	1.4%	0.83%	0.71%	*	0.90%

* CTRL-C encountered difficulty in solving Lyapunov equation for full-order optimal design.

Table 2.4: Performance values of Case 4

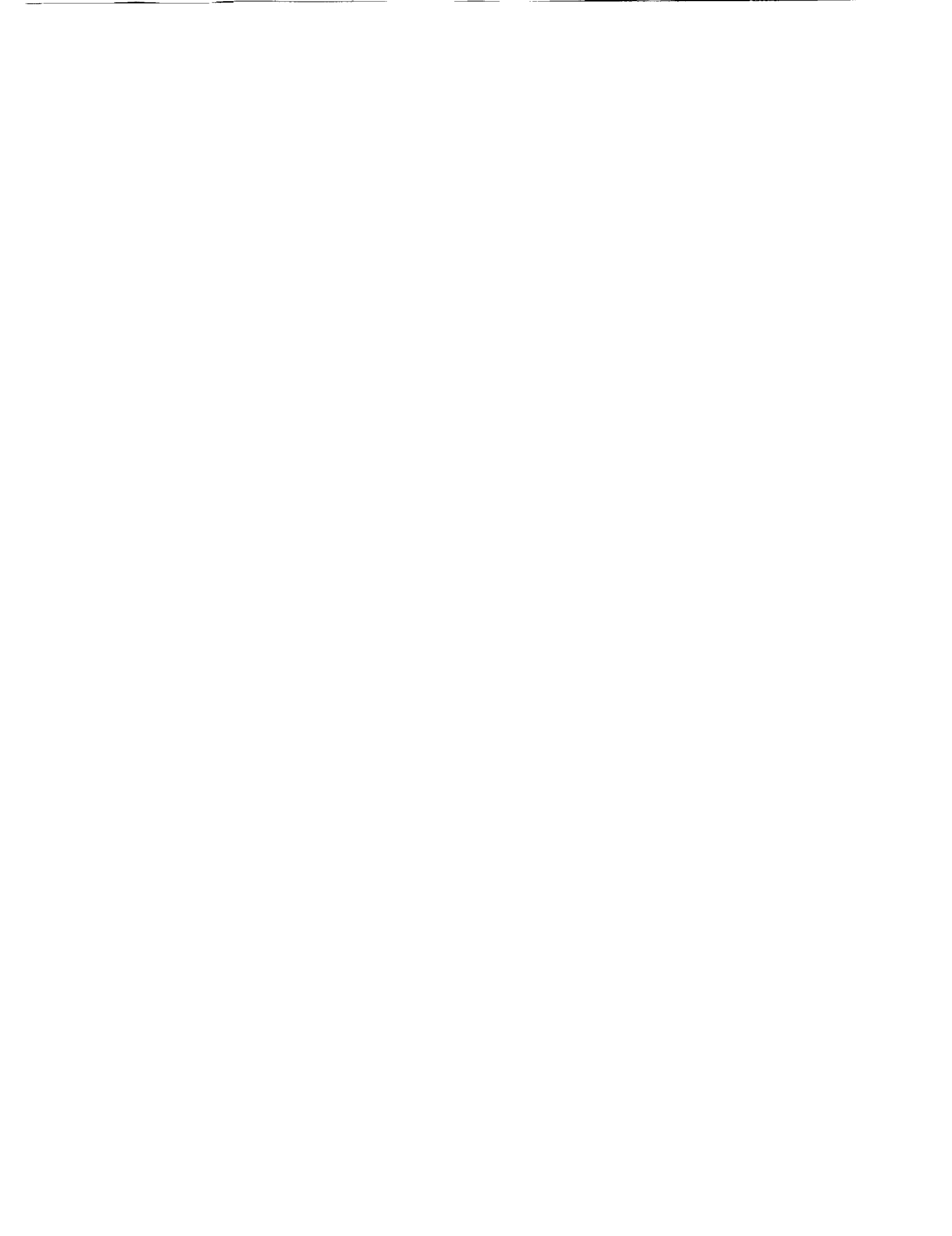
R=	0.01	0.05	0.1	0.5	1	5	10
Optimal	1.3742E-4	1.9240E-4	2.2709E-4	3.4887E-4	4.2544E-4	6.8283E-4	8.4029E-4
SCS method	5.3709E-4	6.6359E-4	7.0535E-4	7.9789E-4	8.4867E-4	1.0293E-3	1.1520E-3
Difference	291%	245%	210%	129%	99%	51%	37%

Table 2.5: Performance values of Case 5

R=	0.01	0.05	0.1	0.5	1	5	10
Optimal	5.9433E-5	8.9437E-5	1.0763E-4	1.6989E-4	2.0863E-4	3.3822E-4	4.1726E-4
SCS method	6.1968E-5	9.1607E-5	1.0989E-4	1.7296E-4	2.1219E-4	3.4275E-3	1.1520E-3
Difference	4.3%	2.4%	2.1%	1.8%	1.7%	1.3%	1.2%

Table 2.6: Comparison of full-order optimal controller and SCS controller

		J_u (Control cost)	J_e (Regulation cost)	J (Performance value)
R=0.0001	OPT	1.6610E-2	4.5665E-4	4.5831E-4
	SCS	8.1847E-3	5.4403E-4	5.4485E-4
	Difference			19%
R=0.001	OPT	4.4901E-3	4.6026E-4	4.6475E-4
	SCS	3.2463E-3	5.4472E-4	5.4800E-4
	Difference			18%
R=0.01	OPT	1.6198E-3	4.6930E-4	4.8550E-4
	SCS	1.3719E-3	5.4458E-4	5.5830E-4
	Difference			15%
R=0.05	OPT	6.8176E-4	4.9123E-4	5.2532E-4
	SCS	5.6477E-4	5.5462E-4	5.8286E-4
	Difference			11%
R=0.1	OPT	4.1564E-4	5.1007E-4	5.5163E-4
	SCS	3.4963E-4	5.6574E-4	6.0070E-4
	Difference			9%
R=0.5	OPT	8.8571E-5	5.8016E-4	6.2444E-4
	SCS	7.8312E-5	6.1235E-4	6.5151E-4
	Difference			4%
R=1.0	OPT	3.6711E-5	6.1606E-4	6.5277E-4
	SCS	3.3248E-5	6.3803E-4	6.7128E-4
	Difference			3%
R=5.0	OPT	2.8869E-6	6.7877E-4	6.9320E-4
	SCS	2.7541E-6	6.8520E-4	6.9897E-4
	Difference			0.8%
R=10.0	OPT	8.2542E-7	6.9266E-4	7.0091E-4
	SCS	8.0024E-7	6.9609E-4	7.0409E-4
	Difference			0.4%
R=100.0	OPT	9.5865E-9	7.0794E-4	7.0900E-4
	SCS	9.5056E-9	7.0831E-4	7.0926E-4
	Difference			0.05%



Chapter 3

MODEL REDUCTION OF FLEXIBLE STRUCTURES

A central issue in the active control of flexible structures is to derive a high-fidelity mathematical model to be used as a basis for dynamic analysis and control design. Although a flexible structure is by nature a distributed-parameter system, for analysis purposes it can be modelled as a finite dimension system by using the Finite Element Method or other discretization approaches. However, for a complex structure, e.g., large space structure like the Space Station Freedom, the Finite Element model usually attains thousands, or tens of thousands of degrees of freedom, which is a major computational task for dynamic analysis not to mention too large a scale for control design. Therefore, for the purposes of efficient computation and easy control implementation, model reduction is an inevitable procedure for dynamic analysis and control design of large space structures. Another fact about space structures is that most space structures will be built with light weight components and will thus tend to be very flexible with closely-spaced frequencies and very light damping.

In this chapter, several frequently used model reduction methods are reviewed. Among a myriad of the existing model reduction methods for structural dynamics systems, modal truncation may be the most popular approach. Modal representation has many advantages: modal frequencies represent resonances of the structure, equations of motion are uncoupled implying saving of

computation time, and modal data can be identified and validated by vibration test. However, selection of modes to be retained in the reduced model may not be an easy task. The simplest approach would be to include all modes within the frequency range of interest. For a large space structure with closely-spaced frequencies, this simplest approach may produce a reduced model whose size is still too large to handle.

An efficient modal truncation criterion is based on balanced singular values. It is shown in Refs. [14] and [23] that if frequencies are sufficiently separated and modal damping is very small, then modal representation of a structural dynamics system is approximately balanced. Therefore, approximate balanced singular values can be calculated by using modal parameters and balanced model reduction can be performed on modal coordinates. Other than singular values, Kabamba introduced an L^2 model reduction basis called balanced gain[24]. In this chapter, an approximate balanced gain for a structural dynamics system is expressed in terms of modal parameters by using the balanced form derived in Ref. [14]. The balanced gain approach can produce more accurate reduced models in the L^2 sense.

In addition to normal modes, there are other Ritz vectors superposition methods for dynamic analysis of structures. The authors presented a Krylov model reduction algorithm in Refs. [36, 37]. Krylov vectors are system static modes generated by a recurrence procedure. In Refs. [30] and [42], similar Ritz vector approaches are proposed for structural dynamic analysis. Recently, several numerical experiments have shown that by augmenting a modal basis with some Ritz vectors, fidelity of the reduced model can be substantially

improved[25]. Such approach will be referred to in this chapter as the mixed-mode method.

This chapter is organized as follows. The Model Reduction Section briefly reviews modal truncation, balanced model reduction, balanced gain approach, Krylov model reduction, and Ritz vectors and mixed-mode method. Then, a plane truss structure with closely-spaced frequencies and light modal damping is used to compare different reduced-order models. Open-loop comparison includes the L^2 error norm of the impulse response function and approximation of the output frequency response function. The control design comparison includes closed-loop stability and control performance. The material in this chapter was presented in an international conference on dynamics of flexible structures in space[8].

3.1 Model Reduction

In this section, several frequently used model reduction methods for structural dynamics systems are briefly reviewed.

3.1.1 Modal Truncation

Let a structural dynamics system be described by the following input-output equations

$$\begin{aligned} M\ddot{x} + D\dot{x} + Kx &= Pu & x \in R^n, u \in R^l \\ y &= Vx + W\dot{x} & y \in R^m \end{aligned} \quad (3.1)$$

where M , D , and K are the system mass, damping, and stiffness matrices respectively; P is the force distribution matrix; and V and W are the displacement and velocity sensor distribution matrices respectively. If the damping

matrix D is proportional, then the above structure model can be transformed into standard modal form as follows:

$$\begin{aligned}\ddot{\eta} + 2Z\Lambda\dot{\eta} + \Lambda^2\eta &= \Phi^T P u \\ y &= V\Phi\eta + W\Phi\dot{\eta}\end{aligned}\tag{3.2}$$

where Φ is the matrix of mode shapes, $\Lambda = \text{diag}[\lambda_i]$ is the diagonal matrix of modal frequencies, and $Z = \text{diag}[\zeta_i]$ is the diagonal matrix of modal damping factors. A simple and frequently used approach to structure model reduction is modal truncation, which retains dominant normal modes in the reduced model. Selection of dominant modes, however, is not as easy a task as it seems to be and requires experienced engineering judgement. The simplest approach is to retain all the modes within the frequency range of interest.

3.1.2 Balanced Reduction

For an asymptotically stable, linear, time-invariant system represented by

$$\begin{aligned}\dot{z} &= Az + Bu \\ y &= Cz\end{aligned}\tag{3.3}$$

the controllability and observability grammians are solutions of the two Lyapunov equations

$$\begin{aligned}AW_c + W_cA^T + BB^T &= 0 \\ A^TW_o + W_oA + C^TC &= 0\end{aligned}\tag{3.4}$$

Neither grammian is invariant under similarity transformation. It is shown in Ref. [29] that there always exists an equivalent system for which the grammians are diagonal and equal, $W_c = W_o = \Sigma = \text{diag}[\sigma_i]$. The quantities σ_i 's are called *second-order modes* or *singular values* of the system. A system representation with equal and diagonal grammians is called *internally balanced*. Balanced

model reduction deletes system state variables associated with the smallest singular values. It is interpreted that those states associated with small singular values require large effort to control and contribute little to the system output. In this sense, balanced model reduction retains the most controllable and observable part of the system in the reduced model. Enns showed in Ref. [11] that there exists an ∞ -norm frequency error bound

$$\|H(j\omega) - H_r(j\omega)\|_{\infty} \leq 2 \sum_{i=r+1}^n \sigma_i \quad r < n \quad (3.5)$$

where $H(j\omega) = C(j\omega I - A)^{-1}B$ is the transfer function matrix of the full-order model and $H_r(j\omega)$ is the transfer function matrix of the r -th order reduced model obtained by retaining the first r singular values.

Recently, Gregory[14] and Jonckheere[23] independently showed that for a flexible structure described by the modal equation (3.2), if the system damping ratios are sufficiently small ($\zeta_i \ll 1$) and the system natural frequencies are well separated (The criterion on separation of frequencies is given by $\max(\zeta_i, \zeta_j) \max(\lambda_i, \lambda_j) / |\lambda_i - \lambda_j| \ll 1$), then the modal model is approximately balanced. The approximate balanced singular values can be expressed in terms of the modal parameters as follows

$$\sigma_i \approx \frac{\sqrt{p_i p_i^T (v_i^T v_i + \lambda_i^2 w_i^T w_i)}}{4 \zeta_i \lambda_i^2} \quad (3.6)$$

where p_i is the i -th row of $\Phi^T P$ matrix, and v_i and w_i are the i -th columns of the $V\Phi$ and $W\Phi$ matrices respectively. It is shown in Ref. [4] that the approximate balanced singular value in Eq. (3.6) is equal to one-half of the peak magnitude of the transfer function at resonant frequencies. Therefore, modal truncation based on singular values preserves modes with largest peak magnitude in the transfer function. .

3.1.3 Balanced Gains

Assume that the system described by Eq. (3.3) is internally balanced and let b_i denote the i -th row of B matrix and c_i denote the i -th column of C matrix. Balanced gain is defined by Kabamba in Ref. [24] as $g_i = b_i^T b_i = c_i c_i^T$. ($b_i^T b_i = c_i c_i^T$ is a property of the balanced realization and can be proved easily by using Eqs. (3.4) and $W_c = W_o = \Sigma$.) Kabamba showed that singular values do not give enough information for model reduction in the L^2 sense. By defining the following inner product and norm of the impulse response function matrix

$$(h_1, h_2) \equiv \text{tr} \left[\int_0^\infty h_1(t) h_2^T(t) dt \right] \quad (3.7)$$

$$\| h \|_{L^2} \equiv (h_1, h_2)^{1/2}$$

it can be shown that for an internally balanced system

$$\| h - h_r \|_{L^2} \geq \left(\sum_{i=1}^n \sigma_i g_i \right)^{1/2} - \left(\sum_{i=r+1}^n \sigma_i g_i \right)^{1/2} \quad (3.8)$$

where h and h_r are the impulse response function matrices of the full-order model and the reduced-order model respectively. From Eq. (3.8), we see that it is the product $\sigma_i g_i$ instead of σ_i alone that serves as a truncation basis for L^2 model reduction.

For structural dynamics systems, the balanced gain for mode i can be obtained by combining the definition of Kabamba[24] and the derivation of Gregory[14].

$$g_i = \frac{\sqrt{p_i p_i^T (v_i^T v_i + \lambda_i^2 w_i^T w_i)}}{\lambda_i} \quad (3.9)$$

Therefore, according to Eq. (3.8), an L^2 norm modal truncation for structural dynamics systems should be based on

$$\sigma_i g_i = \frac{p_i p_i^T (v_i^T v_i + \lambda_i^2 w_i^T w_i)}{4 \zeta_i \lambda_i^3} \quad (3.10)$$

It is noted that the above modal truncation basis is exactly the same as Skelton's modal cost analysis truncation basis derived based on the contribution of each mode to the output energy for an impulse input[4, 34]. For modal cost analysis, if a structure's natural frequencies are widely-spaced and modal damping approaches zero, the total cost can be decomposed into a sum of modal costs, which are equal to $\sigma_i g_i$ in Eq. (3.10).

3.1.4 Krylov Model Reduction

Su and Craig proposed in Refs. [36, 37] a Krylov model reduction algorithm for structural dynamics systems. Basically, Krylov model reduction is an extension of the Lanczos method in Ref. [30] to structural control problems. A Krylov reduced model is obtained by projecting the system dynamic equation onto a subspace called *Krylov subspace*, which is spanned by a set of vectors called a *Krylov vectors*. Krylov vectors are generated by a simple recurrence procedure. For undamped structural dynamics systems, the Krylov procedure is

$$Q_{j+1} = K^{-1}MQ_j \quad (3.11)$$

For damped systems, the Krylov procedure is

$$\begin{Bmatrix} Q_{j+1}^d \\ Q_{j+1}^v \end{Bmatrix} = \begin{bmatrix} -K^{-1}D & -K^{-1}M \\ I & 0 \end{bmatrix} \begin{Bmatrix} Q_j^d \\ Q_j^v \end{Bmatrix} \quad (3.12)$$

With starting vectors appropriately chosen as the system's static deflection due to force and sensor distribution matrices, the Krylov vectors generated by the above procedures can form a basis to produce reduced-order models with parameter-matching properties. Parameter-matching methods constitute a class of efficient model reduction methods for linear systems[41].

Krylov model reduction is essentially a second-order formulation of parameter-matching model reduction method for structural dynamics systems. A Krylov reduced model matches a set of system parameters called *low-frequency moments*. For a linear time-invariant system described by Eq. (3.3), low-frequency moments are defined by $CA^{-i}B$, $i = 1, 2, \dots$, which are coefficient matrices in the Taylor's expansion series of system transfer function $H(j\omega)$. By matching low-frequency moments, the reduced-order model produces accurate steady state step input response and approximates the lower natural frequencies of the full-order model. Another interesting feature about Krylov reduced models, as indicated in Ref. [36], is that for structural control design, the Krylov formulation can eliminate control and observation spillovers, but manifests dynamic spillover terms. This is the basic difference between the Krylov reduction method and the traditional modal truncation methods.

3.1.5 Ritz Vectors and Mixed-Mode Method

Although modal truncation may be the most frequently used reduction method, as stated in Ref. [42] there exists no proof that the use of normal modes in mode superposition analysis is better than any other set of Ritz vectors. (Ritz vector is a general terminology for assumed mode or static mode.) On the other hand, it is also true that one cannot assure that a basis formed solely by Ritz vectors can serve as a better truncation basis than normal modes. Recently, many numerical experiments have shown that by augmenting the normal mode basis with some suitably chosen static modes or Ritz vectors, accuracy of dynamic analysis usually can be substantially improved [5, 25]. Static modes are a system's deflection shapes associated with imposed force

distribution vectors. Krylov vectors and Lanczos vectors can all be considered to be system static modes. By using an rms error estimate, Kline provided several examples in Ref. [25] to show that the addition of static modes to the modal basis can indeed enhance fidelity of reduced-order models for analysis of structural response under the action of time-dependent forcing vectors. The addition of some static modes to the normal mode basis to perform model reduction will be called a mixed-mode method.

3.2 Plane Truss Example

A plane truss structure with closely-spaced frequencies and very small modal damping is used to compare the model reduction methods reviewed in the previous section. Figure 3.1 shows the structure's geometry and material properties, which are chosen to be nondimensional and such that the plane truss represents a very flexible structure with closely-spaced frequencies. The structure has twenty-four degrees of freedom. The damping matrix is chosen to be proportional with 0.1% damping ratio for all modes. The structure's natural frequencies, listed in Table 3.1, range from 1.8677(Rad/sec) to 12.992(Rad/sec). The frequency response function in Figure 3.2 shows that the system natural frequencies are clustered. There is a force actuator applied at "f" and a displacement sensor located at "a". Since the assumption of sufficiently separated frequencies is violated for this example ($\zeta\Delta\lambda/\lambda$ is 0.1 for modes 1 and 2, 0.7 for modes 8 and 9, and 0.15 for modes 17 and 18, which are not very much smaller than 1), the modal representation cannot be considered as approximately internally balanced. However, for analysis and design purpose, we can still proceed with modal truncation by retaining only modes with largest singular values or

balanced gains. The approximate balanced singular value and balanced gain for each mode calculated by using Eq. (3.7) and Eq. (3.10) respectively are summarized in Table 3.2. The balanced reduction criterion requires that $\sigma_i \gg \sigma_{i+1}$ so that the model can be truncated at σ_i . For this example, there is not an obvious cut-off point, which means that it is necessary to preserve a large portion of the system modes in order to produce a high-fidelity reduced-order model.

3.2.1 Open-Loop Comparison

First, error norms of the impulse response function matrix are compared for different reduced-order models. Let (A, B, C) denote the full-order system model and let (A_r, B_r, C_r) denote the reduced-order system model. The impulse response function matrices for the full-order model and the reduced-order model are $h(t) = Ce^{At}B$ and $h_r(t) = C_r e^{A_r t} B_r$, respectively. An easy way to calculate the error norm of the impulse response function matrix is by solving Lyapunov equations. Let the inner product and norm of impulse response function matrix be defined by Eqs. (3.7). Then, the difference between h and h_r can be calculated by

$$\|h - h_r\|_{L^2} = \text{tr}(B^T W_o B) + \text{tr}(B_r^T W_{or} B_r) - 2B_r^T X B$$

where W_o and W_{or} are observability grammians of the full-order and reduced-order models respectively, and X is the solution of

$$A_r^T X + X A + C_r^T C = 0$$

The error norm is defined by

$$Err = \frac{\|h - h_r\|_{L^2}}{\|h\|_{L^2}}$$

The results of the impulse response comparison are summarized in Table 3.3. As expected, the balanced gain approach produces reduced-order models that approximate the impulse response better than any other truncation criterion. Modal truncation based on λ_i , which means by retaining the lowest frequency modes, shows that for an 18th-order model, which contains three-fourth of the system's modes, there is still a 15% error. For this example, Krylov reduced models are poor in tracking the impulse response. The mixed-mode reduced model in Table 3.3 is obtained by augmenting the balanced gain modal basis with two Krylov modes. It is seen that the inclusion of Krylov modes in the modal basis for model reduction does not improve accuracy in simulating impulse response.

Next, we compared the system's output frequency response function for different reduced-order models. The results are summarized by Figures 3.3–3.8. Figures 3.4 and 3.7 show that Krylov reduced models can approximate very well the frequency response function in the lower frequency range. This is because a Krylov reduced model matches low-frequency moments of the full-order model, which causes excellent approximation of $H(j\omega)$ in the neighborhood of $\omega = 0$. Figures 3.3 and 3.6 indicate that the balanced gain approach simply picks up those modes that contribute the most to the L^2 output energy norm. Although peaks of the dominant modes are exactly reproduced, there are static gain errors in the lower frequency range for balanced gain reduced models. To improve the approximation in the lower frequency range, we can include two Krylov modes in the balanced gain modal basis. The reduced model, then, matches the first two low-frequency moments $CA^{-1}B$ and $CA^{-2}B$, which can produce exact steady state step input response $H(0)$ as shown by Figures 3.5 and 3.8.

3.2.2 Control Design

Assume that the actuator is subject to zero-mean white noise with intensity 1 and the sensor is contaminated by a zero-mean white noise disturbance with intensity 10^{-5} . Based on each reduced-order model, an LQG control design can be carried out to minimize the performance index

$$J = \frac{1}{2} \lim_{t \rightarrow \infty} E[\dot{x}_r^T M_r \dot{x}_r + x_r^T K_r x_r + \rho u^T u]$$

in which the first two terms represent the total energy of the reduced system and the third term represents the control cost. The controller designed based on reduced model, then, is applied to control the full-order structure. A positive scalar ρ is used to adjust the relative weighting of the regulation cost and control cost penalties. Overall controller authority, actuator mean-square force levels, and controller bandwidth are all inversely proportional to ρ . The value of ρ was varied from 0.01 to 1000 to study the closed-loop stability and controller performance.

The results are summarized by Table 3.4 and Figure 3.9. The stability comparison in Table 3.4 shows that for this example, modal truncation by retaining the lowest frequency modes yields more stable closed-loop designs than other methods. Krylov reduced model appears to be the worst in the stability comparison. This contradicts the results of another example in Ref. [37], in which control design based on Krylov reduced models indicates much better stability property and performance than controllers designed based on normal mode reduced models. Modal truncation based on singular values and balanced gains, and based on the mixed-mode method are about equal in yielding a stable design. Figure 3.9 compares the performance of control designs based

on different 8th-order reduced models. Modal truncation based on lowest frequency modes has the best performance while Krylov-based control design is the worst. The balanced gain modal basis method and the mixed-mode method exhibit comparable performance.

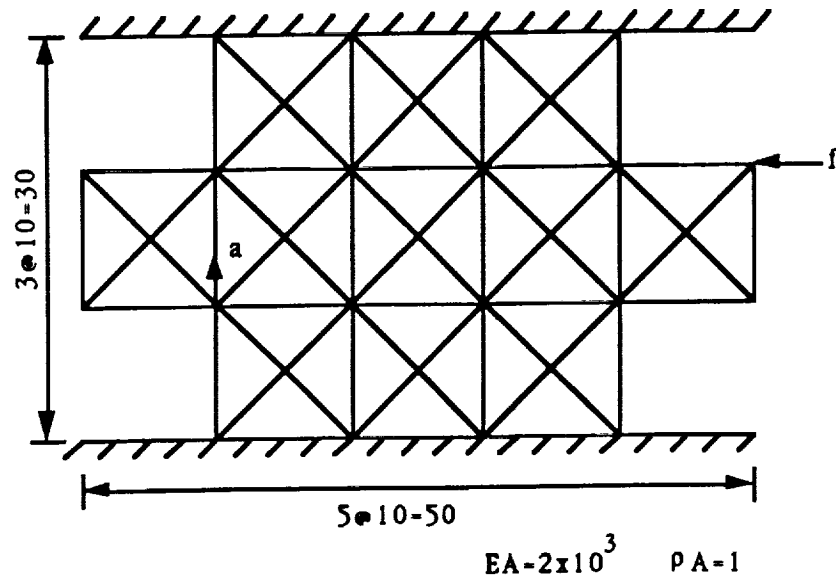


Figure 3.1: Plane truss structure example

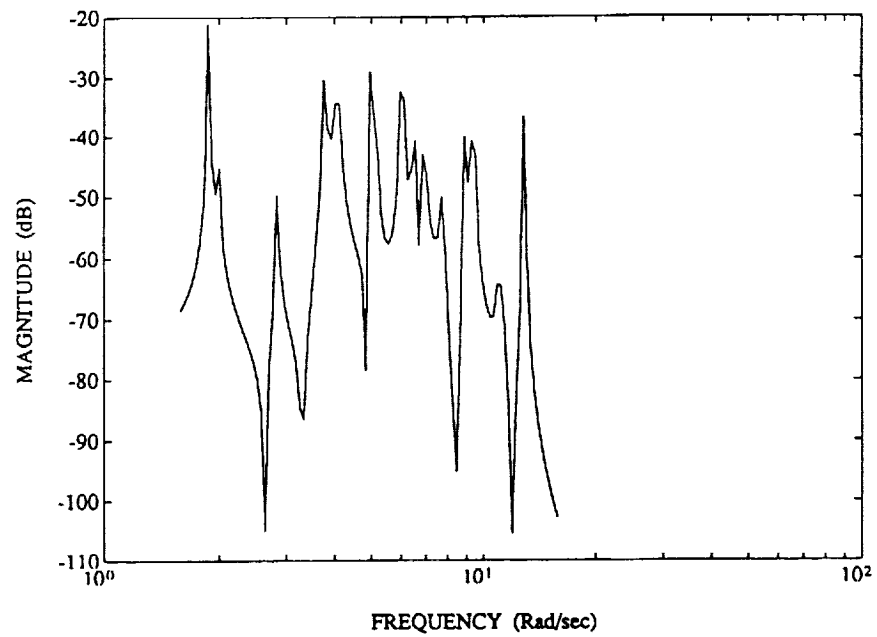


Figure 3.2: FRF of full-order model

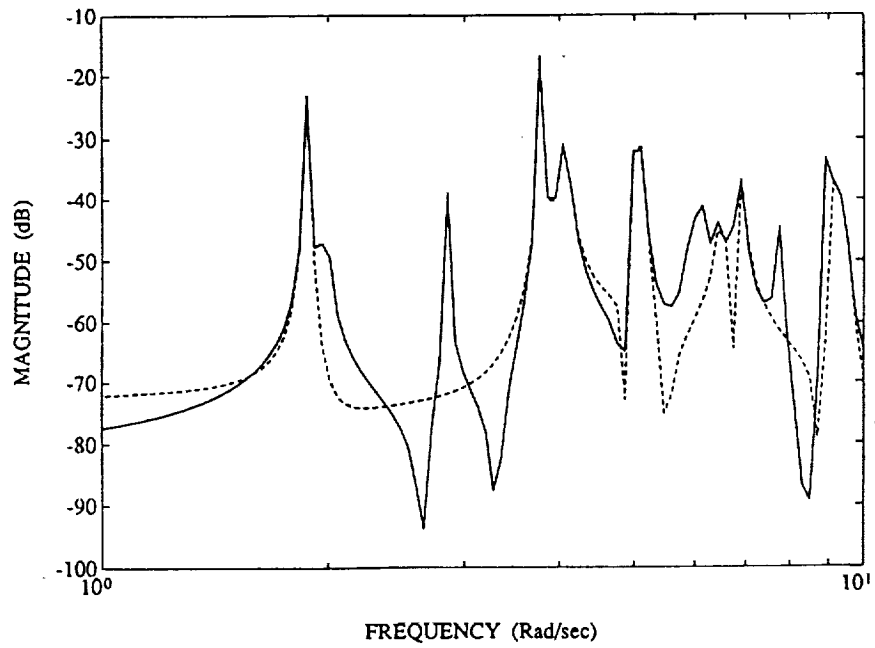


Figure 3.3: FRF of 10th-order reduced model based on balanced gain modal basis

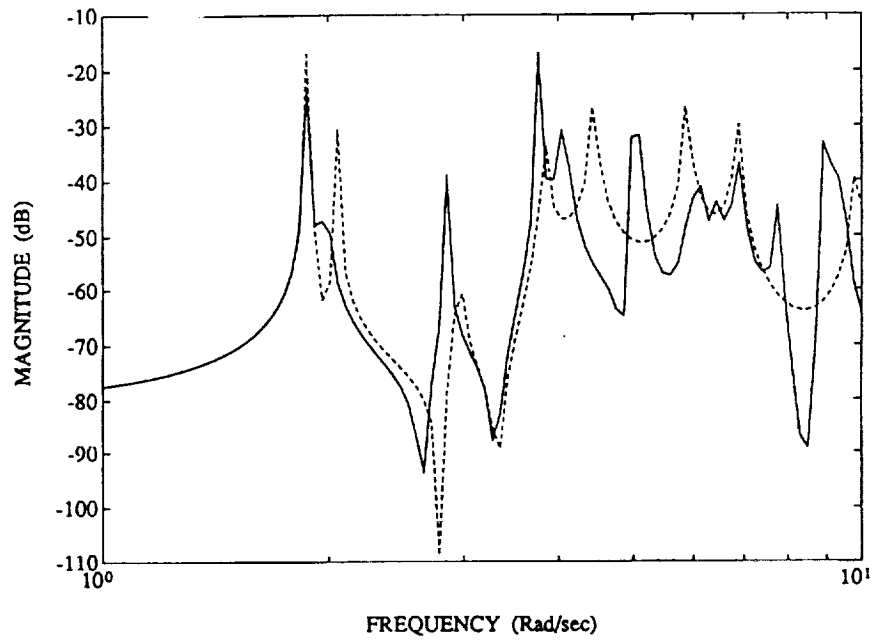


Figure 3.4: FRF of 10th-order reduced model based on Krylov vectors

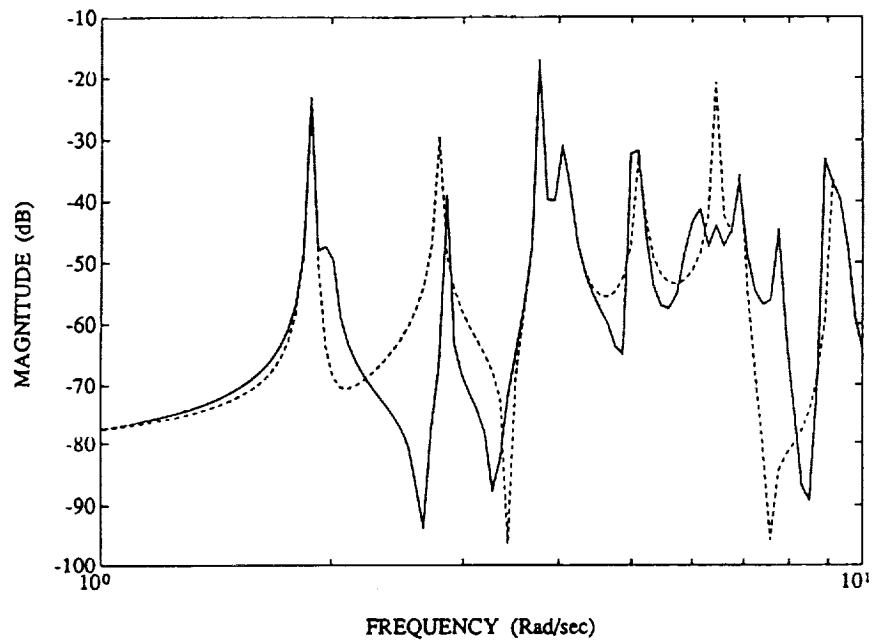


Figure 3.5: FRF of 10th-order reduced model based on 2 Krylov vectors and 8 balanced gain modal basis

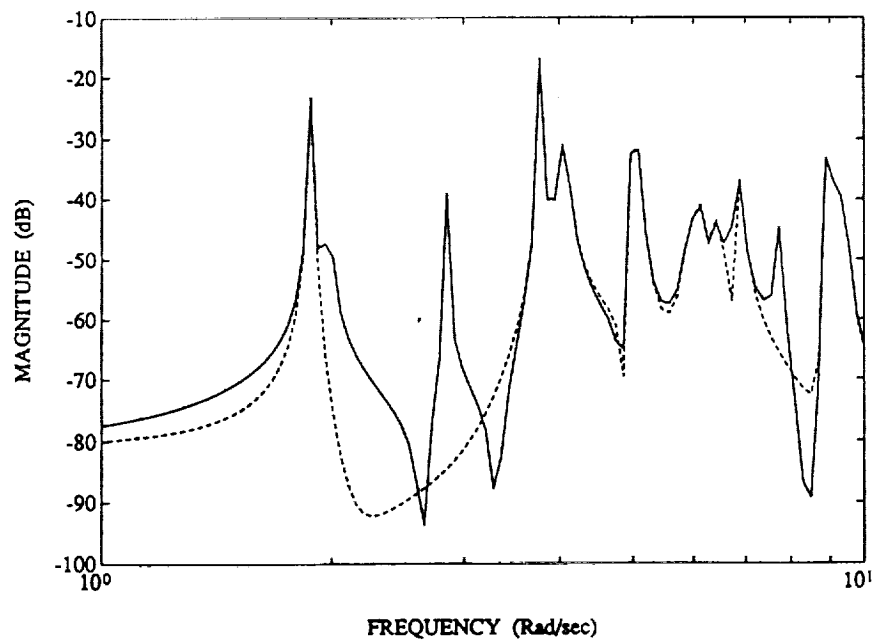


Figure 3.6: FRF of 15th-order reduced model based on balanced gain modal basis

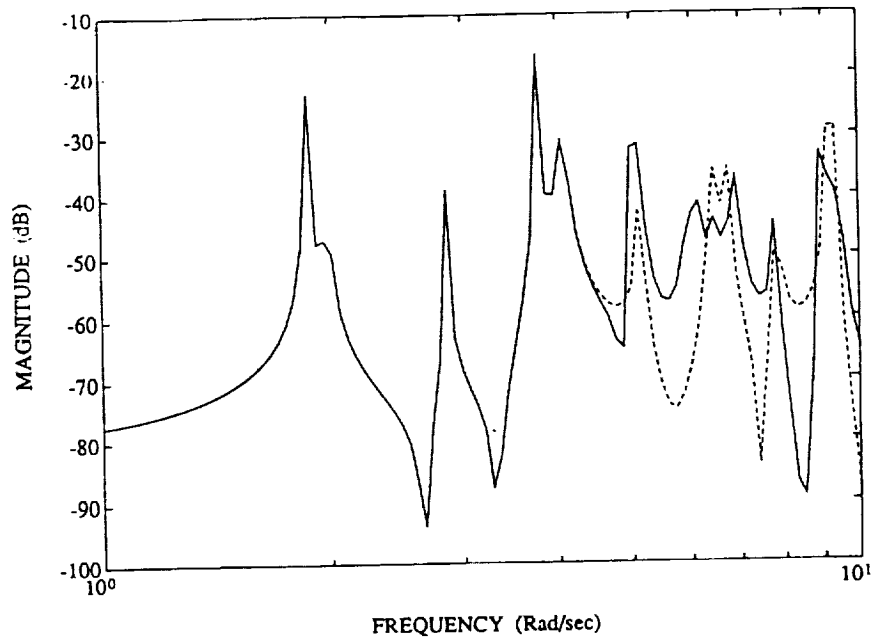


Figure 3.7: FRF of 15th-order reduced model based on Krylov vectors

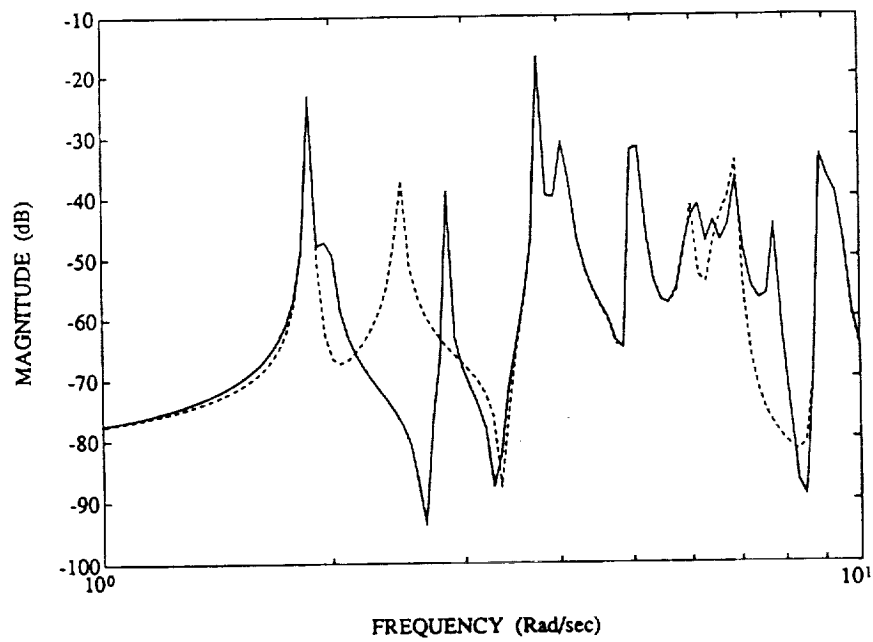


Figure 3.8: FRF of 15th-order reduced model based on 2 Krylov vectors and 13 balanced gain modal basis

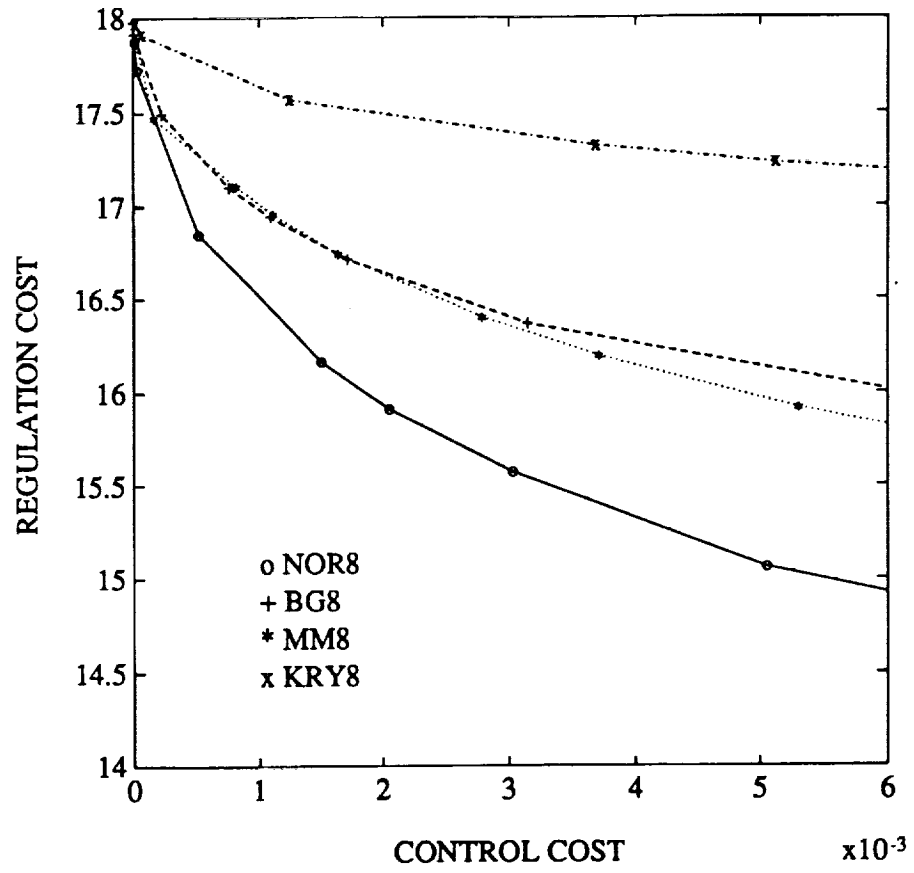


Figure 3.9: Performance plot

Table 3.1: Natural frequencies of plane truss structure

Mode No.	Frequency (Rad/sec)	Mode No.	Frequency (Rad/sec)	Mode No.	Frequency (Rad/sec)
1	1.8677	9	5.1279	17	8.9762
2	1.8861	10	5.9550	18	9.0349
3	1.9849	11	6.0958	19	9.1429
4	2.8460	12	6.5133	20	9.4214
5	3.7640	13	6.7425	21	11.069
6	4.0700	14	6.9224	22	11.558
7	4.9611	15	7.7759	23	12.838
8	5.1206	16	8.8845	24	12.992

Table 3.2: Singular values and balanced gains

Singular Value				Balanced Gain			
Mode	σ_i	Mode	σ_i	Mode	$\sigma_i g_i$	Mode	$\sigma_i g_i$
6	1.0938E-1	16	1.9229E-2	6	1.9477E-4	17	1.3072E-5
1	8.3539E-2	17	1.9080E-2	5	8.2592E-5	11	8.7570E-6
2	7.5481E-2	11	1.8951E-2	8	7.8123E-5	24	7.3362E-6
5	7.4065E-2	15	1.1891E-2	1	5.2137E-5	23	6.3562E-6
8	6.1759E-2	24	1.1881E-2	20	5.2115E-5	15	4.3978E-6
20	3.7187E-2	23	1.1126E-2	2	4.2984E-5	3	3.6599E-6
7	3.3461E-2	4	6.8545E-3	19	3.4265E-5	13	8.0027E-7
14	3.2379E-2	13	5.4472E-3	14	2.9030E-5	4	5.3487E-7
19	3.0609E-2	21	3.3258E-3	12	2.3329E-5	21	4.8973E-7
12	2.9923E-2	9	1.1986E-3	7	2.2218E-5	22	3.1657E-8
10	2.8100E-2	22	8.2749E-4	10	1.8808E-5	9	2.9468E-8
3	2.1470E-2	18	6.1067E-4	16	1.3140E-5	18	1.3477E-8

Table 3.3: Error norms of impulse response function

Model Order	Based on λ_i	Based on σ_i	Based on $\sigma_i g_i$	Krylov Modes	Mixed Modes*
1	9.2897E-1	7.1434E-1	7.1434E-1	1.0082E+0	—
2	8.6593E-1	6.4331E-1	5.9309E-1	1.2159E+0	—
3	8.6056E-1	5.8027E-1	4.8189E-1	1.0367E+0	8.9475E-1
4	8.5978E-1	4.5903E-1	4.1087E-1	5.6607E+0	6.7110E-1
5	7.3878E-1	3.4782E-1	3.3495E-1	1.0683E+0	8.0917E-1
6	4.5287E-1	2.7191E-1	2.7191E-1	4.1616E+0	7.7403E-1
7	4.2073E-1	2.3928E-1	2.2124E-1	1.0384E+0	9.1157E-1
8	3.0904E-1	1.9669E-1	1.7866E-1	2.2132E+0	3.2963E-1
9	3.0899E-1	1.4603E-1	1.4454E-1	2.1238E+0	3.7733E-1
10	2.8115E-1	1.1190E-1	1.1190E-1	2.5662E+0	4.9722E-1
11	2.6834E-1	8.4013E-2	8.4013E-2	2.6191E+0	6.5646E-1
12	2.3406E-1	7.8640E-2	6.6106E-2	2.5230E+0	3.9786E-1
13	2.3296E-1	6.0734E-2	4.7029E-2	1.6895E+0	2.3394E-1
14	1.9036E-1	4.1657E-2	3.4170E-2	1.3701E+0	1.2998E-1
15	1.8390E-1	2.8797E-2	2.3947E-2	1.3418E+0	1.5327E-1
16	1.6622E-1	2.2341E-2	1.4617E-2	6.4551E-1	8.9277E-2
17	1.4654E-1	1.2118E-2	8.1601E-3	8.2138E-1	1.0390E-1
18	1.4657E-1	2.7875E-3	2.7875E-3	7.3783E-1	5.7178E-2
19	9.6817E-2	2.0024E-3	1.6128E-3	7.0348E-1	3.2111E-2
20	2.0318E-2	8.2761E-4	8.2761E-4	5.9209E-1	4.9123E-3
21	1.9600E-2	1.0952E-4	1.0952E-4	6.2487E-1	2.7161E-3
22	1.9553E-2	6.6258E-5	6.3041E-5	5.5446E-1	6.7804E-4
23	1.0769E-2	1.9784E-5	1.9784E-5	1.6457E-1	2.7408E-4

*Mixed-Modes: 2 Krylov modes plus balanced gain modal basis.

Table 3.4: Stability of controllers

Controller	$\rho = 0.01$	0.1	1	10	100	1000
SV8	U	U	U	S	S	S
SV10	U	U	U	S	S	S
SV12	U	U	U	S	S	S
SV14	U	U	U	S	S	S
BG8	U	U	U	U	S	S
BG10	U	U	U	S	S	S
BG12	U	U	U	U	S	S
BG14	U	U	S	S	S	S
MM8	U	U	U	S	S	S
MM10	U	U	U	U	S	S
MM12	U	U	S	S	S	S
MM14	U	U	U	S	S	S
KRY8	U	U	U	U	S	S
KRY10	U	U	U	U	S	S
KRY12	U	U	U	U	S	S
KRY14	U	U	U	S	S	S
NOR8	U	U	S	S	S	S
NOR10	U	U	S	S	S	S
NOR12	U	U	S	S	S	S
NOR14	U	U	S	S	S	S

U: Closed-loop system is unstable. S: Stable.

SV: Singular value modal basis.

BG: Balanced gain modal basis.

MM: 2Krylov modes plus balanced gain modal basis.

KRY: Krylov reduced model.

NOR: Lowest normal mode basis.



Chapter 4

CONTROLLER REDUCTION

Conventional Linear Quadratic Gaussian (LQG) controller design usually leads to a controller with an order about the same as the order of the original system to be controlled. A controller design based on the H^∞ theory may be of much higher order than the plant. For large scale systems it is, in many cases, necessary to reduce the controller to a smaller order for the purpose of easy implementation and economical computation. The reduced-order controller, however, should not affect the closed-loop stability or degrade the performance too much.

In recent years there has been extensive research devoted to the topic of controller reduction. Among a myriad of controller reduction methods, one class of methods based on the state-space formulation can be called projection methods [9, 22, 45]. The controller system equation is usually first projected, or transformed, to new coordinates in which the contribution of each controller state to the overall closed-loop control performance can be meaningfully defined and evaluated. Then, the reduction strategy is to eliminate those states with the least contribution to the performance. This type of approach is referred as Linear-Quadratic Reduction in Ref. [13] because the reduced-order controller is obtained by performing reduction to the full-order LQG controller.

The major task in LQG reduction is to find an appropriate projection

subspace for controller system transformation and reduction. Since controller reduction is a closed-loop problem, it is required to take not only the controller system itself but also the closed-loop system as a whole into consideration in the search for a truncation basis. Therefore, as it is usually addressed in the literature, a controller reduction problem is different from a model order reduction problem. The component cost analysis (CCA) method of Skelton et al.[45] performs reduction based upon the participation of the controller states to a quadratic closed-loop performance metric. The balanced controller reduction method [22] balances the two algebraic Riccati equations which arise in the LQG design. In Ref. [9] there are three more balanced controller reduction algorithms which balance Lyapunov equations involving system and controller matrices. All these methods are projection methods with the choice of projection subspace more or less based upon closed-loop considerations. However, despite the fact that the strategy for controller reduction is somewhat different from that of model order reduction, it is still true that if a reduced-order controller can approximate the input-output characteristics of the full-order LQG controller well, then it should also have a fairly good closed-loop performance. Therefore, an efficient model order reduction scheme might very well be applied to controller reduction.

The controller reduction algorithm presented in this chapter can be considered as a model reduction method applied to controller reduction. The projection subspace used is a Krylov subspace generated by a Krylov recurrence procedure. The reduced-order controller is called an *Equivalent Impulse Response Energy Controller* (EIREC) because it has the same impulse response energy as the full-order controller. Since the proposed controller reduction

method is, in fact, a model-order reduction method applied to a controller, it is applicable to controllers obtained by any of the existing control design approaches and is not restricted to the LQG design. This is one advantage over the balanced controller reduction methods ([9, 22, 46]), which are based upon the two Riccati equations which arise in the LQG design. However, the only controller considered in this chapter is the LQG controller, because the examples illustrated are drawn from other LQG controller reduction literature. Computationally, the method in this chapter requires solving a Lyapunov equation of order equal to the order of the controller to be reduced. For a real large scale system, this can be very expensive. Therefore, the method in this chapter is recommended for order-reduction of controllers with moderate scale. The reduction algorithms developed in this chapter can also be used to reduce the order of an open-loop plant.

The organization of this chapter is as follows. In Section 4.1, the problem of LQG controller reduction is briefly reviewed and the concept of preserving the impulse response energy is introduced. Then, two algorithms for generating projection subspaces for controller system transformation are presented in Section 4.2. In Section 4.3, some properties of the reduced-order controller, like energy-equivalence, stability, minimality, and moment-matching are depicted and proved. Finally, in Section 4.4, two examples drawn from other controller reduction literature are used to test the proposed algorithm. Comparisons with other methods are made. Part of the material in this chapter is presented in Ref. [35].

4.1 LQG Controller Reduction Problem

The system to be controlled is a linear, finite dimensional, time-invariant system described by

$$\begin{aligned} \dot{z} &= Az + Bu + N\varpi \\ y &= Cz + v \end{aligned} \quad (4.1)$$

where $z \in R^n$ is the state variable vector, $y \in R^m$ is the output variable vector, and $u \in R^l$ is the input variable vector. A , B , and C are the system matrix, input distribution matrix, and output distribution matrix, respectively. The disturbance noises ϖ and v are assumed to be uncorrelated zero-mean white noise processes with intensities $W \geq 0$, $V > 0$, respectively. The system is assumed to be controllable and observable. The LQG design problem is to find a controller which minimizes the performance index

$$J = \lim_{t \rightarrow \infty} E[z^T Q z + u^T R u] \quad (4.2)$$

with $Q \geq 0$, and $R > 0$, the weighting matrices. The optimal controller is of the form [26]

$$\begin{aligned} \dot{q} &= Eq + Fy \\ u &= Gq \end{aligned} \quad (4.3)$$

where $q \in R^n$ is the controller state, and

$$\begin{aligned} E &= A + BG - FC \\ F &= \mathcal{P}C^T\mathcal{V}^{-1} \\ G &= -R^{-1}B^T\mathcal{S} \end{aligned} \quad (4.4)$$

where \mathcal{P} and \mathcal{S} satisfy the algebraic Riccati equations

$$\begin{aligned} A\mathcal{P} + \mathcal{P}A^T - \mathcal{P}C^T\mathcal{V}^{-1}C\mathcal{P} + NWN^T &= 0 \\ A^T\mathcal{S} + \mathcal{S}A - \mathcal{S}B R^{-1}B^T\mathcal{S} + Q &= 0 \end{aligned} \quad (4.5)$$

The controller reduction algorithm presented in this chapter is designed to reduce the order of the controller, Eq. (4.3). The projection subspace employed is a Krylov subspace, which is generated by a Krylov recursive process. The recursive process uses the inverse of the controller system matrix E to generate vectors recursively. The starting subspace is chosen to be the F matrix (or G^T matrix) so that the generated Krylov subspace is, in fact, equivalent to the generalized controllability (or observability) subspace. The generated Krylov vectors are normalized such that when the controller system equation is projected onto the Krylov subspace, the controllability (or the observability) grammian is equal to the identity matrix and the transformed G (or F) matrix has a special form with nonzero elements only in the first block.

Since the output of the controller is to be used to control the original system, the proposed reduced-order controller preserves the impulse response energy of the full-order controller. In this way, although the reduced-order controller might have a response profile which deviates very much from that of the full-order controller, the control energy in some sense is the same. The impulse response energy is defined as the L^2 energy norm of the impulse response of the controller

$$\mathcal{E} = \|H\|_{L^2}^2 = \text{tr} \left[\int_0^\infty H^T H dt \right] \quad (4.6)$$

where $H = Ge^{Et}F$ is the impulse response of the controller. It is assumed that the full-order controller is an asymptotically stable system. If the full-order controller is not asymptotically stable, one can separate the unstable part and the stable part and perform model reduction only on the stable part. The

impulse response energy can further be expressed as

$$\begin{aligned}\mathcal{E} &= \text{tr}\left[\int_0^\infty F^T e^{E^T t} G^T G e^{E t} F dt\right] = \text{tr}[F^T W_o F] \\ &= \text{tr}\left[\int_0^\infty G e^{E t} F F^T e^{E^T t} G^T dt\right] = \text{tr}[G W_c G^T]\end{aligned}\tag{4.7}$$

where W_o and W_c are the observability and controllability grammians. From Eq. (4.7) it is clear that the triple (E, F, G) and its dual (E^T, G^T, F^T) have the same impulse response energy. Hence, two equally applicable algorithms, one based on (E, F, W_o) and the other based on (E^T, G^T, W_c) , can be developed for producing an Equivalent Impulse Response Energy Controller.

4.2 Equivalent Impulse Response Energy Controller Reduction Algorithm

In this section, two algorithms for generating projection subspaces for controller system transformation are presented. The new coordinates to which the controller system equation is transformed are called *normalized grammian coordinates* because they are coordinates in which either the controllability grammian or the observability grammian is the identity matrix. Controller reduction is based upon the representation in the new coordinates. The subspace-generating algorithm is a recursive process with either the F matrix or the G^T matrix as the starting subspace. It is assumed that either the number of actuators, l , or the number of sensors, m , is much less than the number of states, n , so that the algorithm can work and the reduction of the controller can actually be achieved. The first algorithm is used to generate a subspace that normalizes the observability grammian.

Algorithm 4.1 (EIRECWo Algorithm)

(1.) Calculate the observability grammian W_o .

$$E^T W_o + W_o E + G^T G = 0, \quad (W_o \geq 0) \quad (4.8)$$

(2.) $i = 1$. Perform singular-value decomposition on $F^T W_o F$.

$$F^T W_o F = U \Sigma U^T$$

$$U = [U_\alpha \ U_\beta], \quad \Sigma = \begin{bmatrix} \Sigma_\alpha & \\ & 0 \end{bmatrix}$$

Retain only the nonzero singular-value portion and perform normalization to get L_1 .

$$L_1 = F U_\alpha \Sigma_\alpha^{-\frac{1}{2}}$$

(3.) Form $R = E^{-1} L_i$.

(4.) Orthogonalize R with respect to L_j , for $j = 1$ to i .

$$R^T W_o L_j = 0, \quad j = 1 \text{ to } i$$

(5.) Perform singular-value decomposition on $R^T W_o R$.

$$R^T W_o R = U \Sigma U^T$$

$$U = [U_\alpha \ U_\beta], \quad \Sigma = \begin{bmatrix} \Sigma_\alpha & \\ & 0 \end{bmatrix}$$

If $\Sigma = 0$ stop; else $L_{i+1} = R U_\alpha \Sigma_\alpha^{-\frac{1}{2}}$.

(6.) $i = i + 1$, go to 3.

The projection subspace is formed as $L = [L_1 \ L_2 \ \dots]$ in which each L_i is a matrix containing a set of vectors and will be referred to as a *block of vectors*, or, simply, a *block*. Since the vectors in L_i are normalized with respect to W_o , the L subspace satisfies

$$L^T W_o L = I \quad (4.9)$$

By using the above identity, the controller system equation can be transformed to the *normalized observability grammian coordinates* as

$$\begin{aligned} \dot{\bar{q}} &= \bar{E}\bar{q} + \bar{F}y \\ u &= \bar{G}\bar{q} \end{aligned} \quad (4.10)$$

where

$$q = L\bar{q}$$

and where the transformed system matrices are given by

$$\begin{aligned} \bar{E} &= L^T W_o E L \\ \bar{F} &= L^T W_o F = [\bar{F}_1^T \ 0 \ 0 \ \dots \ 0]^T \\ \bar{G} &= G L \end{aligned} \quad (4.11)$$

The transformed \bar{F} matrix has nonzero elements only in the first block. \bar{F} attains this special form because the starting subspace is F , and L is W_o -normalized.

As mentioned in Section 4.1, the dual triples (E, F, G) and (E^T, G^T, F^T) have the same impulse response energy. Therefore, we have the following algorithm which normalizes the controllability grammian.

Algorithm 4.2 (EIRECWc Algorithm)

(1.) Calculate the controllability grammian W_c .

$$EW_c + W_c E^T + FF^T = 0, \quad (W_c \geq 0) \quad (4.12)$$

(2.) $i = 1$. Perform singular-value decomposition on $GW_c G^T$.

$$GW_c G^T = U \Sigma U^T$$

$$U = [U_\alpha \ U_\beta], \quad \Sigma = \begin{bmatrix} \Sigma_\alpha & \\ & 0 \end{bmatrix}$$

Retain only the nonzero singular-value portion and perform normalization to get L_1 .

$$L_1 = G^T U_1 \Sigma_1^{-\frac{1}{2}}$$

(3.) Form $R = E^{-T} L_i$.

(4.) Orthogonalize R with respect to L_j , for $j = 1$ to i .

$$R^T W_c L_j = 0, \quad j = 1 \text{ to } i.$$

(5.) Perform singular-value decomposition on $R^T W_c R$.

$$R^T W_c R = U \Sigma U^T$$

$$U = [U_\alpha \ U_\beta], \quad \Sigma = \begin{bmatrix} \Sigma_\alpha & \\ & 0 \end{bmatrix}$$

If $\Sigma = 0$ stop; else $L_{i+1} = R U_\alpha \Sigma_\alpha^{-\frac{1}{2}}$.

(6.) $i = i + 1$, go to 3.

Algorithm 4.2 is the dual version of Algorithm 4.1 for the triple (E^T, G^T, F^T) . Therefore E^T is used for subspace recursion with G^T being the starting subspace. The L subspace generated by Algorithm 4.2 satisfies

$$L^T W_c L = I \quad (4.13)$$

and the transformed controller system matrices in the normalized controllability grammian coordinates are

$$\begin{aligned} \bar{E} &= L^T E W_c L \\ \bar{F} &= L^T F \\ \bar{G} &= G W_c L = [\bar{G}_1 \ 0 \ 0 \ \cdots \ 0] \end{aligned} \quad (4.14)$$

with the transformed \bar{G} matrix having nonzero elements only in the first block.

To perform controller reduction, let the transformed controller system equation (4.10) be partitioned as

$$\begin{aligned} \begin{Bmatrix} \dot{\bar{q}}_R \\ \dot{\bar{q}}_T \end{Bmatrix} &= \begin{bmatrix} \bar{E}_R & \bar{E}_{RT} \\ \bar{E}_{TR} & \bar{E}_T \end{bmatrix} \begin{Bmatrix} \bar{q}_R \\ \bar{q}_T \end{Bmatrix} + \begin{Bmatrix} \bar{F}_R \\ \bar{F}_T \end{Bmatrix} y \\ u &= [\bar{G}_R \ \bar{G}_T] \begin{Bmatrix} \bar{q}_R \\ \bar{q}_T \end{Bmatrix} \end{aligned} \quad (4.15)$$

where subscripts R and T denote retained and truncated portion, respectively.

The reduced-order controller is the R -portion of the above equation

$$\begin{aligned} \dot{\bar{q}}_R &= \bar{E}_R \bar{q}_R + \bar{F}_R y \\ u &= \bar{G}_R \bar{q}_R \end{aligned} \quad (4.16)$$

Obviously, $\bar{E}_R = L_R^T W_o E L_R$ (or $L_R^T E W_c L_R$ for Algorithm 4.2), $\bar{F}_R = L_R^T W_o F$ (or $L_R^T F$), and $\bar{G}_R = G L_R$ (or $G W_c L_R$) if L is partitioned as $L = [L_R \ L_T]$. Therefore, only L_R is needed to produce the reduced-order controller. The subspace recursion process does not have to be carried out completely until it

stops at Step 4. It can be terminated whenever the number of vectors generated is equal to the predetermined order of the reduced controller.

As to which algorithm should be used; it depends on the number of actuators and the number of sensors. It will be shown later that the reduced-order controller has the property of matching a certain number of system parameters of the full-order controller. The more blocks of vectors included in L_R , the more system parameters that are matched. In order to match more system parameters, it is desirable that the size of each block of vectors in L_R be small. Therefore, Algorithm 4.1 is preferred for a system with fewer sensors than actuators; otherwise Algorithm 4.2 is preferred.

4.3 Some Properties of the Equivalent Impulse Response Energy Controller

Some properties discovered for the reduced-order controllers obtained in Section 4.2 are listed here.

Proposition 4.1 *The subspace L generated by either of the Equivalent Impulse Response Energy Controller Reduction Algorithms proposed in Section 4.2 is both controllable and observable. If the algorithm terminates before n vectors are generated, then the full-order controller is not minimal. A minimal optimal controller can be produced by projecting the full-order controller onto the L subspace.*

As noted in Ref. [46], the optimal full-order controller obtained from the LQG design is, in general, not minimal even if the system to be controlled is minimal. In other words, the controller itself is not a completely controllable

and/or not a completely observable system. Therefore, there might exist a controller of order smaller than n which still yields the same performance as the full-order LQG controller. An efficient controller reduction algorithm should have the capability to detect and to produce such a minimal-order controller, if it exists. The reduction method proposed here meets this requirement. Before proving minimality of the reduced-order controller, a relationship between the observable subspace (controllable subspace) and observability grammian (controllability grammian) needs to be clarified. To the author's knowledge, this relationship has not been fully exploited in linear systems textbooks.

Theorem 4.1 *Let the controllability grammian W_c be expressed in the eigenvalue decomposition form*

$$W_c = \Phi \Lambda \Phi^T = [\Phi_c \ \Phi_{uc}] \begin{bmatrix} \Lambda_c & \\ & 0 \end{bmatrix} \begin{bmatrix} \Phi_c^T \\ \Phi_{uc}^T \end{bmatrix} = \Phi_c \Lambda_c \Phi_c^T \quad (4.17)$$

where Φ_c and Φ_{uc} are eigen-subspaces associated with non-zero and zero eigenvalues, respectively. Then, the Φ_{uc} subspace is the uncontrollable subspace of the system. The Φ_c subspace is the controllable subspace, and it is the same subspace spanned by the linearly-independent column vectors of the controllability matrix.

Proof: For an asymptotically stable system (A, B, C) , the controllability grammian satisfies

$$AW_c + W_c A^T + BB^T = 0$$

Under the similarity transformation

$$\bar{A} = \Phi^T A \Phi, \quad \bar{B} = \Phi^T B, \quad \bar{C} = C \Phi$$

the controllability grammian for the transformed system becomes $\Phi^T W_c \Phi = \Lambda$ and satisfies

$$\bar{A}\Lambda + \Lambda\bar{A}^T + \bar{B}\bar{B}^T = 0$$

or, in partitioned form

$$\begin{bmatrix} \bar{A}_{11} & \bar{A}_{12} \\ \bar{A}_{21} & \bar{A}_{22} \end{bmatrix} \begin{bmatrix} \Lambda_c & 0 \\ 0 & 0 \end{bmatrix} + \begin{bmatrix} \Lambda_c & 0 \\ 0 & 0 \end{bmatrix} \begin{bmatrix} \bar{A}_{11}^T & \bar{A}_{21}^T \\ \bar{A}_{12}^T & \bar{A}_{22}^T \end{bmatrix} + \begin{bmatrix} \bar{B}_1\bar{B}_1^T & \bar{B}_1\bar{B}_2^T \\ \bar{B}_2\bar{B}_1^T & \bar{B}_2\bar{B}_2^T \end{bmatrix} = 0$$

The above equation leads to

$$\bar{A}_{11}\Lambda_c + \Lambda_c\bar{A}_{11}^T + \bar{B}_1\bar{B}_1^T = 0$$

and

$$\bar{B}_2 = 0, \quad \bar{A}_{12} = 0, \quad \bar{A}_{21} = 0$$

Therefore, $(\bar{A}_{11}, \bar{B}_1, \bar{C}_1)$ is the controllable part of the system. And hence Φ_c is the controllable subspace and Φ_{uc} is the uncontrollable subspace. ■

There is a similar theorem for the observability grammian.

Theorem 4.2 *Let the observability grammian W_o be expressed in the eigenvalue decomposition form*

$$W_o = [\Phi_o \ \Phi_{uo}] \begin{bmatrix} \Lambda_o & \\ & 0 \end{bmatrix} \begin{bmatrix} \Phi_o^T \\ \Phi_{uo}^T \end{bmatrix} = \Phi_o \Lambda_o \Phi_o^T \quad (4.18)$$

where Φ_o and Φ_{uo} are eigen-subspaces associated with non-zero and zero eigenvalues, respectively. Then, the Φ_{uo} subspace is the unobservable subspace of the system. The Φ_o^T subspace is equivalent to the subspace spanned by the linearly-independent row vectors of the observability matrix.

Proof: Although a proof similar to that for the controllability grammian can be approached from the Lyapunov equation, we will prove it by using the definition of the unobservable subspace. For the triple (A, B, C) , an unobservable state z_0 is a state that has no contribution to the output and satisfies

$$y = Ce^{At}z_0 = 0 \quad \text{for } t \geq 0 \quad (\text{a})$$

We want to prove that if z_0 satisfies Eq. (a), then it is in Φ_{uo} and is orthogonal to Φ_o .

It can be shown that

$$\|y\|^2 = \int_0^\infty y^T y = z_0^T W_o z_0 = z_0^T \Phi_o \Lambda_o \Phi_o^T z_0 \quad (\text{b})$$

If z_0 satisfies Eq. (a), then $\|y\|^2$ in the above equation is equal to zero which leads to $\Phi_o^T z_0 = 0$. If $\Phi_o^T z_0 = 0$, then $\|y\|^2 = 0$ which leads to $y = 0$ and z_0 is an unobservable state. Therefore, the unobservable state is in the subspace Φ_{uo} . Finally, by recalling that Ce^{At} and the observability matrix $[C^T, C^T A^T, \dots, C^T (A^T)^{n-1}]^T$ play same role in the observability study [33], the conditions $\Phi_o^T z_0 = 0$ and $Ce^{At} z_0 = 0$ simply state that Φ_o^T is the same subspace spanned by the row vectors of the observability matrix. This completes the proof. \blacksquare

By using the relationships between the grammians and the observable subspace and controllable subspace, Proposition 4.1 can be proved as follows.

Proof: The following proof is for Algorithm 4.1. The proof for Algorithm 4.2 is similar. Apparently, the R vector generated at Step 3 in Algorithm 4.1 is contained in the generalized controllability matrix $[F \ E^{-1}F \ \dots \ E^{-(i-1)}F]$. Therefore, R is in the controllable subspace. At the normalization step (Step

5, singular-value decomposition), the unobservable part is removed from R because $R^T W_o R = R^T \Phi_o \Lambda_o \Phi_o^T R$ is singular if and only if the column vectors in R are linearly-dependent and/or R is orthogonal to Φ_o . Therefore, to retain only the nonzero singular-value portion is to retain only the observable subspace in L . If the algorithm terminates at Step 5 before n vectors are generated, then, obviously, the full-order controller is not minimal. The reduced-order controller obtained by projecting the full-order controller onto the L subspace is a minimal controller. ■

The full-order controller is assumed to be asymptotically stable. The reduced-order controller has the following stability property.

Theorem 4.3

- (1.) *The reduced-order controller obtained by Algorithm 4.1 is asymptotically stable if and only if (\bar{E}_R, \bar{G}_R) is observable.*
- (2.) *The reduced-order controller obtained by Algorithm 4.2 is asymptotically stable if and only if (\bar{E}_R, \bar{F}_R) is controllable.*
- (3.) *The unstable poles of the reduced-order controller lie on the imaginary axis.*

Proof: There is a similar proof in Ref. [41]. The proof shown here is based upon the previous formulation.

- (1). Premultiply and postmultiply Eq. (4.8) by L_R^T and L_R respectively.

$$L_R^T E^T W_o L_R + L_R^T W_o E L_R + L_R^T G^T G L_R = 0$$

Then,

$$\bar{E}_R^T + \bar{E}_R + \bar{G}_R^T \bar{G}_R = 0 \quad (4.19)$$

By the uniqueness of the solution of

$$\bar{E}_R^T \bar{W}_{oR} + \bar{W}_{oR} \bar{E}_R + \bar{G}_R^T \bar{G}_R = 0$$

if \bar{E}_R is asymptotically stable, then the observability grammian for (\bar{E}_R, \bar{G}_R) is the identity matrix, which is nonsingular, and hence (\bar{E}_R, \bar{G}_R) is observable. And, if (\bar{E}_R, \bar{G}_R) is observable, then the observability grammian of (\bar{E}_R, \bar{G}_R) is the identity matrix, which is positive definite, and hence \bar{E}_R is asymptotically stable.

(2). The proof is similar.

(3). A proof for the location of unstable poles is given in Ref. [32] and reproduced in Ref. [41]. Therefore, it is omitted here. ■

The reduced-order controller is called an Equivalent Impulse Response Energy Controller because it conserves the impulse response energy of the full-order controller.

Proposition 4.2 *If the reduced-order controller obtained by Algorithm 4.1 or Algorithm 4.2 is asymptotically stable, then it has the same impulse response energy as the full-order controller. The impulse response energy is defined as the L^2 -norm of the impulse response of the controller, Eqs. (4.6), (4.7).*

Proof: For Algorithm 4.1, the observability grammian for the controller system in L -coordinates is the identity matrix. Since the defined impulse response energy is invariant under coordinate transformation, it can be shown that

$$\mathcal{E} = \text{tr}[F^T W_o F] = \text{tr}[\bar{F}^T \bar{F}] = \text{tr}[\bar{F}_R^T \bar{F}_R] \quad (4.20)$$

due to the special form of the \bar{F} matrix.

The proof for Algorithm 4.2 is similar. ■

In fact, as will be depicted in Theorem 4.4, the reduced-order controller matches a set of system parameters of the full-order controller, and the impulse response energy is one of the parameters matched. Furthermore, the following proposition, which is similar to the one in Ref. [24] can be used to calculate the error norm of the impulse response energy.

Proposition 4.3 *The error of the impulse response $H_e = H - H_R$ can be measured by*

$$\|H_e\|_{L^2}^2 = \text{tr}\left[\int_0^\infty H_e^T H_e dt\right] = 2\text{tr}[F^T W_o F] - 2\text{tr}[\bar{F}_R^T \mathcal{Z} \bar{F}] \quad (4.21)$$

where \mathcal{Z} satisfies

$$\bar{E}_R^T \mathcal{Z} + \mathcal{Z} \bar{E} + \bar{G}_R^T \bar{G} = 0$$

or by

$$\|H_e\|_{L^2}^2 = \text{tr}\left[\int_0^\infty H_e H_e^T dt\right] = 2\text{tr}[G W_c G^T] - 2\text{tr}[\bar{G}_R \mathcal{X} \bar{G}^T] \quad (4.22)$$

where \mathcal{X} satisfies

$$\bar{E}_R \mathcal{X} + \mathcal{X} \bar{E}^T + \bar{F}_R \bar{F}^T = 0$$

Proof: For Eq. (4.21),

$$\begin{aligned} \|H_e\|_{L^2}^2 &= \|H\|_{L^2}^2 + \|H_R\|_{L^2}^2 - 2\text{tr}\left[\int_0^\infty \bar{F}_R^T e^{\bar{E}_R^T t} \bar{G}_R^T \bar{G} e^{\bar{E} t} \bar{F} dt\right] \\ &= 2\text{tr}[F^T W_o F] - 2\text{tr}[\bar{F}_R^T \mathcal{Z} \bar{F}] \end{aligned}$$

with \mathcal{Z} satisfying the corresponding Lyapunov equation. Eq. (4.22) can be proved similarly. ■

Another interesting property of the reduced-order controller, in addition to preserving the impulse response energy, is that it matches a set of system parameters. This set of parameters includes the so called low-frequency moments and low-frequency power moments [41]. For the triple (A, B, C) , low-frequency moments, sometimes called time moments [15], are defined as $CA^{-i}B$ for $i > 0$, which are the coefficient matrices of the Taylor series expansion of the transfer function. Low-frequency power moments are defined in Ref. [41] as $CA^{-i}W_c(A^T)^{-j}C^T$ with $i, j > 0$ and W_c the controllability grammian. Besides low-frequency moments and low-frequency power moments, other meaningful parameters are Markov parameters CA^iB and the high-frequency power moments $CA^iW_c(A^T)^jC^T$. The q -COVER method of Yousuff et al. [47] produces a reduced-order controller that matches q Markov parameters and q high-frequency power moments $CA^iW_cC^T$ which are the derivatives of the output covariance matrix. Since these parameters and moments constitute sets of data that can describe the system transfer function and output autocorrelation, it is reasonable to seek a reduced-order system that matches as many parameters of the full-order system as possible. The reduced-order controller proposed here turns out to match the low-frequency moments and low-frequency power moments because the projection subspace is the generalized controllability (or observability) matrix.

Theorem 4.4:

- (1.) *If the full-order controller is observable, then the reduced-order controller $(\bar{E}_R, \bar{F}_R, \bar{G}_R)$ obtained by Algorithm 4.1 matches:*

$$\text{low-frequency moments} \quad GE^{-i}F, \quad i = 1, 2, \dots, k - 1$$

low-frequency power moments $F^T(E^T)^{-i}W_oE^{-j}F$, $i, j = 1, 2, \dots, k-1$

where k is number of blocks contained in the projection subspace $L_R = [L_1 \ L_2 \ \dots \ L_k]$.

- (2.) If the full-order controller is controllable, then the reduced-order controller $(\bar{E}_R, \bar{F}_R, \bar{G}_R)$ obtained by Algorithm 4.2 matches:

low-frequency moments $GE^{-i}F$, $i = 1, 2, \dots, k-1$

low-frequency power moments $GE^{-i}W_c(E^T)^{-j}G^T$, $i, j = 1, 2, \dots, k-1$

where k is number of blocks contained in the projection subspace $L_R = [L_1 \ L_2 \ \dots \ L_k]$.

- (3.) If the full-order controller is neither controllable nor observable, but has the same controllable subspace as observable subspace, then the above moment-matching properties still hold.

Proof: (Part of the proof shown here follows a similar proof given in Ref. [41]).

- (1). If the full-order controller is observable, then the subspace L_R is equal to the generalized controllability subspace $[F \ E^{-1}F \ E^{-2}F \ \dots \ E^{-(k-1)}F]$. So $E^{-i}F$ can be represented as a linear combination of L_R

$$E^{-i}F = L_R\alpha$$

Then,

$$L_R L_R^T W_o E^{-i} F = L_R L_R^T W_o L_R \alpha = L_R \alpha = E^{-i} F, \quad \text{for } i = 0, 1, \dots, k-1$$

Secondly, by using the above equality, it can be shown that

$$\begin{aligned}
L_R^T W_o E^{-i} F &= (L_R^T W_o E_R)^{-i} (L_R^T W_o E_R)^i L_R^T W_o E^{-i} F \\
&= (L_R^T W_o E_R)^{-i} (L_R^T W_o E_R)^{i-1} L_R^T W_o E (L_R L_R^T W_o E^{-i} F) \\
&= (L_R^T W_o E_R)^{-i} (L_R^T W_o E_R)^{i-1} L_R^T W_o E^{-(i-1)} F \\
&\vdots \\
&= (L_R^T W_o E L_R)^{-i} L_R^T W_o F \\
&= (\bar{E}_R)^{-i} \bar{F}_R \quad \text{for } i = 0, 1, \dots, k-1
\end{aligned}$$

Therefore,

$$\bar{G}_R (\bar{E}_R)^{-i} \bar{F}_R = G L_R (L_R^T W_o E^{-i} F) = G E^{-i} F, \quad \text{for } i = 0, 1, \dots, k-1$$

The low-frequency power moment matching property can be proved similarly.

$$\bar{F}_R^T (\bar{E}_R^T)^{-i} (\bar{E}_R)^{-j} \bar{F}_R = F^T (E^T)^{-i} W_o L_R L_R^T W_o E^{-j} F = F^T (E^T)^{-i} W_o E^{-j} F$$

for $i, j = 0, 1, \dots, k-1$.

(2). Similar proof for Algorithm 4.2.

(3). If the controllable subspace and the observable subspace are the same, then it is true that L_R is equal to $[F \ E^{-1}F \ E^{-2}F \ \dots \ E^{-(k-1)}F]$ for (1), and the same proof follows. \blacksquare

It is to be pointed out here that the low-frequency power moments $F^T (E^T)^{-i} W_o E^{-j} F$ in (1) are not the same as the low-frequency power moments defined in Ref. [41]. The low-frequency power moments defined here are not related to the coefficient matrices of the Laurent series of the output power spectral density. Nevertheless, they still constitute pieces of data for parameter matching. The other thing to be mentioned is that if E instead of E^{-1} is

used in the Algorithm 4.1 to generate the projection subspace, then the generated subspace is equivalent to $[F \ EF \ E^2F \ \dots \ E^{i-1}F]$. The reduced-order controller would match the Markov parameters and high-frequency power moments and hence would be a q -COVER. However, numerical experience shows that matching high-frequency moments gives a poor reduced-order controller compared with matching low-frequency moments. At least for the two examples shown in the following section, matching low-frequency moments produces a reduced-order model with much better closed-loop performance.

4.4 Examples

4.4.1 Controllers For A Four-Disk System

The first example is given by Enns [10] and is used in Ref. [13] and Ref. [28] to compare six different controller reduction methods. It is used as an example here to illustrate the efficiency of the current controller reduction method. The plant to be controlled is a four-disk system and is linear, time-invariant, SISO, neutrally-stable, non-minimum phase, and of eighth order. Numerical values of the system A , B , and C matrices (in observable canonical form), the weighting matrices Q and R , and the noise intensities \mathcal{V} and \mathcal{W} are

$$A = \begin{bmatrix} -0.1610 & 1 & 0 & 0 & 0 & 0 & 0 & 0 \\ -6.0040 & 0 & 1 & 0 & 0 & 0 & 0 & 0 \\ -0.5822 & 0 & 0 & 1 & 0 & 0 & 0 & 0 \\ -9.9835 & 0 & 0 & 0 & 1 & 0 & 0 & 0 \\ -0.4073 & 0 & 0 & 0 & 0 & 1 & 0 & 0 \\ -3.9820 & 0 & 0 & 0 & 0 & 0 & 1 & 0 \\ 0 & 0 & 0 & 0 & 0 & 0 & 0 & 1 \\ 0 & 0 & 0 & 0 & 0 & 0 & 0 & 0 \end{bmatrix}$$

$$B^T = [0, 0, 0.0064, 0.00235, 0.0713, 1.0002, 0.1045, 0.9955]$$

$$C = [1 \ 0 \ 0 \ 0 \ 0 \ 0 \ 0 \ 0]$$

$$N = B$$

$$Q = (1.0 \times 10^{-6})H^T H; \quad H = [0 \ 0 \ 0 \ 0 \ 0.55 \ 11 \ 1.32 \ 18.0]$$

$$R = 1$$

$$\mathcal{W} = q_2 \quad (q_2 = 0.01, 0.1, 1, 10, 100, 1000, 2000)$$

$$\mathcal{V} = 1$$

Disturbance noise intensity parameter q_2 is used as a design parameter. For this SISO system, we can use either Algorithm 4.1 or Algorithm 4.2. These two algorithms give exactly the same results.

First, different full-order optimal controllers are obtained by LQG design for different values of q_2 ($q_2 = 0.01, 0.1, 1, 10, 100, 1000, 2000$). Then, order reduction is carried out on each full-order controller. We have checked the closed-loop system stability of each reduced-order controller and summarized the results in Table 4.1 to compare the current method (EIREC method) with the other methods. N_c in Table 4.1 is the order of the reduced-order controller. We see that only the optimal projection method produces stable designs for all cases. This is because the optimal projection method is not a linear quadratic reduction method which performs reduction to the full-order optimal controller obtained by LQG design. Instead, the system matrices of an optimal projection reduced-order controller are obtained by solving a parameter optimization problem which minimizes the performance index J in Eq. (4.2). Therefore, in theory, the optimal projection method should produce an

optimal reduced-order controller which is guaranteed to stabilize the closed-loop system, if the solution scheme converges to an appropriate solution at all. Hence, at least from a theoretical point of view, all the other methods cannot compete with the optimal projection method in regard to stability and performance. However, computationally, the other linear quadratic reduction methods are certainly more efficient than the optimal projection method. Here we compare the current method only with the other linear quadratic reduction methods.

The stability comparison is apparent from Table 4.1. The EIREC method is better than Glover's method[12], Davis and Skelton's balanced controller reduction method[9], and Yousuff and Skelton's Component Cost Analysis (CCA) method[45], but is not so good as Enns' method[10] and Liu and Anderson's method[28] as far as absolute percentage of stable designs is concerned. However, one interesting thing to note is that the current method seems to have a trend that if the lower-order reduced controller can produce a stable closed-loop system, then the higher-order one also can. This trend is not seen in the other methods. It is usually expected and preferred that a higher-order controller has better performance and stability than a lower-order controller. In addition to stability comparisons, the accuracy of closed-loop response is also compared. Comparisons of unit step responses and unit impulse responses for a second-order controller designed with $q_2 = 1.0$ and a fifth-order controller designed with $q_2 = 100$ are shown in Figures 4.1-4.8. It is seen that for the low noise intensity case, the second-order controller produced by the current method has about the same performance as the controller obtained by methods 1 and 5. For the high noise intensity case, although the fifth-order controller

produced by the current method gives a stable closed-loop system, the damping is very low (the closed-loop pole with the least damping is $-0,0022 \pm 1.3792i$). However, the sixth-order controller has quite accurate closed-loop responses (Figures 4.9, 4.10).

4.4.2 Controllers For A Solar Optical Telescope Spacecraft

The second example considered here is the pointing and shape control of the “Solar Optical Telescope” spacecraft example discussed in Ref. [45] and Ref. [16]. The original model has 44 modes and is reduced to 10 modes by modal cost analysis as discussed in Ref. [45]. In the first-order state-space form, the matrices describing this 20-state problem are given by

$$A = \begin{bmatrix} 0 & I_{10} \\ -\omega^2 & -2\zeta\omega \end{bmatrix}, \quad B = N = \begin{bmatrix} 0 \\ \beta \end{bmatrix}, \quad C = [\mathcal{P} \ 0]$$

$$\zeta = 0.001$$

$$\omega = \text{diag}[14.853, 0.914, 10.817, 3.652, 153.43, 53.861, 3.63, 149.37, 0, 0]$$

$$Q = \begin{bmatrix} \mathcal{P}^T \\ 0 \end{bmatrix} \begin{bmatrix} 1 & 0 & 0 \\ 0 & 10 & 0 \\ 0 & 0 & 10^{-3} \end{bmatrix} [\mathcal{P} \ 0], \quad R = \rho I_8$$

$$\mathcal{W} = 10^{-4} I_8, \quad \mathcal{V} = 10^{-15} I_3$$

with matrices β and \mathcal{P} given in Table II of Ref. [45].

Design parameter ρ in the control weighting matrix R was varied to study controllers of different bandwidth. Since in this problem there are fewer sensors than actuators, Algorithm 4.1 is used to carry out the reduction. The design comparison is to plot the regulation cost $J_e = E[x^T Q x]$ versus the control cost

$J_u = E[u^T u]$ for different orders of controller and for different values of ρ . The results are shown in Figures 4.11–4.13. Comparing Figures 4.11 and 4.12, it is seen that the tenth-order reduced-order controller obtained by the current method has a slightly better performance than the tenth-order controller obtained by component cost analysis. The sixth-order case of the current method is, however, not as good as the one produced by the component cost analysis. The fourth-order case of the current method is not shown in Figure 4.12 because the curve lies outside of the window (For $\rho = 0.5, 1, 5, 10$ the control costs are $1.3897E-7, 1.3650E-5, 1.3240E-5, 1.3114E-5$, and the regulation costs are $7.9732E-8, 1.3105E-7, 4.2024E-7, 6.9699E-7$). Figure 4.13 shows smoother cost curves of the sixth, tenth, and twelfth-order reduced controllers of the current method. It is seen again here that the higher-order controller tends to have better performance than the lower-order controller. In contrast to this appealing result, component cost analysis produces a fourth-order controller with better performance than the sixth and tenth-order controllers (see Figure 4.11). In addition to this performance comparison, we have also checked the closed-loop stability. It is seen that for the current method, all of the reduced-order controllers with order higher than three produce stable closed-loop systems for all ρ values from 0.01 to 1000. On the other hand, the tenth-order controller and the fourth-order controller of component cost analysis fail to give stable designs for $\rho < 0.05$ and $\rho < 0.5$, respectively.

From the above two examples, one can see that the present controller reduction method produces fairly good closed-loop designs. Computationally, the current method is also economical compared with the other methods. Enns' frequency-weighted balanced realization method requires solving two Lyapunov

equations of order larger than n (order of the full-order controller), depending on the order of the input and output weightings, in addition to solving one unsymmetric eigenvalue problem of order n . The stable factorization and balancing method of Liu and Anderson [28] and the two balanced controller reduction algorithms of Yousuff and Skelton [46] and of Davis and Skelton [9] all involve the solution of two Lyapunov equations and two singular-value decompositions of order n . The component cost analysis method requires solving one Lyapunov equation and two singular-value decompositions of order n . The current controller reduction method needs to solve only one Lyapunov equation of order n and to perform some small scale singular-value decompositions. Therefore, the computational burden of the current method is lower than that of the other methods.

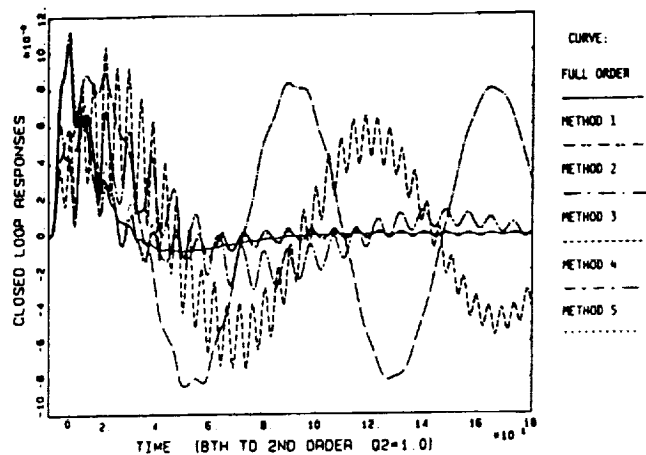


Figure 4.1: Comparison of impulse responses of second-order compensators given by methods 1-5 with full-order design (small q_2).

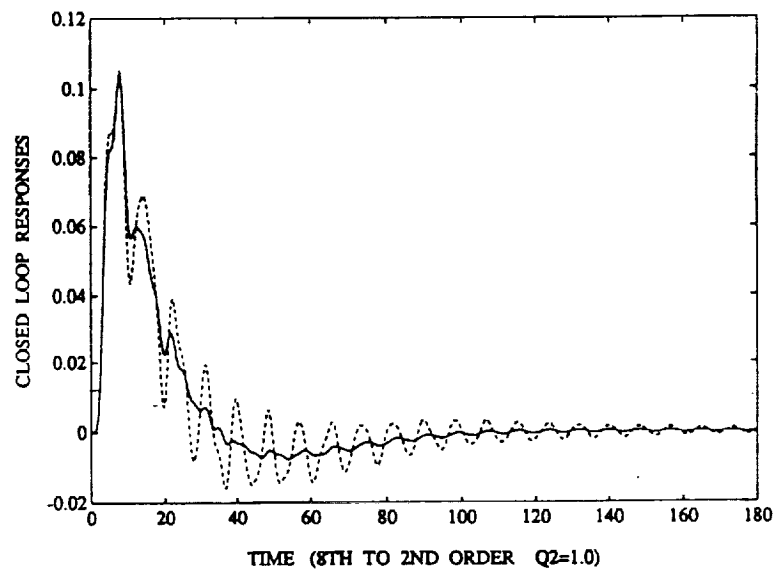


Figure 4.2: Comparison of impulse response of second-order compensator given by current method with full-order design (small q_2).

ORIGINAL PAGE IS
OF POOR QUALITY

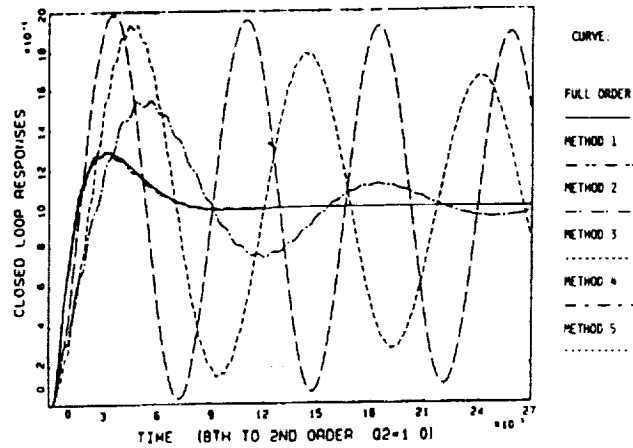


Figure 4.3: Comparison of step responses of second-order compensators given by methods 1-5 with full-order design (small q_2).

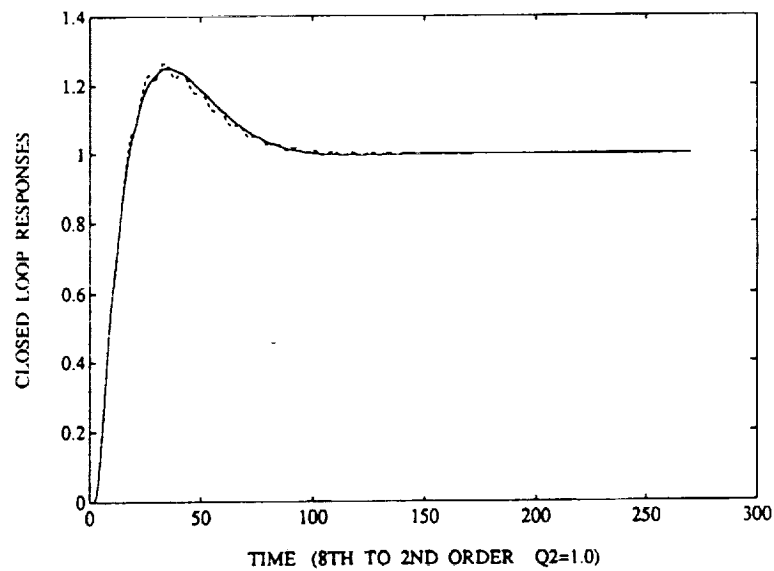


Figure 4.4: Comparison of step response of second-order compensator given by current method with full-order design (small q_2).

ORIGINAL PAGE IS
OF POOR QUALITY

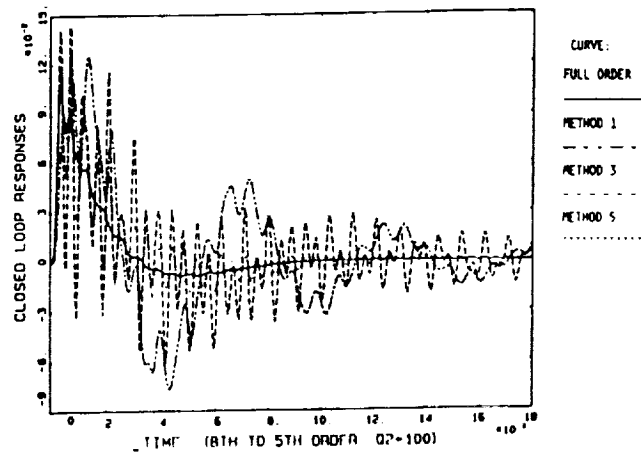


Figure 4.5: Comparison of impulse responses of fifth-order compensators given by methods 1, 3, 5 with full-order design (large q_2).

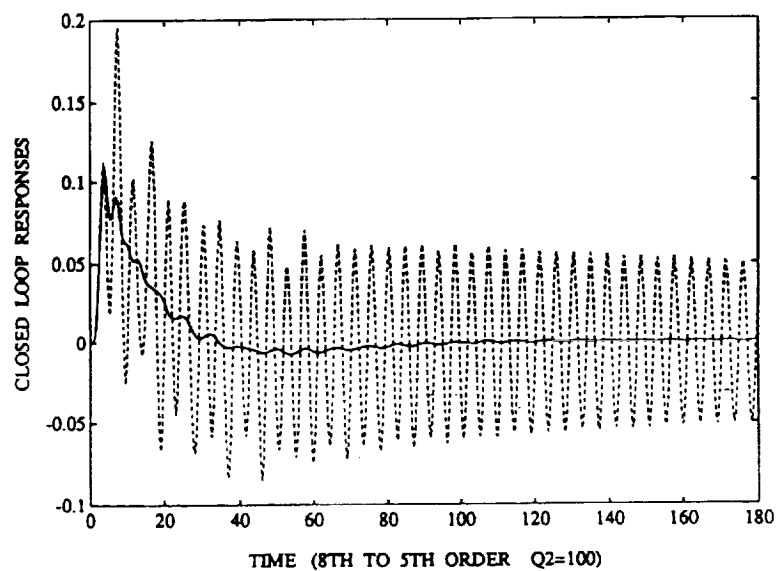


Figure 4.6: Comparison of impulse response of fifth-order compensator given by current method with full-order design (large q_2).

ORIGINAL PAGE IS
OF POOR QUALITY

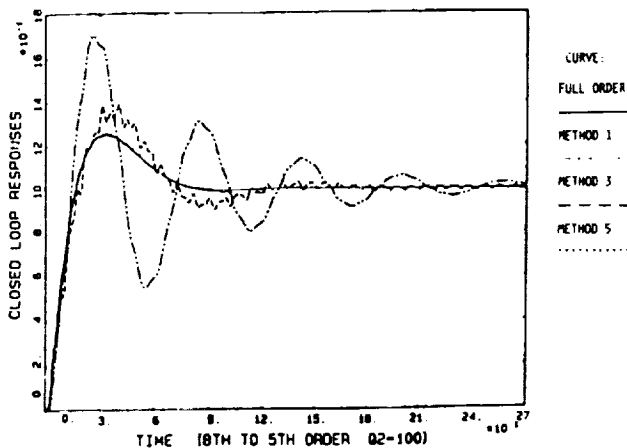


Figure 4.7: Comparison of step responses of fifth-order compensators given by methods 1, 3, 5 with full-order design (large q_2).

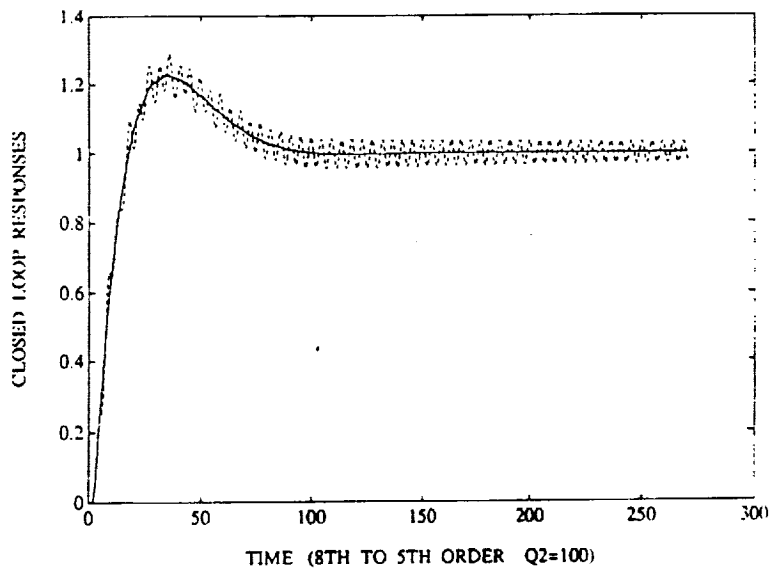


Figure 4.8: Comparison of step response of fifth-order compensator given by current method with full-order design (large q_2).

ORIGINAL PAGE IS
OF POOR QUALITY

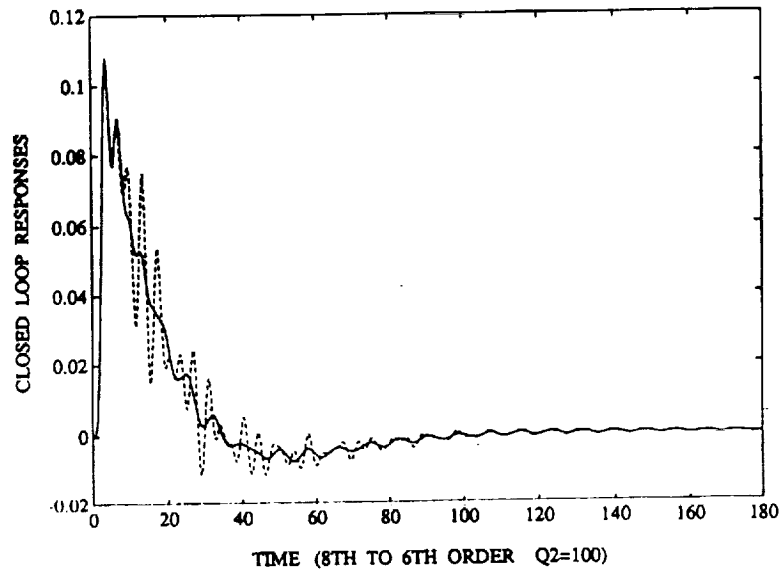


Figure 4.9: Comparison of impulse response of sixth-order compensator given by current method with full-order design (large q_2).

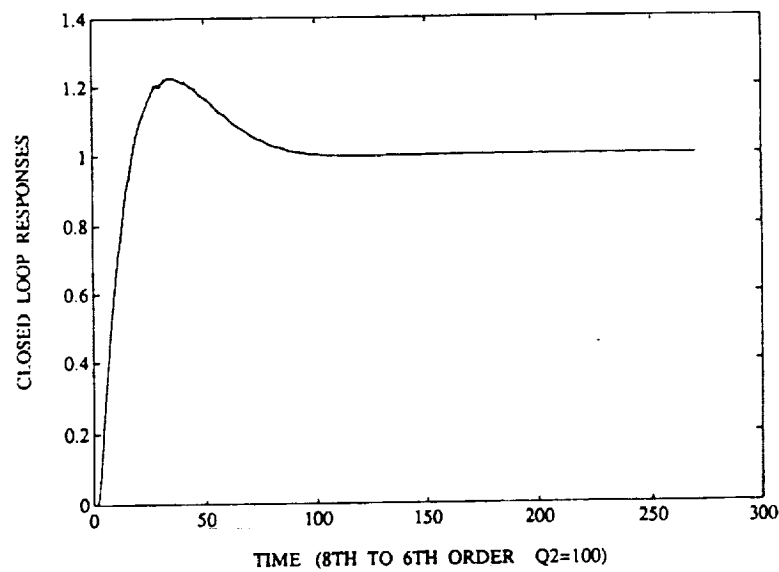


Figure 4.10: Comparison of step response of six-order compensator given by current method with full-order design (large q_2).

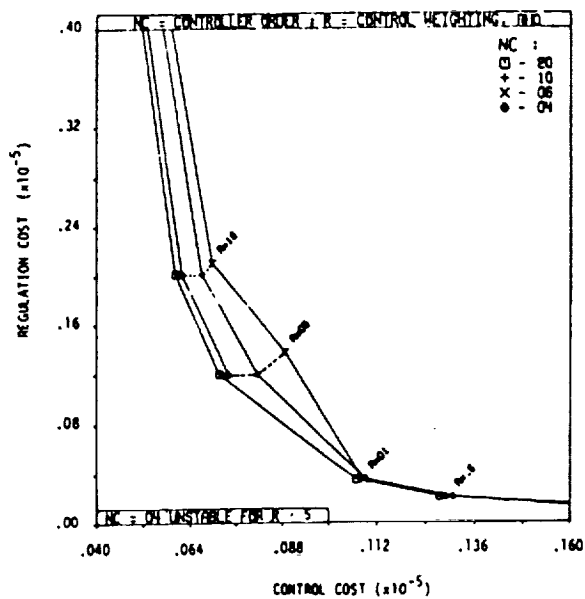


Figure 4.11: Performance plot of Component Cost Analysis method

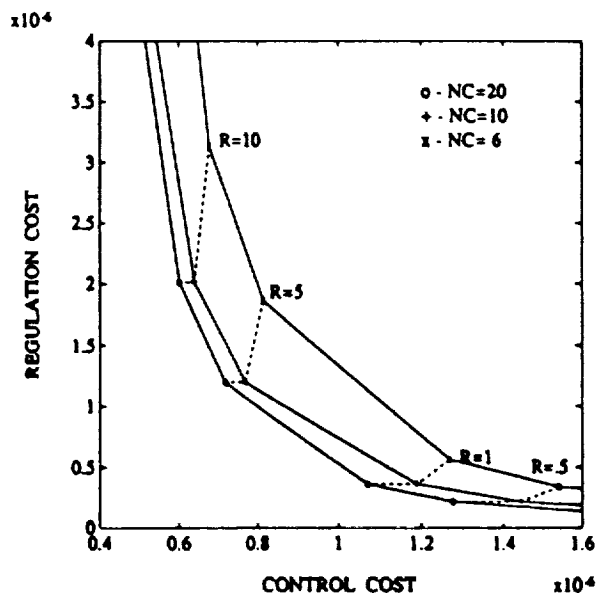


Figure 4.12: Performance plot of current method

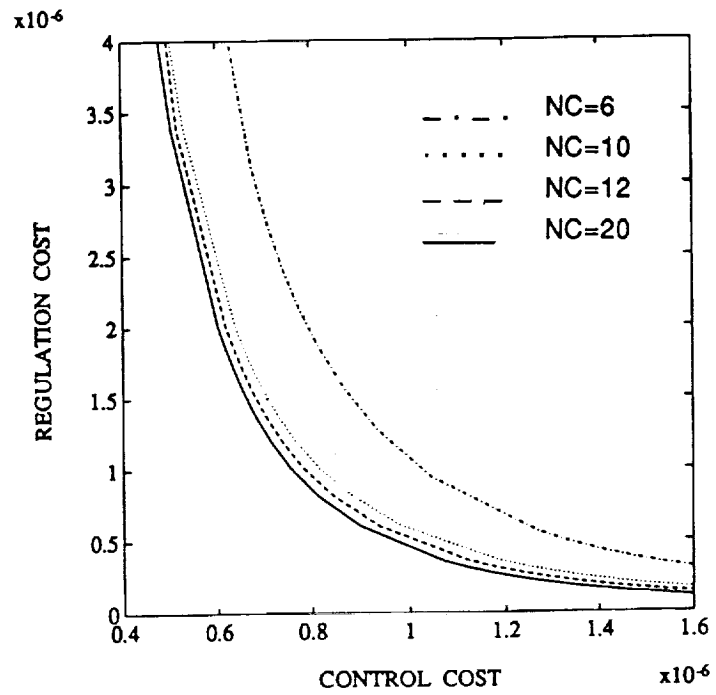


Figure 4.13: Performance plot of current method with smoother curves

Table 4.1: Stability of the reduced-order controller by different methods

Method	N_c	$g_2=.01$	0.1	1	10	100	1000	2000
1 Enns[10]	7	S	S	S	S	S	S	S
	6	SS	SS	SS	SS	SS	SS	SS
	5	SSS	SSS	SSS	SSS	SSS	SSS	SSS
	4	SSSS	SSSS	SSSS	SSSS	SSSS	SSSS	SSSS
	3	SSSSS	SSSSS	SSSSS	SSSSS	SSSSS	SSSSS	SSSSS
2 Glover[12]	7	S	S	S	S	S	U	S
	6	SS	SS	SS	SS	SS	UU	UU
	5	SSS	SSS	SSS	SSS	SSS	UUU	UUU
	4	SSSS	SSSS	SSSS	SSSS	SSSS	UUUU	UUUU
	3	SSSSS	SSSSS	SSSSS	SSSSS	SSSSS	UUUUU	UUUUU
3 Davis & Skelton[9]	7	S	U	U	S	S	S	S
	6	SS	S	S	SS	SS	SS	SS
	5	SSS	U	S	SSS	SSS	SSS	SSS
	4	SSSS	S	U	SSSS	SSSS	SSSS	SSSS
	3	SSSSS	U	U	SSSSS	SSSSS	SSSSS	SSSSS
4 Yousuff & Skelton[46]	7	S	S	S	S	U	U	U
	6	SS	SS	SS	SS	UU	UU	UU
	5	SSS	SSS	SSS	SSS	UUU	UUU	UUU
	4	SSSS	SSSS	SSSS	SSSS	UUUU	UUUU	UUUU
	3	SSSSS	SSSSS	SSSSS	SSSSS	UUUUU	UUUUU	UUUUU
5 Liu & Anderson[28]	7	S	S	S	S	S	S	U
	6	SS	SS	SS	SS	SS	SS	SS
	5	SSS	SSS	SSS	SSS	SSS	SSS	SSS
	4	SSSS	SSSS	SSSS	SSSS	SSSS	SSSS	SSSS
	3	SSSSS	SSSSS	SSSSS	SSSSS	SSSSS	SSSSS	SSSSS
6 Optimal Projection[13]	7	S	S	S	S	S	S	S
	6	SS	SS	SS	SS	SS	SS	SS
	5	SSS	SSS	SSS	SSS	SSS	SSS	SSS
	4	SSSS	SSSS	SSSS	SSSS	SSSS	SSSS	SSSS
	3	SSSSS	SSSSS	SSSSS	SSSSS	SSSSS	SSSSS	SSSSS
7 EIREC Method	7	S	S	S	S	S	S	S
	6	SS	SS	SS	SS	SS	SS	SS
	5	SSS	SSS	SSS	SSS	SSS	SSS	SSS
	4	SSSS	SSSS	SSSS	SSSS	SSSS	UUUU	UUUU
	3	SSSSS	SSSSS	SSSSS	SSSSS	SSSSS	UUUUU	UUUUU

S: the closed-loop system is stable. U: unstable

Chapter 5

CONCLUSIONS

A decentralized suboptimal linear quadratic design procedure which combines substructural synthesis, model reduction, decentralized control design, and controller reduction is proposed for the control design of flexible structures. The structure to be controlled is decomposed into several substructures by using substructuring decomposition. Then, a Krylov model reduction algorithm is employed to reduce the order of each substructure to a size that is Riccati-solvable. For each substructure, a subcontroller is designed by using a linear quadratic optimal control method. After all subcontrollers are designed, a controller synthesis scheme called Substructural Controller Synthesis is used to assemble all subcontrollers into a global controller. Finally, a controller reduction scheme which produces a reduced-order controller with equivalent impulse response energy is used to reduce the order of the global controller to a reasonable size for implementation.

Substructural Controller Synthesis (SCS) is a decentralized control design scheme for flexible structures. The method relieves the computational burden associated with dimensionality. The SCS design scheme is a highly adaptable controller synthesis method for structures with varying configuration, or varying mass and stiffness properties.

Equivalent Impulse Response Energy Controller (EIREC) Reduction Al-

gorithm is an efficient controller reduction method. The method produces a reduced-order controller that preserves impulse response energy and matches low-frequency moments and low-frequency power moments of the full-order controller. It is a model reduction algorithm applied to controller reduction and is applicable to controllers designed by any existing methods.

Some recommendations for future research direction are listed below.

- Robustness of SCS controllers is an interesting topic and needs to be investigated.
- Application of substructuring decomposition and Substructural Controller Synthesis to general linear time-invariant systems needs to be explored. A system representation in Lanczos coordinates may be a good starting point for substructuring decomposition and SCS analysis.
- Incorporation of Substructural Controller Synthesis with the well-developed Component Mode Synthesis (CMS) is another possibility for designing controllers for flexible structures.
- Suboptimality and stability of SCS controllers is an important topic. It would elevate the SCS method from a design technique level to a control theory level if a suboptimality study similar the one in Ref. [20] can be accomplished.

BIBLIOGRAPHY

- [1] Ahmed, N. U., *Optimal Control of Distributed Parameter Systems*, Nasir Uddin, NY, 1981.
- [2] Bantell, M. H., "Precision Pointing and Control of Flexible Spacecraft," *Structural Dynamics and Control Interaction of Flexible Structures*, Proceedings of a workshop held at NASA Marshall Space Flight Center, Huntsville, AL, April 22-24, 1986, pp. 505-537.
- [3] Benfield, W. A. and Hruda, R. F., "Vibration Analysis of Structures by Component Mode Substitution," *AIAA Journal*, Vol. 9, No. 7, pp. 1255-1261, 1971.
- [4] Blueloch, P. A. and Carney, K. S., "Modal Selection In Structural Dynamics," *Proc. 7th International Modal Analysis Conference*, Union College, Schenectady, NY, pp. 742-749, 1989.
- [5] Cornwell, R. E., Craig, R. R., Jr., and Johnson, C. P., "On the Application of the Mode Acceleration Method to Structural Engineering Problems," *Earthquake Eng. & Struc. Dyn.*, Vol. 11, pp. 679-688, 1983.
- [6] Craig, R. R. Jr., *Structural Dynamics - An Introduction to Computer Methods*, John Wiley & Sons, Inc. NY, 1981.
- [7] Craig, R. R. Jr., "A Review of Time-Domain and Frequency-Domain Component Modes Synthesis Methods," *Combined Experimental/Analytical*

Modeling of Dynamic Structural Systems, AMD-Vol. 67, ASME, NY, pp. 1-30, 1985. Also *International Journal of Analytical and Experimental Modal Analysis*, Vol. 2, No. 2, pp. 59-72, April 1987.

- [8] Craig, R. R., Jr. and Su, T. J., "A Review of Model Reduction Methods For Structural Control Design," *International Conference on Dynamics of Flexible Structures*, Cranfield Institute of Technology, United Kingdom, May 15-18, 1990.
- [9] Davis, J. A. and Skelton, R. E., "Another Balanced Controller Reduction Algorithm," *System Control Lett.*, Vol. 4, 1984, pp. 79-83.
- [10] Enns, D. F., "Model Reduction for Control System Design," Ph.D. Dissertation, Stanford University, Palo Alto, CA, 1984.
- [11] Enns, D. F., "Model Reduction With Balanced Realizations: An Error Bound And A Frequency Weighted Generalization," *Proc. 23rd Conference on Decision and Control*, Las Vegas, NV, pp. 127-132, Dec. 1984.
- [12] Glover, H., "All Optimal Hankel-Norm Approximations of Linear Multi-variable Systems and Their L -Error Bounds," *Int. J. Contr.*, Vol. 39, 1984, pp. 1115-1193.
- [13] Greeley, S. W. and Hyland, D. C., "Reduced-Order Compensation: Linear-Quadratic Reduction Versus Optimal Projection," *J. Guidance, Control, and Dynamics*, Vol. 11, No. 4, 1988, pp. 328-335.
- [14] Gregory, C. Z., "Reduction of Large Flexible Spacecraft Models Using Internal Balancing Theory," *AIAA J. Guidance, Control, and Dynamics*,

- Vol. 7, No. 6, pp. 725–732, 1984.
- [15] Hickin, J. and Sinha, N. K., “Model Reduction for Linear Multivariable Systems,” *IEEE Trans. Automat. Contr.*, Vol. 25, No.6, pp. 1121–1127, 1980.
- [16] Hyland, D. C., “Comparison of Various Controller-Reduction Methods: Suboptimal versus Optimal Projection,” *AIAA Dynamics Specialists Conf.*, Palm Springs, CA, May 1984, pp. 381–389.
- [17] Hyland, D. C. and Bernstein, D. S., “The Optimal Projection Equations for Fixed-Order Dynamic Compensation,” *IEEE Trans. Automat. Contr.*, Vol. 29, No. 11, pp. 1034–1037, 1984.
- [18] Ikeda, M. and Šiljak, D. D., “Overlapping Decompositions, Expansions, and Contractions of Dynamic Systems,” *Large Scale Systems*, Vol. 1, pp. 29–38, 1980.
- [19] Ikeda, M., Šiljak, D. D., and White, D. E., “An Inclusion Principle for Dynamic Systems,” *IEEE Trans. Automat. Control*, Vol. 29, No. 3, pp. 244–249, 1984.
- [20] Ikeda, M., Šiljak, D. D., and White, D. E., “Decentralized Control With Overlapping Information Sets,” *J. Optim. Theory Appl.*, Vol. 34, No. 2, pp. 279–309, 1981.
- [21] Johnson, M. A. and Grimble M. J., “Recent Trends in Linear Optimal Quadratic Multivariable Control System Design,” *IEE Proceedings*, Vol. 134, No. 1, pp. 53–71, 1987.

- [22] Jonckhere, E. A. and Silverman, L. M., "A New Set of Invariants for Linear Systems - Application to Reduced Order Compensator Design," *IEEE Trans. Automat. Control*, Vol. 28, No. 10, 1983, pp.953-964.
- [23] Jonckheere, E. A., "Principal Component Analysis of Flexible Systems - Open-Loop Case," *IEEE Trans. Automat. Control*, Vol. AC-29, No. 12, pp. 1095-1097, 1984.
- [24] Kabamba, P. T., "Balanced Gains and Their Significance for L^2 Model Reduction," *IEEE Trans. Automat. Control*, Vol. 30, No. 7, 1985, pp. 690-693.
- [25] Kline, K. A., "Dynamic Analysis Using a Reduced Basis of Exact Modes and Ritz Vectors," *AIAA Journal*, Vol. 24, No. 12, pp. 2022-2029, 1986.
- [26] Kwakernaak, H. and Sivan, R., *Linear Optimal Control Systems*, New York: Wiley, 1972.
- [27] Lions, J. L., *Optimal Control of Systems Governed by Partial Differential Equations*, Berlin, 1971.
- [28] Liu, Y. and Anderson, B. D. O., "Controller Reduction Via Stable Factorization and Balancing," *Int. J. Contr.*, Vol. 44, No. 2, 1986, pp. 507-531.
- [29] Moore, B. C., "Principal Component Analysis in Linear Systems: Controllability, Observability, and Model Reduction," *IEEE Trans. Automat. Control*, Vol. AC-26, No. 2, pp. 17-32, 1981.

- [30] Nour-Omid, B. and Clough, R. W., "Dynamic Analysis of Structures Using Lanczos Co-ordinates," *Earthquake Eng. & Struc. Dyn.*, Vol. 13, pp. 271-275, 1983.
- [31] Nurre, G. S., Ryan, R. S., Scofield, H. N., and Sims, J. L., "Dynamics and Control of Large Space Structures," *J. Guidance, Control, and Dynamics*, Vol. 7, No. 5, pp. 514-526, 1984.
- [32] Pernebo, L. and Silvermann, L. M., "Model Reduction via Balanced State Space Representations," *IEEE Automat. Control*, Vol. 27, No. 2, 1982, pp. 382-387.
- [33] Reid, J. G., *Linear System Fundamentals*, McGraw-Hill Book Co., 1983.
- [34] Skelton, R. E. and Hughes, P. C., "Modal Cost Analysis for Linear Matrix-Second-Order Systems," *J. Dynamic Systems, Measurement, and Control*, Vol. 102, pp. 151-158, 1980.
- [35] Su, T. J. and Craig, R. R. Jr., "Controller Reduction by Preserving Impulse Response Energy," presented at *1989 AIAA Guidance, Navigation and Control Conference*, Boston, MA, pp. 55-64, August 14-16, 1989.
- [36] Su, T. J. and Craig, R. R., Jr., "Krylov Model Reduction Algorithm For Undamped Structural Dynamics Systems," accepted for publication by *J. Guidance, Control, and Dynamics*.
- [37] Su, T. J. and Craig, R. R., Jr., "Model Reduction and Control of Flexible Structures Using Krylov Vectors," to appear *J. Guidance, Control, and*

Dynamics. Also *30th AIAA/ASME/ASCE/AHS/ASC Structures, Structural Dynamics and Materials Conference*, Mobile, AL, pp. 691–700, April 1989.

- [38] Su, T. J. and Craig, R. R. Jr., “Substructuring Decomposition and Controller Synthesis,” *31st AIAA/ASME/ASCE/AHS/ASC Structures, Structural Dynamics and Materials Conference*, San Diego, CA, April 1990.
- [39] Su, T. J. and Craig, R. R. Jr., “Substructural Controller Synthesis,” presented *3rd Annual Conference on Computational Control*, Oxnard, CA, August 1989.
- [40] Verriest, E. I., “Suboptimal LQG-Design and Balanced Realizations,” *Proc. 20th IEEE Conf. Decision and Contr.*, pp. 686–687, Dec. 1981.
- [41] Villemagne, C. D. and Skelton, R. E., “Model Reduction Using a Projection Formulation,” *IEEE Trans. Automat. Contr.*, Vol. 46, No.6, pp. 2141–2169, 1987.
- [42] Wilson, E. L., Yuan, M. W., and Dickens, J. M., “Dynamic Analysis by Direct Superposition of Ritz Vectors,” *Earthquake Eng. & Struc. Dyn.*, Vol. 10, pp. 813–821, 1982.
- [43] Young, K. D., “Approximate Finite Element Models for Structural Control,” *Proceedings of the 24th IEEE Conference on Decision and Control*, Fort Lauderdale, FL, pp. 940–945, December 11–13, 1985.

- [44] Young, K. D., "Controlled Component Synthesis," Preprint paper, UCRL 98063, Lawrence Livermore National Laboratory, University of California, Livermore, CA, December 21, 1987.
- [45] Yousuff, A. and Skelton, R. E., "Controller Reduction by Component Cost Analysis," *IEEE Trans. Automat. Control*, Vol. 29, No. 6, pp. 520-530, 1984.
- [46] Yousuff, A. and Skelton, R. E., "A Note on Balanced Controller Reduction," *IEEE Trans. Automat. Control*, Vol. 29, No. 3, pp. 254-256, 1984.
- [47] Yousuff, A., Waige, D. A., and Skelton, R. E., "Linear System Approximation via Covariance Equivalent Realizations," *J. Math. Anal. & Appl.*, Vol. 106, pp. 91-115, 1985.
- [48] Yousuff, A., "Application of Inclusion Principle to Mechanical Systems," *Proceedings of 1988 American Control Conference*, Atlanta, GA, June 15-17, pp. 1516-1520, 1988.
- [49] *Advances in Large Scale Systems*, Ed. Jose B. Cruz, Jr., Volume 1, Jai Press Inc., Greenwich, Connecticut, 1984.
- [50] *Control and Dynamics Systems, Advances in Theory and Applications*, Ed. C. T. Leondes, Vols. 22, 23, 24: Decentralized/Distributed Control and Dynamics Systems, Academic Press, Inc., London, 1985, 1986.

